nature biotechnology

SUPPLEMENTARY INFORMATION

https://doi.org/10.1038/s41587-020-0531-2

In the format provided by the authors and unedited.

A lipidome atlas in MS-DIAL 4

Hiroshi Tsugawa[1,2] ✉, Kazutaka Ikeda[1,3], Mikiko Takahashi[2], Aya Satoh[2], Yoshifumi Mori[4], Haruki Uchino[1,5], Nobuyuki Okahashi[1,6], Yutaka Yamada[2], Ipputa Tada[7], Paolo Bonini[8], Yasuhiro Higashi[2], Yozo Okazaki[2,9], Zhiwei Zhou[10,11], Zheng-Jiang Zhu[10], Jeremy Koelmel[12,13], Tomas Cajka[14], Oliver Fiehn[15], Kazuki Saito[2,16], Masanori Arita[2,17] and Makoto Arita[1,5,18] ✉

[1]RIKEN Center for Integrative Medical Sciences, Yokohama, Japan. [2]RIKEN Center for Sustainable Resource Science, Yokohama, Japan. [3]Department of Applied Genomics, Kazusa DNA Research Institute, Chiba, Japan. [4]Bruker, Yokohama, Japan. [5]Graduate School of Pharmaceutical Sciences, Keio University, Tokyo, Japan. [6]Graduate School of Information Science and Technology, Osaka University, Osaka, Japan. [7]Department of Genetics, The Graduate University for Advanced Studies, SOKENDAI, Miura, Japan. [8]NGAlab, Tarragona, Spain. [9]Graduate School of Bioresources, Mie University, Tsu, Japan. [10]Interdisciplinary Research Center on Biology and Chemistry, Shanghai Institute of Organic Chemistry, Chinese Academy of Sciences, Shanghai, China. [11]University of Chinese Academy of Sciences, Beijing, China. [12]Department of Pathology, University of Florida, Gainsville, FL, USA. [13]Department of Environmental Health Sciences, Yale School of Public Health, New Haven, CT, USA. [14]Institute of Physiology of the Czech Academy of Sciences, Prague, Czech Republic. [15]West Coast Metabolomics Center, UC Davis, Davis, CA, USA. [16]Graduate School of Pharmaceutical Sciences, Chiba University, Chiba, Japan. [17]National Institute of Genetics, Mishima, Japan. [18]Graduate School of Medical Life Science, Yokohama City University, Yokohama, Japan. ✉e-mail: hiroshi.tsugawa@riken.jp; makoto.arita@riken.jp

Supplementary Information: a combined PDF file containing the following information

- Supplementary Note 1 | Details of the biological samples and analytical platforms
- Supplementary Note 2 | Details of tandem mass spectrometry (MS/MS) characterization for 117 lipid subclasses
- Supplementary Fig. 1 | Details of tandem mass spectrometry (MS/MS) characterization of 117 lipid subclasses categorized as LipidMAPS Fatty Acyls [FA], Glycerolipids [GL], Glycerophospholipids [GP], Sphingolipids [SP], Sterol Lipids [ST], and Prenol Lipids [PR].

Supplementary Note 1 │ Details of the biological samples and analytical platforms

A total of 36 unique tissues/species which contain human plasma, 19 mouse tissues, 4 mammalian cultured cell types, 9 algal species, and 3 plant species from 10 different analytical platforms were processed by MS-DIAL 4.0. The detail of biological samples and internal standards were described in **Supplementary Table 1 and 2**.

LC-MS/MS and LC-IM-MS/MS methods

Method 1: SCIEX TripleTOF DDA high mass range method

Methanol, isopropanol, and acetonitrile of LC-MS grade were purchased from Wako. Ammonium acetate and EDTA were purchased from Wako and Dojindo, respectively. Milli-Q water was purchased from Millipore. SPLASH Lipidomics I or EquiSPLASH used as internal standards were purchased from Avanti Polar Lipids.

The LC system consisted of a Waters Acquity UPLC system. Lipids were separated on an Acquity UPLC Peptide BEH C18 column (50 × 2.1 mm; 1.7 μm) (Waters, Milford, MA, USA). The column was maintained at 45°C at a flow-rate of 0.3 mL/min. The mobile phases consisted of (A) 1:1:3 (v/v/v) acetonitrile:methanol:water with ammonium formate (5 mM) and 10 nM EDTA and (B) 100% isopropanol with ammonium formate (5 mM) and 10 nM EDTA. A sample volume of 0.5−3 μL, which depended on biological samples, was used for the injection. The separation was conducted under the following gradient: 0 min 0% (B); 1 min 0% (B); 5 min 40% (B); 7.5 min 64% (B); 12 min 64% (B); 12.5 min 82.5% (B); 19 min 85% (B); 20 min 95% (B); 20.1 min 0% (B); and 25 min 0% (B). Sample temperature was maintained at 4°C.

Mass spectrometric detection of lipids was performed on a quadrupole/time-of-flight mass spectrometer TripleTOF 5600 or 6600 (SCIEX, Framingham, MA, USA). All analyses were performed

at the high resolution mode in MS1 (~35,000 full width at half maximum (FWHM)) and at the high sensitivity mode (~20,000 FWHM) in MS2. Data dependent MS/MS acquisition (DDA) was used. The parameters were MS1 and MS2 mass ranges, *m*/*z* 70–1750; MS1 accumulation time, 200 ms; MS2 accumulation time, 70 ms; collision energy, +40/–42 eV; collision energy spread, 15 eV; cycle time, 1370 ms; curtain gas, 30; ion source gas 1, 40(+)/50(–); ion source gas 2, 80(+)/50(–); temperature, 250°C(+)/300°C(-); ion spray voltage floating, +5.5/–4.5 kV; declustering potential, 80 V. The other DDA parameters were dependent product ion scan number, 16; intensity threshold, 100 cps; exclusion time of precursor ion, 0s; mass tolerance, 20 ppm; ignore peaks, within *m/z* 200; and dynamic background subtraction, True. The mass calibration was automatically performed using an APCI positive/negative calibration solution via a calibration delivery system (CDS).

Method 2: SCIEX TripleTOF DDA normal mass range method

The LC-MS machine platform was the same as Method 1, and the LC condition was also the same as Method 1. The mass spectrometer settings were changed for scanning *m*/*z* 70–1250 mass range accordingly: MS1 and MS2 mass ranges, *m*/*z* 70–1250; MS1 accumulation time, 250 ms; MS2 accumulation time, 100 ms; cycle time, 1300 ms. The other parameters were the same as Method 1.

Method 3: Bruker timsTOF Pro DDA for plant lipidomics

Methanol, isopropanol, and acetonitrile of LC-MS grade were purchased from Wako. Ammonium formate and formic acid were purchased from Wako. Water was purchased from Millipore. The LC system consisted of a Bruker Elute UHPLC system. Lipids were separated on an Acquity UPLC HSS T3 C18 column (50 × 1.0 mm; 1.8 μm) (Waters, Milford, MA, USA). The column was maintained at 55°C at a flow-rate of 0.15 mL/min. The mobile phases consisted of (A) 200:800:10:1 (v/v/v/v)

acetonitrile:water:1M ammonium formate:formic acid and (B) 100:900:10:1 (v/v/v/v) acetonitrile:isopropanol:1M ammonium formate:formic acid. A sample volume of 2 μL was used for the injection. The separation was conducted under the following gradient: 0 min 35% (B); 3 min 70% (B); 7 min 85% (B); 10 min 90% (B); 12 min 90% (B); 12.5 min 35% (B); and 15 min 35% (B). Sample temperature was maintained at 10°C.

Mass spectrometric detection of lipids was performed on a hybrid trapped ion mobility-quadrupole time-of-flight mass spectrometer (timsTOF Pro, Bruker Daltonics, Bremen, Germany). Data dependent MS/MS acquisition (DDA) was used. The parameters were MS1 mass ranges, *m*/*z* 200–1600 and MS2 mass ranges, *m*/*z* 50–1600; MS1 cycle time time, 0.5 sec; MS2 accumulation, 14 Hz ; collision energy, 30 eV; end plate offset, 500 V; capillary voltage, +4.2/–4.2 kV; nebulizer pressure, 2 bar; dry gas, 8.0 l/min; dry temperature, 200°C; funnel 1 RF (radio frequency), 300 Vpp; funnel 2 RF, 250 Vpp; multipole RF, 200 Vpp; deflection delta, 70 V; quadrupole ion energy, 5 eV; collision transfer energy, 8 eV; collision RF, 1100 Vpp; transfer time, 54 μs; pre-pulse Storage, 5 μs; intensity threshold, 31cts.; exclusion time of precursor ion, 0.2 min. The mass calibration was automatically performed using 5 mM sodium formate calibration solution.

Method 4: Bruker timsTOF Pro PASEF for plant lipidomics

The LC-MS machine platform was the same as Method 3, and the regents and LC conditions were the same as Method 3. The PASEF mode acquisition, i.e. data dependent MS/MS acquisition with the ion mobility separation, was performed by the following parameters. The parameters were MS1 mass ranges, *m/z* 200–1600 and MS2 mass ranges, *m/z* 50–1600; MS1 and MS2 accumulation time, 148.5 ms; mobility range 0.55–1.9; collision energy 30 eV; end plate offset, 500 V; capillary voltage, +4.2/–4.2 kV; nebulizer pressure, 2 bar; dry gas, 8.0 l/min; dry temperature, 200°C; funnel 1 RF (radio frequency), 300 Vpp; funnel

2 RF, 250 Vpp; multipole RF, 200 Vpp; deflection delta, 70 V; quadrupole ion energy, 5 eV; collision transfer energy, 15 eV; collision RF, 1100 Vpp; transfer time 54 μs; pre-pulse storage, 5 μs; tims transfer *Δ*1, –20 V/+20 V; tims transfer *Δ*2, -120 V/+120 V; tims transfer *Δ*3, +70 V/–70 V; tims transfer *Δ*4, +100 V/-100 V; tims transfer *Δ*5, 0 V; tims transfer *Δ*6, +100 V/–100 V; intensity threshold, 2500 cts; target intensity, 20000 cts; exclusion time of precursor ion, 0.1 min. The mass calibration was automatically performed using 5 mM sodium formate calibration solution.

Method 5: Bruker timsTOF Pro DDA for mouse tissue lipidomics

Methanol, isopropanol, and acetonitrile of LC-MS grade were purchased from Wako. Ammonium acetate and EDTA were purchased from Wako and Dojindo, respectively. Milli-Q water was purchased from Millipore. The LC-MS machine system was the same as Method 3 and 4, and the LC condition was the same as Method 1. Data dependent MS/MS acquisition (DDA) was used. The parameters were MS1 mass ranges, *m*/*z* 200–2500 and MS2 mass ranges, *m*/*z* 50–2500; MS1 cycle time, 0.5 sec; MS2 accumulation 14 Hz ; collision energy, 30 eV; end plate offset, 500 V; capillary voltage, +4.5 kV/–4.2 kV; nebulizer pressure, 2 bar; dry gas, 10.0 l/min; dry temperature, 220°C/200°C; funnel 1 RF, 300 Vpp; funnel 2 RF, 200 Vpp/250 Vpp; multipole RF, 200 Vpp; deflection delta, +70 V/–70 V; quadrupole ion energy, 6 eV/5 eV; collision transfer energy, 14 eV/15 eV; collision RF, 1100 to 1800 Vpp stepping; transfer time 45 to 75 μs stepping; pre-pulse storage, 10 μs/5 μs; intensity threshold, 31cts.; exclusion time of precursor ion, 0.2 min. The mass calibration was automatically performed using 5 mM sodium acetate calibration solution.

Method 6: Bruker timsTOF Pro PASEF for mouse tissue lipidomics

The regents and LC conditions were the same as Method 5. Data dependent MS/MS acquisition (DDA) was used. The parameters were MS1 and MS2 mass ranges, *m/z* 50–2500; MS1 and MS2 accumulation time, 100 ms; mobility range, 0.55–1.90; collision energy 30 eV; end plate offset, 500 V; capillary voltage, +4.5 kV/–4.2 kV; nebulizer pressure, 2 bar; dry gas, 10.0 L/min; dry temperature, 220°C; funnel 1 RF, 300 Vpp; funnel 2 RF, 200 Vpp/250 Vpp; multipole RF, 200 Vpp; deflection delta, 70 V/–70 V; quadrupole ion energy, 6 eV/5 eV; collision transfer energy, 14 eV/15 eV; collision RF, 1500 Vpp/1100 Vpp; transfer time 75 μs/54 μs; pre-pulse storage, 10 μs/5 μs; tims transfer *Δ*1, –20 V/20 V; tims transfer *Δ*2, –120 V/120 V; tims transfer *Δ*3, 70 V/–70 V; tims transfer *Δ*4, 100 V/–100 V; tims transfer *Δ*5, 0 V; tims transfer *Δ*6, 100 V/–100 V; intensity threshold, 250 cts.; target intensity, 4000 cts; exclusion time of precursor ion, 0.1 min. The mass calibration was automatically performed using 5 mM sodium acetate calibration solution. For the confirmation of ESI(+)-MS/MS spectra for phosphatidylcholine, the positive ion mode data was acquired with the following setting. The parameters were dry temperature, 200°C; funnel 2 RF, 250 Vpp; quadrupole ion energy, 5 eV; collision transfer energy, 15 eV; collision RF, 1100 Vpp; and transfer time 54 μs; pre-pulse storage, 5 μs. The other parameters were the same as above.

Method 7: Waters XevoG2 QTOF DDA for plant lipidomics

Methanol, isopropanol, and acetonitrile of LC-MS grade were purchased from Wako. Ammonium acetate, formic acid, methyl *tert*-butyl ether (MTBE), and water were also purchased from Wako. 1,2-Didecanoyl-*sn*-glycero-3-phosphocholine used for the internal standard was purchased from Sigma-Aldrich.

The LC system consisted of a Waters Acquity UPLC system. Lipids were separated on the mostly same condition as described in Method 3 except for using ammonium acetate instead of ammonium formate. The LC system consisted of a Waters Acquity UPLC system. Lipids were separated on an Acquity UPLC HSS T3 C18 column (50 × 1.0 mm; 1.8 μm) (Waters, Milford, MA, USA). The column

was maintained at 55°C at a flow-rate of 0.15 mL/min. The mobile phases consisted of (A) 200:800:10:1 (v/v/v/v) acetonitrile:water:1 M ammonium acetate:formic acid and (B) 100:900:10:1 (v/v/v/v) acetonitrile:isopropanol:1 M ammonium acetate:formic acid. A sample volume of 1 µL was used for the injection. The separation was conducted under the following gradient: 0 min 35% (B); 3 min 70% (B); 7 min 85% (B); 10 min 90% (B); 12 min 90% (B); 12.5 min 35% (B); and 15 min 35% (B). Sample temperature was maintained at 10°C.

Mass spectrometric detection of lipids was performed on a quadrupole/time-of-flight mass spectrometer Xevo G2 QTOF MS (Waters, Milford, MA, USA). MS2 analyses were performed at the sensitivity mode. Data dependent MS/MS acquisition (DDA) was used for MS2. The conditions for recording were as follows: source capillary, 3.0 (positive ion mode) and 2.5 kV (negative ion mode); sampling cone, 20 (positive) and 40 (negative); extraction cone, 4.0; source temperature, 120°C; desolvation temperature, 450°C; cone gas flow, 50 L/h; desolvation gas flow, 600 L/h; scan ranges, *m*/*z* 100–1600; MS1 scan time, 200 ms (centroid); MS2 scan time, 100 ms (centroid); collision energy, 20–50 eV (ramp mode). The other DDA parameters were event number, 6; scan repeat, 3; peak selection mode to trigger MS/MS, intensity-based detection; deisotope peak detection, yes; ionization mode, ESI; and correction by lock mass function, yes.

Method 8: SCIEX TripleTOF 6600 SWATH for NIST SRM 1950 human plasma

Water, isopropanol, and acetonitrile were purchased from Fisher Optima. Methanol was purchased from J.T. Baker. Ammonium formate, ammonium acetate, formic acid, and methyl *tert*-butyl ether (MTBE) were purchased from Sigma–Aldrich. Odd chain and deuterated lipids used as internal standards were purchased from Avanti Polar Lipids, CDN Isotopes, Cayman Chemical, and Sigma–Aldrich.

The LC system consisted of an Agilent 1290 system (Agilent Technologies Inc.) with a pump (G4220A), a column oven (G1316C), and an autosampler (G4226A). Lipids were separated on an Acquity UPLC CSH C18 column (100 × 2.1 mm; 1.7 µm) coupled to an Acquity UPLC CSH C18 VanGuard precolumn (5 × 2.1 mm; 1.7 µm) (Waters, Milford, MA, USA). The column was maintained at 65°C at a flow-rate of 0.6 mL/min. For LC–ESI(+)-MS analysis the mobile phases consisted of (A) 60:40 (v/v) acetonitrile:water with ammonium formate (10 mM) and formic acid (0.1%) and (B) 90:10:0.1 (v/v/v) isopropanol:acetonitrile:water with ammonium formate (10 mM) and formic acid (0.1%). For LC–ESI(–)-MS analysis the organic solvents for mobile phases were the same with the exception of using ammonium acetate (10 mM) as mobile-phase modifier. A sample volume of 3 µL was used for the injection in both ESI(+) and ESI(–). The separation was conducted under the following gradient in ESI(+): 0 min 15% (B); 0−2 min 30% (B); 2−2.5 min 48% (B); 2.5−11 min 82% (B); 11−11.5 min 99% (B); 11.5−12 min 99% (B); 12−12.1 min 15% (B); and 12.1−15 min 15% (B). The separation was conducted under the following gradient in ESI(–): 0 min 15% (B); 0−2 min 30% (B); 2−2.5 min 48% (B); 2.5−9.5 min 76%; 9.5−9.6 min 99% (B); 9.6−10.5 min 99% (B); 10.5−10.6 min 15% (B); 10.6−13.5 min 15% (B). Sample temperature was maintained at 4°C.

Mass spectrometric detection of lipids was performed on a quadrupole/time-of-flight mass spectrometer TripleTOF 6600 (SCIEX, Framingham, MA, USA). All analyses were performed at the high resolution mode in MS1 (~35,000 full width at half maximum (FWHM)) and at the high sensitivity mode (~15,000 FWHM) in MS2. For ESI(+), the SWATH parameters were MS1 accumulation time, 100 ms; MS1 mass range, *m*/*z* 100–1700; MS2 accumulation time, 10 ms; collision energy, 45 eV; collision energy spread, 15 eV; cycle time, 550 ms; Q1 window, 20 Da; SWATH mass range, *m*/*z* 300–1100; number of SWATH experiments, 40; MS2 mass range: *m*/*z* 80–1100. Other parameters were curtain gas, 35; ion source gas 1, 60; ion source gas 2, 60; temperature, 350°C; ion spray voltage floating, 4.5 kV; declustering

potential, 80 V. For ESI(–), the SWATH parameters were MS1 accumulation time, 100 ms; MS1 mass range, *m*/*z* 100–1700; MS2 accumulation time, 10 ms; collision energy, −50 eV; collision energy spread, 10 eV; cycle time, 550 ms; Q1 window, 15 Da; SWATH mass range, *m*/*z* 400–1000; number of SWATH experiments, 40; MS2 mass range: *m*/*z* 80–1000. Other parameters were curtain gas, 35; ion source gas 1, 60; ion source gas 2, 60; temperature, 350°C; ion spray voltage floating, −4.5 kV; declustering potential, −80 V. The mass calibration was automatically performed using an APCI positive/negative calibration solution via a calibration delivery system (CDS).

Method 9: Thermo Q Exactive Plus DDA for NIST SRM 1950 human plasma

Water was purchased from VWR International, isopropanol from Merck, and acetonitrile from Honeywell. MTBE, ammonium formate, ammonium acetate, formic acid, and acetic acid were purchased from Sigma–Aldrich. Odd chain and deuterated lipids used as internal standards were purchased from Avanti Polar Lipids, Chromsystems, Cayman Chemical, and Sigma–Aldrich.

The LC system consisted of a Vanquish UHPLC system (Thermo Fisher Scientific, Bremen, Germany) with a pump, a column oven and an autosampler. Lipids were separated on an Acquity UPLC BEH C18 column (50 × 2.1 mm; 1.7 µm) coupled to an Acquity UPLC BEH C18 VanGuard precolumn (5 × 2.1 mm; 1.7 µm) (Waters, Milford, MA, USA). The column was maintained at 65°C at a flow-rate of 0.6 mL/min. For LC–ESI(+)-MS analysis the mobile phases consisted of (A) 60:40 (v/v) acetonitrile:water with ammonium formate (10 mM) and formic acid (0.1%) and (B) 90:10:0.1 (v/v/v) isopropanol:acetonitrile:water with ammonium formate (10 mM) and formic acid (0.1%). For LC–ESI(–)-MS analysis the organic solvents for mobile phases were the same with the exception of using ammonium acetate (10 mM) and acetic acid (0.1%) as mobile-phase modifiers. A sample volume of 2 µL and 3 µL was used for the injection in ESI(+) and ESI(–), respectively. Separation was conducted under

the following gradient for LC–ESI(+): 0 min 15% (B); 0–1 min 30% (B); 1–1.3 min from 30% to 48% (B); 1.3–5.5 min from 48% to 82% (B); 5.5–5.8 min from 82% to 99% (B); 5.8–6 min 99% (B); 6–6.1 min from 99% to 15% (B); 6.1–7.5 min 15% (B). For LC–ESI(–), the following gradient was used: 0 min 15% (B); 0–1 min 30% (B); 1–1.3 min from 30% to 48% (B); 1.3–4.8 min from 48% to 76% (B); 4.8–4.9 min from 76% to 99% (B); 4.9–5.3 min 99% (B); 5.3–5.4 min from 99% to 15% (B); 5.4–6.8 min 15% (B). Sample temperature was maintained at 4°C.

Mass spectrometric detection of lipids was performed on a quadrupole/orbital ion trap mass spectrometer Q Exactive Plus with a HESI-II ion source (Thermo Fisher Scientific, Bremen, Germany). Simultaneous MS1 and MS/MS (data-dependent MS/MS) acquisition was used. The parameters were as follows: sheath gas pressure, 60; aux gas flow, 25; sweep gas flow, 2; spray voltage, 3.6 kV and −3.0 kV for ESI(+) and ESI(–), respectively; capillary temperature, 300°C; aux gas heater temperature, 370°C; MS1 mass range, *m*/*z* 200–1700; MS1 resolving power, 35,000 FWHM (*m*/*z* 200); number of data-dependent scans per cycle: 3; MS/MS resolving power, 17,500 FWHM (*m*/*z* 200); MS1 ion time: 100 ms; MS2 ion time: 50 ms; normalized collision energy, 20% for ESI(+) and 10, 20, 30% for ESI(–). The instrument was tuned using a Thermo positive and negative ion mode calibration solutions.

Method 10: Agilent 6546 LC-QTOF/MS DDA for NIST SRM 1950 human plasma

Ultrapure water was produced with a Milli-Q Integral system equipped with a LC-Pak Polisher and a 0.22 μm point-of-use membrane filter cartridge (EMD Millipore, Billerica, MA, USA). Ammonium fluoride and LC/MS grade ammonium acetate were purchased from Millipore Sigma (St. Louis, MO, USA). Isopropanol of LC/MS grade "LiChrosolv" was purchased from Sigma Aldrich. HPLC-grade acetonitrile and methanol were purchased from Honeywell (Morristown, NJ, USA). SPLASH lipidomics I used as

internal standards were purchased from Avanti Polar Lipids. Chloroform was purchased from Honeywell (Charlotte, North Carolina).

The LC system consisted of an Agilent 1290 Infinity II (Agilent Technologies, Santa Clara, CA, USA) with a pump, a column oven and an autosampler. Lipids were separated on an Agilent InfinityLab Poroshell 120 EC-C18 column (100 × 3.0 mm; 2.7 μm) coupled to an Agilent InfinityLab Poroshell 120 EC-C18 column precolumn (5 × 3.0 mm; 2.7 μm). The column was maintained at 50°C at a flow-rate of 0.6 mL/min. The mobile phases consisted of (A) 9:1 (v/v) water:methanol with ammonium acetate (10 mM) and ammonium fluoride (0.2 mM) and (B) 2:3:5 (v/v/v) acetonitrile:methanol/isopropanol with ammonium formate (10 mM) and ammonium fluoride (0.2 mM). A sample volume of 5 μL was used for tinjections in ESI(+) and ESI(–). Separation was conducted under the following gradient: 0 min 70% (B); 1 min 70% (B); 3.5 min 86% (B); 10.0 min 86% (B); 11.0 min 100% (B); 17.0 min 100% (B); 17.1 min 70% (B); 19.0 min 70% (B). Sample temperature was maintained at 4°C.

Mass spectrometric detection of lipids was performed on a quadrupole/time-of-flight mass spectrometer 6546 Q-TOF (Agilent Technologies, Santa Clara, CA, USA). Simultaneous MS1 and MS/MS (data-dependent MS/MS) acquisition was used. The parameters were as follows: gas temperature, 200°C; gas flow, 10 L/min; nebulizer (psig), 50; sheath gas temperature, 300°C; sheath gas flow, 12 L/min; VCap, 3.5 kV and −3.0 kV for ESI(+) and ESI(–), respectively; nozzle voltage, 0 V; fragmentor, 150 V; skimmer, 65 V; octupole RF Vpp, 750 V; MS1 and MS2 mass range, *m/z* 40–1700; min MS and MS/MS acquisition rate: 3 spectra/s; isolation width, narrow (~1.3 *m/z*); max precursors per cycle, 3; precursor abundance-based scan speed, target 25,000 counts/spectrum; use MS/MS accumulation time limit, yes; reject precursors that cannot reach target TIC, no; threshold for MS/MS, 5,000 counts and 0.001%; active exclusion enabled, one repeat, then exclude for 0.05 minutes; purity, stringency 70%, cut off 0%; isotope model, common organic molecules; sort precursors, 1,2,unknown; static exclusion ranges,

m/z 40 to 151 for ESI(+) and *m/z* 40 to 210 for ESI(–); collision energy, 20 eV for ESI(+) and 25 eV for ESI(–). The instrument was tuned using a reference mass *m/z* 121.050873, *m/z* 1221.990637 (+) and *m/z* 119.03632, *m/z* 980.016375 (–).

Biological resources

NIST SRM 1950 human plasma

As the benchmark to prone the scalability of MS-DIAL 4.0, NIST SRM 1950 human plasma sample was analyzed by eight platforms (Method 1, 2, 5, 6, 7, 8, 9, 10), and the experimental protocols for each platform were described as follows.

For method 1, 2, 5, and 6, an aliquot of 20 μL of NIST SRM 1950 human plasma sample (National Institute of Standards and Technology) was added to 100 μL of ice cold chloroform and vortexed for 10 s. After 1-h incubation on ice, 200 μL of ice cold MeOH containing 5 μL of EquiSPLASH, 10 μM palmitic acid-d_3, and 10 μM stearic acid-d_3 was added and vortexed for 10 s. After 2-h incubation on ice, the solvent tube was centrifuged at 2000×*g* for 10 min at 4°C. 200 μL of supernatant was transferred to LC-MS vial. For method 7, after the same procedure as described above is performed, the supernatant was dried with a vacuum dryer and resuspended in 200 μL of ethanol. The solvent was transferred to LC-MS vial.

For method 8, an aliquot of 20 μL of NIST SRM 1950 human plasma sample (National Institute of Standards and Technology) was added to 225 μL of ice cold MeOH and vortexed for 10 s. Then, 750 μL of ice cold MTBE was added and vortexed for 10 s. After shaking for 6 min at 4°C in the orbital mixer, 188 μL LC-MS-grade water was added and vortexed for 20 s. After centrifugation for 2 min at 14,000 rcf, 350 μL of the supernatant was transferred to a new 1.5 mL Eppendorf tube and evaporated to dryness in the Labconco Centrivap cold trap concentrator. The dried sample was resuspended in 110 μL MeOH:toluene 9:1 (v/v) containing CUDA (12-[[(cyclohexylamino)carbonyl]amino]-dodecanoic acid)

internal standard (50 ng/mL). After vortexing for 20 s the samples were centrifuged for 2 min at 14,000 rcf and 100 µL of the supernatant was transferred to a glass amber vial with micro-insert.

For method 9, an aliquot of 25 µL of NIST SRM 1950 human plasma sample was added to a mixture of 165 µL of ice cold MeOH and 600 µL of ice cold MTBE. After shaking for 30 s in a cold block, 165 µL of 10% MeOH/90% water (v/v) mixture was added followed by shaking for 30 s. After centrifugation for 5 min at 16,000 rcf, 100 µL of the supernatant was transferred to a new 1.5 mL Eppendorf tube and evaporated to dryness in the Labconco Centrivap cold trap concentrator. The dried sample was resuspended in 100 µL MeOH containing CUDA internal standard (200 ng/mL). After shaking for 30 s the samples were centrifuged for 5 min at 16,000 rcf and 90 µL of the supernatant was transferred to a glass amber vial with micro-insert.

For method 10, 50 µL of NIST SRM 1950 human plasma sample was added to 50 µL SPLASH LIPIDOMIX I and 400 µL of ice cold MeOH. After vortexed briefly, then sonicated for five minutes, 800 µL of chloroform was added followed by shaking for 1 min. 240 µL of water was added for phase partitioning followed by shaking for 1 min. After centrifugation for 4 min at 16,000 g, the lower layer was carefully removed with a gas-tight glass syringe, and transferred to a 2 mL Agilent A-Line amber glass vial. To re-extract the remaining interphase and upper phase layers, 900 µL chloroform/methanol/water (86:14:1, v/v/v) was added, and the mixture was vortexed for one minute and centrifuged again. The combined lower layers from ten 50 µL extractions (ESI-) were combined, and the lower layers from a single 50 µL extraction (ESI+) were combined and dried by a vacuum concentrator. The dried samples were resuspended in 100 µL of a MeOH/chloroform mixture (9:1, v/v). After shaking for 1 min, the samples were centrifuged for 4 min at 16,000 g and the supernatants were transferred to glass amber vials with micro-inserts.

Mouse tissues

The adrenal gland, brain, brown adipose tissue, eye, feces, heart, kidney, large intestine, liver, lung, pancreas, skeletal muscle, skin (ear), small intestine, spleen, testis, and white adipose tissues of 8–10 weeks male mice (C57BL/6 J background, CLEA Japan, Tokyo, Japan) were harvested according to the ethical protocol approved by the RIKEN Center for Integrative Medical Sciences (2019-015(2)). The detail of diet and genetics background was described in **Supplementary Data 1**. Tissues were frozen immediately after dissection and stored at −80°C until lipid extraction. The lipid extraction was performed according to the previously reported method[20,23] where the mixed solvent containing methanol, chloroform, and water (MeOH:$CHCl_3$:H_2O, 1:2:0.2, v/v/v) was utilized. The detail of solvent volumes and internal standards used in this study was described in **Supplementary Table 1 and 2**. The tissues were homogenized by a multi-beads shocker (YASUI KIKAI, Japan) with a metal cone (YASUI KIKAI, Japan) at 1500×*g* for 15 s × 2, and MeOH was added to the homogenate according to the tissue weight. After the solvent was homogenized again by the same condition, the appropriate amount of MeOH (<100 μL) solving 10 mg tissue weight was transferred to a 2-mL glass tube. After the solvent was messed up to 175 μL by MeOH, 25 μL of MeOH containing internal standards was added to the solvent, and vortexed for 10 s. After the solvent was incubated for 2 hours on ice, 100 μL of chloroform was added, and vortexed for 10 s. After the solvent was incubated for 1 hour on ice, 20 μL of Milli-Q water was added, and vortexed for 10 s. After 10 min incubation on ice, the solvent was centrifugated at 2000×*g* for 10 min at 4°C, and the supernatant was transferred to the LC-MS vial (Agilent Technologies). The biological samples were analyzed by Method 1, 5, or 6.

Cultured cells

3T3-L1 cell line was seeded by 5×10^4 cells/well, cultured in 1 mL D-MEM (high glucose) with L-glutamine and phenol red (Wako, Japan) and incubated in 5% CO_2 at 37°C in 12-well cell culture multiwell plates (Greiner bio-one). After 2 days where cells were reached to a confluency of ~70%, the medium was removed and cells were cultured in 1 mL MDI composing of 0.5 mM IBMX (Sigma–Aldrich), 1 μM dexamethasone (Sigma–Aldrich), and 10 μg/mL insulin (Sigma–Aldrich). After 2 days, the MDI induction medium was removed and replaced with 1 mL insulin medium. After 2 days, the insulin medium was removed and replaced with fresh D-MEM. After 4 days where the medium was changed every 2 days, the medium was aspirated, and cells were washed on the plates with PBS buffer. The solution was transferred to a new glass tube, and then dried with a vacuum dryer.

C2C12 cell line was seeded by 1×10^5 cells/well, cultured in 1 mL D-MEM (high glucose) with L-glutamine and phenol red (Wako, Japan) containing 10% fetal bovine serum (FBS) and Pen Strep glutamine (PSG), and incubated in 5% CO_2 at 37°C in 24-well cell culture multiwell plates (Greiner bio-one). After over-night cultivation, the medium was aspirated, and cells were washed on the plates with PBS. After the PBS buffer was aspirated, 600 μL of MeOH was added and the cells were detached by cell scraper. The solution was transferred to a new glass tube, and then dried with a vacuum dryer.

The HeLa and HEK293 cells were cultivated as described previously[23]. HEK293- and HeLa cell lines were cultured in D-MEM (high-glucose) with L-glutamine (Wako) containing 10% fetal bovine serum (FBS) and Pen Strep glutamine (PSG), and incubated in 5% CO_2 at 37°C in six-well cell culture multiwell plates (Greiner bio-one). After 1 hour cultivation, the medium was aspirated, and cells were washed on the plates with 10 mM Tris–HCl (pH 8.0) buffered saline.

The lipid extraction was performed by the same mixed solvent protocol (MeOH:$CHCl_3$:H_2O, 1:2:0.2, v/v/v) as described in human plasma (for method 1 and 2) section. First, chloroform was added to dried cells in a tube, followed by 30-s sonication. After 60-min incubation at room temperature, methanol

was added and vortexed for 10 s. After 120-min incubation, Milli-Q water was added, vortexed for 10 s, and left the tube to stand for 10 min. The cells were then centrifuged at 2000×*g* for 10 min at 20°C. Supernatant was transferred to LC/MS vials to determine the phosphorous contents of the lipid fraction. The phosphorus content of the extracted lipids was quantified by the method of Bartlett[43], and then the extracted lipids were gently dried with N_2 and reconstituted with the mixed solvent of chloroform and methanol (1:2, v/v) to 0.5 mM, 0.8 mM, 1.0 mM, and 1.5 mM phosphorus for C2C12, HEK293, HeLa, and 3T3-L1, respectively, and transferred to the LC-MS vial. The biological samples were analyzed by method 2.

Plant materials

The heat-stressed/non-stressed Arabidopsis leaves were prepared as the benchmark for plant lipidomics using liquid chromatography ion mobility-tandem mass spectrometry (LC-IM-MS/MS). In addition, the lipid extracts from Arabidopsis (*Arabidopsis thaliana*), rice (*Oryza sativa*), and eggplant (*Solanum melongena*) were analyzed as the benchmark in using a conventional LC-MS/MS (DDA) method.

For method 3 and 4, plant growth condition was described previously[44]. *Arabidopsis thaliana* ecotype Columbia (Col-0) was used. Arabidopsis seeds were surface-sterilised and sown on an agar-solidified Murashige and Skoog medium containing 0.5% (w/v) sucrose. Plants were grown at 22°C under a 16-h-light/8-h-dark cycle (40 to 75 μmol photons s^{-1} m^{-2} of fluorescent lamp). Seventeen-day-old Col-0 plants at about 3 h after the onset of the light phase were subjected to heat stress at 38°C for one day (biological replicate $n = 3$). Plants grown at 22°C were examined as the normal growth condition. Whole upper-ground parts from two different plants were harvested and pooled as a biological replicate. The plant material was immediately weighed in a 2.0-mL microcentrifuge tube (Sarstedt), frozen in liquid nitrogen and stored at −80°C until use.

The method for lipid extraction was described previously[45]. Under cryogenic conditions with liquid nitrogen, the plant material in the 2.0-mL microcentrifuge tube was milled by shaking at 900 rpm for 2 min on the Shake Master Neo (BMS, Tokyo, Japan) using a zirconia bead. From the frozen powdered plant material, total lipids were extracted by adding a 20-fold volume of extraction solvent (20 μL/mg F.W. plant sample) (chloroform/methanol/water, 50/100/31.45, v/v/v) with 1 μM 1,2-didecanoyl-*sn*-glycero-3-phosphocholine, Sigma-Aldrich) as the internal standard (20 pmol mg^{-1} F.W. plant sample). After stirring on a vortex mixer vigorously, the homogenate was incubated for 5 min at room temperature and centrifuged at 10,000×*g* for 10 min at room temperature. Supernatant (200 μL) was transferred to a new 1.5-mL microcentrifuge tube and mixed with chloroform (52.6 μL) and water (52.6 μL). After stirring on a vortex mixer vigorously, the mixture in the 1.5-mL microcentrifuge tube was incubated on ice for 10 min in darkness and centrifuged at 1,000×*g* for 10 min. The lower organic layer (85 μL) was transferred to a new 1.5-mL microcentrifuge tube and dried by the centrifugal concentrator (ThermoSavant SPD2010, Thermo Fisher Scientific) at room temperature. The dried lipid extract was dissolved in 160 μL of ethanol, centrifuged at 14,000×*g* for 10 min and transferred to a vial with a glass insert for LC-MS analysis.

For method 7, Arabidopsis (*Arabidopsis thaliana* ecotype Columbia (Col-0)), rice (*Oryza sativa* cv. Nipponbare), and eggplant (*Solanum melongena*) were used in this study. Arabidopsis and eggplant were grown on soil (PROMIX BX (Premier Horticulture Inc., Quakertown, PA): vermiculite = 2:1) supplemented with fertilizer in a greenhouse at 22°C under fluorescent light (16 h light/8 h dark cycle, 55 μmol photons s^{-1} m^{-2}) for 7 weeks and 37 days, respectively. Rice was grown on wet commercial soil (Bonsol II (Sumitomo Chemical, Tokyo, Japan)) in a greenhouse with sunlight under a 16-h fluorescent light (28°C)/8-h dark (20°C) cycle[46]. Plants were kept under constant subirrigation conditions with tap water and fertilizer for 5 weeks. The entire aboveground (aerial) parts were harvested, immediately frozen in liquid nitrogen and lyophilized by the freeze dryer FDU-2200 (EYELA, Tokyo, Japan).

The method for lipid extraction was described previously[47]. The freeze-dried plant material was milled by a blender (IFM-800DG, Iwatani, Tokyo, Japan), filtered with a screen (0.5 mm) and transferred into a 2.0-mL microcentrifuge tube containing a zirconia bead. Lipids were extracted from the freeze-dried powdered plant material with a 160-fold volume of extraction solvent (160 μL mg^{-1} D.W. plant sample) (methyl *tert*-butyl ether/methanol = 3/1, (v/v) with 1 μM 1,2-didecanoyl-*sn*-glycero-3-phosphocholine, Sigma-Aldrich) as the internal standard (160 pmol mg^{-1} D.W. plant sample). After vigorous stirring on a vortex mixer, a 50-fold volume of water (50 μL mg^{-1} D.W. plant sample) was added to the homogenate. After vigorous stirring on a vortex mixer and dark incubation for 15 min on ice, the homogenate was centrifuged at 3,000×*g* for 10 min. The upper layer (160 μL) was transferred to a new 1.5-mL microcentrifuge tube. The organic phase was dried by the centrifugal concentrator (ThermoSavant SPD2010, Thermo Fisher Scientific) at room temperature. The dried lipid extract was dissolved in 200 μL of ethanol, centrifuged at 14,000×*g* for 10 min and transferred to a vial with a glass insert for LC-MS analysis.

Published data resources

At RIKEN DropMet website (http://prime.psc.riken.jp), the ID-DM0022[21] for nine algal lipidomics data using SCIEX TripleTOF 5600 DDA and the ID-DM0030[20] for 11 mouse tissues data using SCIEX TripleTOF 5600 DD were downloaded and reanalyzed by MS-DIAL 4.0.

Reference (Supplementary Note 1)

43. Bartlett G., R. *J. Biol. Chem.* **234**, 466–468 (1959).

44. Higashi, Y. *et al. Plant Cell* **30**, 1887–1905 (2018).

45. Okazaki, Y., Kamide, Y., Hirai, M. Y. & Saito, K. *Metabolomics* **9**, 121–131 (2013).

46. Matsuda, F. *et al. Plant J.* **81**, 13–23 (2015).

47. Okazaki Y., Nishizawa T., Takano K., Ohnishi M., Mimura T., and Saito K. *Physiol Plant* **155**, 33–42 (2015).

Supplementary Note 2 │ Details of tandem mass spectrometry (MS/MS) characterization for 117 lipid subclasses (also see Supplementary Fig. 1)

We describe the details of mass fragmentation for 117 lipid subclasses. Note that the peak quantification of lipids to create our lipidomics database was performed according to the representative adduct type in each lipid subclass. For example, the ceramide containing sphingosine and nonhydrolyzed acyl chain, termed as Cer-NS, was quantified by $[M+CH_3COO]^-$ in negative ion mode although the molecule can also be characterized as $[M+H]^+$ and $[M-H]^-$ in MS-DIAL 4. The adduct type for lipid quantification was determined by the ion sensitivity and the practical annotation handiness. Moreover, the description for MS/MS spectrum annotation for the acetate adduct form could be replaced by the formate adduct form. The only difference of mass spectra between acetate and formate adduct forms is the *m/z* value of the precursor ion derived from the CH_2 (14.016 Da) difference, whereas the MS/MS pattern of product ions when using ammonium acetate as the LC solvent is almost equivalent as that obtained using ammonium formate according to our experience. The acyl chain moiety is characterized by the carbon and double bond numbers, such as 18:2 indicating 18 carbon and 2 double bonds in the acyl chain. The number of oxygen atoms involved with acyl chain incorporation; e.g., in oxidized phospholipids and ceramides, is separated by a semi-colon: e.g., Cer 18:1;O2/18:0;O, which is usually described in mammalian studies as Cer d18:1/18:0h, incorporating sphingosine and hydroxy fatty acid in the acyl chain moiety. When the hydroxy position can be determined from the MS/MS information, the description becomes Cer 18:1;(1OH, 3OH)/18:0;(2OH) which is known as Cer-AS in mammalian ceramides[18]. The ether- and vinyl ether linkages are described by O-18:0 and P-18:0, respectively. The *N*-acyl linkage is described by N-18:0 except for ceramide species. Underlining "_" is used to describe acyl chain compositions if the *sn1*, *sn2*, *sn3*, and *sn4* positional isomers are uncharacterized whereas the virgule (/) character is used if the acyl chain position is determined in a specific position such as *N*-acyl chain, ether chain, or acyl sugar.

The annotation is mostly performed according to the fragment ion of the alkyl ketone (termed as "Acyl ion"), dehydromonoacylglycerol (termed as "DMAG ion"), dehydrodiacylglycerol (termed as "DDAG ion"), or the neutral loss of alkyl ketone (termed as "Acyl loss") in positive ion mode and by the fragment ion of fatty acid (termed as "FA ion") in negative ion mode, respectively, in addition to lipid subclass specific diagnostic ions. The ontology, nomenclature for species level and molecular species level, and confirmation level are exemplified as {ontology, species level, molecular species level (if needed), confirmation level}.

Annotations in LipidMAPS Fatty Acyls [FA]. Acyl carnitine (CAR, CAR 18:1, level 1) was confirmed as the $[M]^+$ form by the unique product ion of *m/z* 85.028 ($C_4H_5O_2^+$) in positive ion mode. *N*-acyl ethanolamine (NAE, NAE 20:4, level 1) and fatty acid (FA, FA 18:1, level 1) were only confirmed by the consistency with the experimental or predicted retention times and precursor *m/z* values in positive and negative ion mode, respectively. The fatty acid ester of hydroxyl fatty acid (FAHFA, FAHFA 34:1, FAHFA 16:0/18:1, level 1) was confirmed as the $[M-H]^-$ form by the product ion and the neutral loss of esterified fatty acid in negative ion mode. *N*-acyl amides including *N*-acyl glycine[17,48] (NAGly, NAGly 31:0, NAGly 15:0/16:0, level 2), *N*-acyl glycyl serine[17,48] (NAGlySer, NAGlySer 31:0, NAGlySer 15:0/16:0, level 2), and *N*-acyl ornithine[17,48] (NAOrn, NAOrn 31:0, NAOrn 15:0/16:0, level 2) were mainly assigned and quantified as the $[M+H]^+$ form, and were double-checked in negative ion mode data where the metabolites were observed as $[M+CH_3COO]^-$ or $[M-H]^-$. The *m/z* 76.039, 106.05, 145.062, and 115.087 in positive ion mode constituted the characteristic ions for glycine, serine, glycyl serine, and ornithine moieties, respectively. The fatty acid ester form was characterized in this study, and the acyl chain moiety of esterified fatty acid was characterized by the acyl plus H_2O neutral losses in both positive and negative ion mode data.

Annotations in LipidMAPS Glycerolipids [GL]. For monoacylglycerolipids, monoacylglycerol (MG, MG 18:0, level 1) was assigned as the $[M+NH_4]^+$ form, and the neutral loss (35 Da) of NH_3 and H_2O from the precursor *m/z* was used for the lipid class confirmation. The lysodiacylglyceryl-3-O-carboxyhydroxymethylcholine[49] (LDGCC, LDGCC 16:0, level 2) was characterized as the $[M+H]^+$ form using the product ions of *m/z* 104.107 ($C_5H_{14}NO^+$) and 132.102 ($C_6H_{14}NO_2^+$) associated with the polar head moiety. The lysodiacylglyceryltrimethylhomoserine (LDGTS, LDGTS 18:1, level 2) and lysodiacylglyceryl hydroxymethyl-*N*,*N*,*N*-trimethyl-β-alanine (LDGTA, LDGTA 18:1, level 2) lipid subclasses[21] could not be distinguished at least in our low-energy collision induced dissociation (CID) condition, and the annotation was determined as LDGTS/A through the confirmation of *m/z* 144.102 ($C_7H_{14}NO_2^+$) and 236.149 ($C_{10}H_{22}NO_5^+$) values.

For diacylglycerolipids, the diacylglyceryl glucuronide (DGGA, DGGA 34:2, DGGA 16:0_18:2, level 1) was basically characterized and quantified as $[M-H]^-$ in negative ion mode because of higher sensitivity than that in positive ion mode whereas the DGGA lipid subclass could be characterized in positive ion mode by the unique neutral loss of 211.07 Da ($C_6H_{10}O_7$ and NH_3). According to our observation, the sensitivity of sulfoquinovosyl diacylglycerol (SQDG, SQDG 34:1, SQDG 16:0_18:1, level 1) is often higher in negative ion mode than that of positive ion mode. However, this depends on the injection volume and the matrix effect in biological samples. Moreover, the characterization for both lipid class and acyl chain moieties for SQDG is easier in positive ion mode than in negative ion mode because of the low sensitivities of fragment ions in negative ion mode. Therefore, the representative adduct type for SQDG lipid quantification was determined in each study independently. The neutral loss of $C_6H_{10}O_7S$ (sulfoquinovosyl moiety) plus NH_3 (adduct ion moiety) and the product ion of *m/z* 225.007 ($C_6H_9O_7S^-$) were used to characterize the SQDG lipid subclass in positive and negative ion mode, respectively. Both

mono-galactosyl/glucosyl diacylglycerol (MGDG, MGDG 34:1, MGDG 16:0_18:1, level 1) and di-galactosyl/glucosyl diacylglycerol (DGDG, DGDG 34:1, DGDG 16:0_18:1, level 1) lipid subclasses were characterized and quantified as $[M+CH_3COO]^-$ and the product ions of *m/z* 253.093 (monohexosyl moiety, $C_9H_{17}O_8^-$) and *m/z* 397.135 (dihexosyl moiety, $C_{15}H_{25}O_{12}^-$) were used to characterize the MGDG and DGDG lipid subclasses, respectively. Note that the stereoisomer of glucosyl and galactosyl moieties in MGDG and DGDG is not distinguished in our method. As the sensitivity of the MGDG-specific product ion, i.e. *m/z* 253.093, is often very low in negative ion mode, the classification of MGDG lipid in negative ion mode was performed only by checking the FA ions from two acyl chain moieties whereas the lipid class could be double-checked in positive ion mode by the neutral loss of $C_6H_{12}O_6$ (monogalactocyl moiety) plus NH_3 (adduct moiety). The DGTS[22] (DGTS 34:1, DGTS 16:0_18:1, level 2) and DGCC[49] (DGCC 34:1, DGCC 16:0_18:1, level 2) lipid classes could be characterized by the same characteristic ions as described in the lyso-type of LDGTS and LDGCC. The acyl chains were elucidated according to the acyl losses.

For alkylacylglycerolipids, our platform distinguished the ether type molecule from the ester type one of the same polar head lipid class by the accurate mass and the unique fragmentation associated to ether chains. The alkylacyl form of MGDG[50] (EtherMGDG, MGDG O-34:1, MGDG O-16:0_18:1, level 2) could be characterized and quantified as $[M+CH_3COO]^-$ in negative ion mode by the confirmation of the FA ion and the acyl loss derived from the ester-linked acyl chain moiety. The EtherMGDG lipid could also be annotated as $[M+NH_4]^+$ by the confirmation of the DMAG ion and neutral loss of $C_6H_{12}O_6$ plus NH_3 as described in the MGDG subclass. Notably, the same polar head lipid class could also be distinguished by the 30–40 mDa mass difference of precursor *m/z* values: for example, the *m/z* value of MGDG O-16:0_16:0 (*m/z* 775.59409) in $[M+CH_3COO]^-$ adduct type exhibits 36 mDa difference from that of MGDG 15:0_16:0 (*m/z* 775.5577) in the same adduct type, demonstrating that high resolution MS

offers a distinct advantage in lipid profiling. The seminolipid[50] (EtherSMGDG, SMGDG O-30:0, SMGDG O-16:0_14:0, level 2) was characterized as $[M-H]^-$ according to the product ions of *m/z* 241.002 ($C_6H_9O_8S^-$) and *m/z* 96.96 (HSO_4^-). The acyl chain moiety was determined by the neutral loss of acyl 14:0 and H_2O. The alkylacyl form of DGDG (EtherDGDG, DGDG O-34:2, DGDG O-18:2_16:0, level 3) could only be characterized as $[M+CH_3COO]^-$ in this study, and the annotation could be performed by the presence of the FA ion and the acyl loss from the ester-linked acyl moiety. Note that the product ion of the digalactosyl moiety observed as *m/z* 397.135 in DGDG could not be detected in the alkylacyl form. The alkylacyl type of DG[52] (EtherDG, DG O-34:1, DG O-16:0_18:1, level 2) was characterized as $[M+NH_4]^+$ by confirming the DMAG ion derived from the ester-linked moiety.

For triacylglycerols, the triacylglycerol lipid class (TG, TG 56:8, TG 16:0_18:2_22:6, level 1) was characterized as $[M+NH_4]^+$ and the acyl chains could be annotated by the neutral losses of acyl and H_2O. The sodium adduct type of TG ($[M+Na]^+$) was also characterized in our platform to reduce the chances of false positive annotations by the other lipid classes. The alkyldiacyl type of TG[51] (EtherTG, TG O-56:7, TG O-16:0_18:1_22:6, level 2) was characterized as $[M+NH_4]^+$: the EtherTG lipids eluted later than normal TG lipids. The acyl chain moieties could be characterized by the neutral losses of acyl and H_2O where the neutral loss of alkyl chain could also be observed. The acylated DGGA (ADGGA, ADGGA 50:2, ADGGA 16:0_16:1_18:2, level 3) was characterized and quantified as $[M+NH_4]^+$ because the unique product ion of the acylated glucuronosyl moiety could be detected in positive ion mode whereas the other acyl chains were characterized by DMAG ions. Therefore, the acyl chain linked to the glucuronosyl moiety was separated by chain length with the brackets from the other acyl chain descriptions; for example, ADGGA (O-16:0)16:1_18:2 indicated that FA 16:0 is incorporated into the glucuronosyl moiety and the others are linked to the glycerol moiety. Alternatively, all chain compositions

were connected by an underline, such as ADGGA 16:0_16:1_18:1 because the acyl chains could only be characterized by FA ions in negative ion mode.

Annotations in LipidMAPS Glycerophospholipids [GP]. Among monoacylglycerophospholipids, lysophosphatidylcholine (LPC, LPC 18:1, level 1) and its alkyl type[51] (EtherLPC, LPC O-18:1, level 2) were quantified as $[M+H]^+$ and could also be characterized as $[M+CH_3COO]^-$. The product ion of *m/z* 184.074 ($C_5H_{15}NO_4P^+$) and the neutral loss of 74.037 ($CH_3COOH+CH_2$) were used as the diagnostic fragment ion for LPC and Ether LPC for positive and negative ion mode, respectively. According to a previous report[52], the acyl chain position of LPC is determined as *sn1* by default if the ion abundance of *m/z* 104.107 ($C_5H_{14}NO^+$) exceeds 10% of the base peak. In addition, the ion from the neutral loss of C_3H_9N (59.073) was used as the characteristic ion for the sodium adduct type of LPC. The lysophosphatidylethanolamine (LPE, LPE 18:1, level 1) and its alkyl type[51] (EtherLPE, LPE O-18:1, level 1) were quantified as $[M+H]^+$ and could also be characterized as $[M-H]^-$. The neutral loss of $C_2H_8NO_4P$ (141.02 Da) and the product ion of *m/z* 196.036 ($C_5H_{11}NO_5P^-$) were utilized as the diagnostic criteria for these lipid classes in positive and negative ion mode, respectively. Because of the low sensitivity of *m/z* 196.036, confirmation of the FA ion must be performed in negative ion mode. In addition, the EtherLPE was annotated as the plasmenyl type (plasmalogen) if the "Ether" fragment ion was observed (annotated as LPE P-18:0): the fragment is defined by cleavage of the ether link, resulting in the product ion of R-C=C–O^- where R denotes the acyl moiety. The lysophosphatidic acid (LPA, LPA 16:0, level 1) was quantified as $[M-H]^-$, and *m/z* 152.996 ($C_3H_6O_5P^-$) was utilized as the diagnostic ion. Note that the FA ion was basically not detected from LPA lipids. The lysophosphatidylglycerol (LPG, LPG 18:1, level 1) and its alkyl type[51] (EtherLPG, LPG O-18:1, level 2) were characterized and quantified as $[M-H]^-$, where *m/z* 152.996 ($C_3H_6O_5P^-$) was utilized for the diagnostic ion. Because of the low sensitivity of *m/z* 152.996, the

FA ion was practically utilized for LPG characterization. When the Ether ion was detected, the Ether LPG was annotated as the plasmenyl type as described in EtherLPE. Both lysophosphatidylserine (LPS, LPS 18:0, level 1) and lysophosphatidylinositol (LPI, LPI 18:1, level 1) were quantified as $[M-H]^-$. The product ions of *m/z* 241.008 ($C_6H_{10}O_8P^-$) and *m/z* 315.049 ($C_9H_{16}O_{10}P^-$) were used for LPI and the neutral loss of $C_3H_5NO_2$ (87.032 Da) were used for LPS annotations, respectively: the FA ion especially for LPI was used for the diagnostic criterion because of the low sensitivity of phosphoinositol moiety-derived ions.

For diacylglycerophospholipids, all lipid classes except for bismonoacylglycerophosphate (BMP, BMP 40:5, BMP 18:1_22:4, level 1) and plasmenyl PE (EtherPE_P, PE P-38:3, PE P-18:0_20:3, level 1) were quantified in negative ion mode because both acyl chains and lipid class specific ions could easily be detected, decreasing the number of false positive annotations. Phosphatidic acid (PA, PA 34:1, PA 16:0_18:1, level 1) was only characterized as $[M-H]^-$ in negative ion mode by the confirmation of FA ions from both acyl chains. The phosphatidylcholine (PC, PC 38:4, PC 18:0_20:4, level 1) lipid exhibited the unique product ion of *m/z* 184.074 ($C_5H_{15}NO_4P^+$) and the neutral loss of 74.037 ($CH_3COOH+CH_2$) for $[M+H]^+$ and $[M+CH_3COO]^-$ forms, respectively, as described in the lyso-type form. The acyl chains could easily be determined based on FA ions in negative ion mode whereas they could also be characterized by acyl losses in positive ion mode although the sensitivity was quite low. The sodium adduct form of PC was characterized by two neutral losses of C_3H_9N (59.073 Da) and $C_5H_{14}NO_4P$ (183.066 Da). The plasmenyl or plasmanyl type of PC (EtherPC, PC O-38:4, PC O-18:0_20:4, level 1) could also be confirmed by the same lipid class specific ions of PC whereas the acyl chain was only determined in negative ion mode according to the confirmation of the FA ion derived from the ester-linked moiety. Note that the plasmanyl and plasmenyl types were not distinguished in our annotation pipeline for EtherPC because of the low sensitivity of plasmenyl-specific product ions. Phosphatidylethanolamine (PE, PE 38:4, PE 18:0_20:4, level 1) was characterized as $[M+H]^+$ and $[M-H]^-$ by the neutral loss of $C_2H_8NO_4P$ (141.02

Da) and the product ion of *m/z* 196.038 ($C_5H_{11}NO_5P^-$) in positive- and negative ion mode, respectively. The product ions of alkyl ketones (termed as "Acyl ion") and FA ions were utilized to characterize the acyl chain moieties in positive and negative ion mode, respectively, although the sensitivity of the acyl ion was very low. The sodium adduct type of PE was annotated according to the neutral losses of C_2H_5N (43.04 Da) and $C_2H_8NO_4$ (110.045 Da). The plasmanyl (EtherPE_O, PE O-34:1, PE O-16:0_18:1, level 1) and plasmenyl (EtherPE_P, PE P-38:3, PE P-18:0_20:3, level 1) types of PE could be characterized in positive ion mode whereas the difference between vinyl ether and normal ether types was not observed in ESI (−)-MS/MS. The plasmalogen type of PE was characterized by the existence of the DMAG ion derived from the neutral loss of the vinyl ether acyl moiety whereas the fragment ion could not be observed in the plasmanyl type of PE in which only the neutral loss of the PE polar head ($C_2H_8NO_4P$, 141.02 Da) and the acyl ion were detected. Alternatively, the plasmenyl/plasmanyl type of PE (EtherPE) could easily be characterized in negative ion mode by the FA ion and acyl loss derived from the ester chain moiety. Phosphatidylglycerol (PG, PG 38:4, PG 18:0_20:4, level 1) was characterized as $[M+NH_4]^+$ and $[M-H]^-$ by the neutral loss of 171.006 Da ($C_3H_9O_6P+NH_3$) and the product ion of *m/z* 152.996 ($C_3H_6O_5P^-$), respectively. Because of the low ion sensitivity of *m/z* 152.996, the PG lipid was annotated as molecular species level if both FA ions of the two acyl chains were observed in ESI (−)-MS/MS. In comparison, the DMAG ions were used as the diagnostic ions in in ESI (+)-MS/MS: the lipid was annotated as molecular species level when both DMAG ions were detected. The alkylacyl type of PG[51] (EtherPG, PG O-34:1, PG O-18:1_16:0, level 2) was only characterized in negative ion mode by the confirmation of FA ion derived from the ester-linked chain moiety. According to our observation, the ether ion where an oxygen atom was rearranged to the ether chain moiety could be observed in the EtherPG lipid and might occur in the plasmalogen type of EtherPG. As we could not find an EtherPG lipid having no double bond in the alkyl chain moiety in this study, the issue will be resolved in future work. The BMP lipid (BMP 40:5, BMP

18:1_22:4, level 1) was only characterized in positive ion mode by the confirmation of DMAG ions from both acyl chains because the MS/MS spectrum could not be distinguished from PG lipid in negative ion mode. Phosphatidylinositol (PI, PI 38:4, PI 18:0_20:4, level 1) could be characterized as $[M+NH_4]^+$, $[M+Na]^+$, and $[M-H]^-$ where the acyl chains could be resolved in negative ion mode. The neutral loss of 277.056 Da ($C_6H_{14}O_9P+NH_3$) and the product ion of *m/z* 283.019 ($C_6H_{13}O_9PNa^+$) were used as the PI-specific ion in $[M+NH_4]^+$ and $[M+Na]^+$, respectively. The product ions of *m/z* 241.008 ($C_6H_{10}O_8P^-$) and *m/z* 315.049 ($C_9H_{16}O_{10}P^-$) served as the PI class specific ions in $[M-H]^-$ and the annotation was exported as acyl-chain resolved when FA ions from both acyl chains were detected. The alkyl type of PI[51] (EtherPI, PI O-36:4, PI O-16:0_20:4, level 2) was annotated by the FA ion from the ester chain moiety with the confirmation of PI-specific ions. Phosphatidylserine (PS, PS 38:4, PS 18:0_20:4, level 1) was characterized as $[M+H]^+$, $[M+Na]^+$, and $[M-H]^-$ by the neutral losses of $C_3H_8NO_6P$ (185.009 Da) and $C_3H_5NO_2$ (87.032 Da) in positive- and negative ion mode, respectively. The acyl losses and FA ions were utilized for the annotation of acyl chains in $[M+H]^+$ and $[M-H]^-$, respectively. The alkyl type of PS[51] (EtherPS, PS O-38:6, PS O-16:0_22:6, level 2) was characterized as $[M-H]^-$ by the confirmation of acyl loss from the ester chain moiety with the PS-specific neutral loss of 87.032 Da. Dilysocardiolipin[53] (DLCL, DLCL 34:2, DLCL 16:0_18:2, level 2) was characterized as $[M-H]^-$, and the fragment ion matched with the LPA moiety was utilized rather than the FA ion for acyl chain annotations. The product ion of *m/z* 152.996 ($C_3H_6O_5P^-$) was used as the diagnostic ion for the DLCL lipid class. Phosphatidylmethanol (PMeOH, PMeOH 34:2, PMeOH 16:0_18:2, level 1) and phosphatidylethanol (PEtOH, PEtOH 38:4, PEtOH 18:0_20:4, level 1) were characterized by the existence of FA ions from both acyl chain moieties because of the low sensitivity of the product ions of *m/z* 110.985 ($CH_4O_4P^-$) and *m/z* 125.001 ($C_2H_6O_4P^-$), which could be utilized as PMeOH and PEtOH-specific fragment ions, respectively.

The oxidized phospholipids were characterized and quantified in negative ion mode. The oxidized PC, PE, PG, PI, and PS (OxPC, OxPE, OxPG, OxPI, and OxPS, level 2[49]) were first confirmed by their lipid class-specific ions of 74.037 Da neutral loss, *m/z* 196.038 product ion, *m/z* 152.996 product ion, *m/z* 241.008/315.049 product ions, and 87.032 Da neutral loss, respectively. With regard to nomenclature, the oxidized form was described using a semi-colon (;) and the additional oxygen count as in PE 18:0_20:4;4O. Because the current program does not target the oxidized lipid having two oxidized acyl chains, the non-oxidized fatty acid ion was secondly utilized as the diagnostic ion. Because the oxidized fatty acid ion could be detected as the native fatty acid form, one H_2O-loss form, or two H_2O-loss form, depending on the oxidation number and structural conformation, the annotation was successful if at least one of these three forms was confirmed in the MS/MS spectrum. The alkyl type of OxPE[49] (EtherOxPE, PE O-38:6;O, PE O-16:0_22:6;O, level 2) was annotated by the product ion and neutral loss of the ester-linked oxidized fatty acid moiety.

The lyso-type of *N*-acyl PE[54] (LNAPE, LNAPE 34:2, LNAPE 16:0/N-18:2, level 2) and *N*-acyl PS[54] (LNAPS, LNAPS 34:0, LNAPS 18:0/N-16:0, level 2) were quantified and characterized in negative ion mode. In contrast to PE, the product ion of *m/z* 196.038 was not observed in LNAPE form; instead, the product ion of *m/z* 152.996 was detected. Moreover, the fragment ion of *N*-acyl chain was not detected at least in our experimental condition whereas the FA ion from the ester-link moiety was used for the acyl chain characterization. In comparison to PS, identically, the neutral loss of 74.037 Da was not observed in LNAPS and the product ion of *m/z* 152.996 was detected instead. The product ion matched with the LPA moiety containing an ester-linked fatty acid could be used to characterize the acyl chain moiety.

For triacylglycerophospholipids, hemibismonoacylglycerophosphate (HBMP, HBMP 52:3, HBMP 18:1/16:1_18:1, level 1) was quantified as ether $[M+NH_4]^+$ or $[M-H]^-$, depending on the biological sample and the injection volume. The acyl chain of the LPG moiety was characterized in positive ion

mode by the dehydrodiacylglycerol ion (termed as "DDAG" ion) containing two acyl chains of the PG substructure. The DMAG ions derived from the PG moiety were used to determine the other acyl chains. Alternatively, the FA ions from the PG moiety were detected in negative ion mode, and the product ion of DMAG plus the phosphate moiety was used to characterize the acyl chain involved in the LPG moiety. Lysocardiolipin[55] (MLCL, MLCL 56:7, MLCL 16:0_16:0_16:0, level 2) was quantified and characterized in negative ion mode, and the product ion of *m/z* 152.996 was utilized as the diagnostic ion of glycerophospholipid. Three FA ions derived from ester-linked moieties were used for acyl chain characterizations.

For cardiolipin (CL, level 1) incorporating four ester-linked acyl chains, the quantification was performed as $[M-H]^-$ because four acyl chains could be characterized by FA ions with the characteristic ion of *m/z* 152.996 in negative ion mode whereas the acyl chains were semi-resolved in positive ion mode: the DDAG ions incorporating two acyl chains were only available from the $[M+NH_4]^+$ form, resulting in the annotation as e.g. CL 34:0_36:2 for CL 16:0_18:0_18:1_18:1 at least in our experimental condition.

Annotations in LipidMAPS Sphingolipids [SP]. The sphingobase (SPB) moiety was described as (carbon number):(double bond);(hydroxy moiety count); for example, SPB 18:1;2O for sphingosine d18:1, indicating that the chain had one nitrogen, two hydroxy moieties, 18 carbons, and 1 double bond. When the hydroxy positions could be determined by the MS/MS spectrum, the sphingobase description became SPB 18:1;(1OH,3OH) for sphingosine d18:1. Moreover, the term of "SPB 18:1;2O ion" was used to describe the characteristic ion for the sphingobase moiety in both positive and negative ion mode. The term "SPB 18:1;2O" ion indicates *m/z* 300.2897 ($C_{18}H_{38}NO_2^+$) and *m/z* 298.2752 ($C_{18}H_{36}NO_2^-$) derived by the hydrogen rearrangement (HR) rule[28] P2 and rule N1 in positive and negative ion mode, respectively. The SPB ion could often be detected in the form of one or two H_2O losses, with the product ion being

described as "SPB 18:0;2O-H_2O" or "SPB 18:0;2O-2H_2O", respectively. For the intact sphingobase molecules, the sphinganine (DHSph, SPB 17:0;2O, level 1) and sphingosine (Sph, SPB 18:1;2O, level 1) were characterized as $[M+H]^+$ by the neutral losses of H_2O, double H_2O, and CH_4O_2 moieties, and the phytosphingosine (PhytoSph, SPB 18:0;3O, level 1) was also characterized as $[M+H]^+$ by the neutral losses of double and triple H_2O and CH_6O_3 moieties.

For sphingolipids incorporating the phosphocholine polar head, the normal sphingomyelin (SM, SM 34:1;2O, SM 18:1;2O/16:0, level 1) was quantified as $[M+CH_3COO]^-$. The SM lipid class could be characterized by the specific product ion of *m/z* 168.043 ($C_4H_{11}NO_4P^+$) and neutral loss of 74.037 Da ($CH_3COOH+CH_2$) in negative ion mode, and the product ion of *m/z* 184.074 ($C_5H_{15}NO_4P^+$) was used in positive ion mode. The acyl chain was annotated by the neutral loss of acyl and methyl moieties and the product ion of "SPB-H_2O" in negative and positive ion mode, respectively. Because of the low sensitivity of acyl chain-related ions, the sphingomyelin was often annotated by the summed form, such as SM 34:1;2O for SM 18:1;2O/16:0. The sodium adduct form of SM was characterized by the neutral losses of C_3H_9N (59.073 Da) and $C_5H_{14}NO_4P$ (183.066 Da). The SM lipid incorporating the phytosphingosine or a hydroxy fatty acid[56] (SM+O, SM 34:1;3O, level 2) was quantified as $[M+CH_3COO]^-$, and it could be characterized by the same characteristic ions of normal SM lipid class as $[M+H]^+$ and $[M+CH_3COO]^-$. Notably, the acyl chain specific ion could not be observed in our experimental data set, and therefore the SM+O lipid class was only reported as the summed description. The acylated SM (ASM, SM 52:2;3O, SM 34:1;2O(FA 18:0), level 3) was quantified as $[M+CH_3COO]^-$, and characterized in both positive and negative ion modes. The acylated position was defined at the hydroxy moiety in the sphingobase because it was the only plausible position for the ester reaction. In addition to the SM characteristic ions, the FA ion and the neutral loss derived from the acylated moiety could be detected in negative ion mode, and the neutral loss of the acylated moiety was also used for the characterization in positive ion mode. Moreover,

the diagnostic ion to characterize the sphingobase and *N*-acyl chain moieties could not be detected in our experimental data set; therefore, the ceramide moiety was reported as the summed description.

The description and characterization of ceramide lipid classes have been reported previously for negative ion mode data[18]. The ceramide lipids were basically quantified as $[M+CH_3COO]^-$ except for di- and tri-hexosyl ceramides because the hydroxy position of *N*-hydroxy fatty acid could be determined in ESI(−)-MS/MS. In addition, the sensitivity was higher in acetate adduct form than that of proton loss form. Moreover, the example lipid structure was used to explain the diagnostic ions for ceramide characterizations because the mass fragmentation was more complex than that of glycerolipids. The ceramide lipid (Cer-NDS[23], Cer 34:0;2O, Cer 18:0;2O/16:0, level 2) incorporating sphinganine (DS) and fatty acid moieties (N) could be characterized as $[M+H]^+$, $[M-H]^-$, and $[M+CH_3COO]^-$. For the acetate adduct form of Cer 18:0;2O/16:0 in ESI(−)-MS/MS, the product ions of *m/z* 280.264 (Acyl 16:0+C_2H_3N), *m/z* 239.238 (SPB 18:0;2O-C_2H_7NO), and *m/z* 237.246 (Acyl 16:0-2H) were used to characterize the acyl chain moieties whereas the lipid class was determined by confirming the product ion of $[M-H]^-$ (*m/z* 538.53) and the neutral losses of CH_4O (32.04 Da) and CH_4O_2 (48.03 Da) from the $[M-H]^-$ peak. Alternatively, the product ions of *m/z* 284.285 (SPB 18:0;2O-H_2O), *m/z* 266.284 (SPB 18:0;2O-$2H_2O$), and *m/z* 254.284 (SPB 18:0;2O-CH_4O_2) were used to characterize the acyl chains in positive ion mode. The ceramide lipid (Cer-NS, Cer 34:1;2O, Cer 18:1;2O/16:0, level 1) incorporating sphingosine (S) and fatty acid (N) moieties was also characterized as $[M+H]^+$, $[M-H]^-$, and $[M+CH_3COO]^-$. The scheme of mass fragmentation was the same as described in Cer-NDS where the *m/z* values were changed by the difference of double bond number in the sphingobase. The ceramide lipid (Cer-AP, Cer 38:0;4O, Cer 18:0;3O/20:0;(2OH), level 1) incorporating phytosphingosine (P) and alpha-hydroxy fatty acid (A) was characterized as $[M+H]^+$, $[M-H]^-$, and $[M+CH_3COO]^-$. For the acetate adduct form of Cer 18:0;3O/20:0;(2OH) in ESI(−)-MS/MS, the unique ion characterizing the hydroxyl position was detected

as *m/z* 281.285 (Acyl 20:0;O-CH_2O, $C_{19}H_{37}O^-$) and the product ions of *m/z* 382.332 (Acyl 20:0;O+C_3H_5NO, $C_{23}H_{44}NO_3^-$) and *m/z* 328.291 (Acyl 20:0;O+O, $C_{20}H_{39}O_3^-$) were used for acyl chain characterizations. The product ions of *m/z* 316.285 (SPB 18:0;3O, $C_{18}H_{38}NO_3^+$), *m/z* 298.274 (SPB 18:0;3O-H_2O, $C_{18}H_{36}NO_2^+$), *m/z* 280.264 (SPB 18:0;3O-2H_2O, $C_{18}H_{34}NO^+$), and *m/z* 262.253 (SPB 18:0;3O-3H_2O, $C_{18}H_{32}N^+$) were the characteristic ions to determine acyl chains in positive ion mode.

The ceramide (Cer-ADS[23], Cer 34:0;3O, Cer 18:0;2O/16:0;(2OH), level 2) incorporating sphinganine (DS) and alpha-hydroxy fatty acid (A) moieties was characterized as $[M-H]^-$ and $[M+CH_3COO]^-$. For the acetate adduct form of Cer 18:0;2O/16:0;(2OH), the product ion of *m/z* 225.222 (Acyl 16:0;O-CH_2O) was used to characterize the hydroxy position and the product ions of *m/z* 282.28 (SPB 18:0;2O-H_2O, $C_{18}H_{36}NO^-$) and *m/z* 253.217 (Acyl 16:0;O-2H, $C_{16}H_{29}O_2^-$) were used to characterize the acyl chain moieties. Furthermore, the product ion of *m/z* 239.238 (SPB 18:0;2O-C_2H_7NO, $C_{16}H_{31}O^-$) was the unique ion characterizing the hydroxy position at γ-C in the sphinganine moiety. The ceramide (Cer-AS, Cer 34:1;3O, Cer 18:1;2O/16:0;(2OH), level 1) incorporating sphingosine (S) and alpha-hydroxy fatty acid (A) was characterized by the product ions derived from the same fragmentation scheme as those of Cer-ADS. The ceramide (Cer-BDS[23], Cer 34:0;3O, Cer 18:0;2O/16:0;(3OH), level 2) incorporating sphinganine (DS) and beta-hydroxy fatty acid (B) was characterized as $[M-H]^-$ and $[M+CH_3COO]^-$. For the acetate adduct form of Cer 18:0;2O/16:0;(3OH), the product ions of *m/z* 342.301 (SPB 18:0;2O+C_2H_2O, $C_{20}H_{40}NO_3^-$) and *m/z* 310.275 (*m/z* 342.301-CH_4O, $C_{19}H_{36}NO_2^-$) were used to characterize the hydroxy position and the sphingosine moiety. Furthermore, the product ion of *m/z* 239.238 (SPB 18:0;2O-C_2H_7NO, $C_{16}H_{31}O^-$) was the unique ion characterizing the γ-hydroxy position in the sphingosine moiety. The ceramide (Cer-BS[23], Cer 40:1;3O, Cer 16:1;2O/24:0;(3OH), level 2) incorporating sphingosine (S) and beta-hydroxy fatty acid (B) was characterized by the product ions derived from the same fragmentation scheme as those of Cer-BDS. In comparison, the hydroxy position

of *N*-acyl chain could not be characterized in ESI(+)-MS/MS, and therefore the character of "H" instead of "A" or "B" was utilized to describe the existence of the hydroxy moiety in the *N*-acyl chain in the MS-DIAL ontology. For the $[M+H]^+$ form of Cer 20:1;2O/24:0;O incorporating SPB 20:1;2O (S) and hydroxy fatty acid 24:0;O (H), the product ions of *m/z* 310.311 (SPB 20:1;2O-H_2O, $C_{20}H_{40}NO^+$), *m/z* 292.3 (SPB 20:1;2O-$2H_2O$, $C_{20}H_{38}N^+$), and *m/z* 280.3 (SPB 20:1;2O-CH_4O_2, $C_{19}H_{38}N^+$) were used to characterize the acyl chain moieties. Moreover, the ceramide (Cer-HDS[23], Cer 38:0;3O, Cer 18:0;2O/20:0;O, level 2) incorporating sphinganine (DS) and hydroxy fatty acid (H) was characterized by the product ions derived from the same fragmentation scheme as those of Cer-HDS. In negative ion mode, the term of "A" and "B" was replaced by "H" when the product ion characterizing the hydroxy position was not observed in ESI(−)-MS/MS. According to our experience and a previous study[57], the case was considered as the ceramide incorporating omega-hydroxy fatty acid (O), which is known as the precursor of acyl ceramide at least in mammalian tissues.

The ceramide (Cer-EOS[23], Cer 70:3;4O, Cer 18:1;2O/32:0;O(FA 18:2), level 2) incorporating sphingosine (S), omega-hydroxy fatty acid (O), and esterified fatty acid (E) linked to the omega hydroxy moiety was characterized as $[M+H]^+$, $[M-H]^-$, and $[M+CH_3COO]^-$. For the acetate adduct form of Cer 18:1;2O/32:0;O(FA 18:2), the product ion of *m/z* 279.233 (FA 18:2) denoted the esterified fatty acid, and the neutral loss of Acyl 18:2 was also used to characterize the esterified acyl chain. The product ion of *m/z* 494.494 (*N*-acyl 32:0;O, $C_{32}H_{64}NO_2^-$) was used to characterize the *N*-acyl chain moiety. Because of the low sensitivity of the product ion involved with the *N*-acyl chain, the annotation was performed by the summed form as Cer d50:1(FA 18:2) if the ion was not detected in ESI(−)-MS/MS: the annotation term of "chain semi-resolved" was used in such case. Alternatively, the product ions of *m/z* 282.279 (SPB 18:1;2O-H_2O, $C_{18}H_{36}NO^+$), *m/z* 264.269 (SPB 18:1;2O-$2H_2O$, $C_{18}H_{34}N^+$), and *m/z* 252.269 (SPB 18:1;2O-CH_4O_2, $C_{17}H_{34}N^+$) were used to characterize the sphingosine moiety in ESI(+)-MS/MS whereas no

fragment ion characterizing the other acyl chains was detected, at least in our experimental condition. Therefore, the annotation was described as the semi-resolved form as Cer 18:1;2O/52:3;2O: Note that the double bond for the ketone moiety was also counted, resulting in the term of 52:3;2O for summing 32:0;O(FA 18:2). The ceramide (Cer-EODS[23], Cer 49:1;4O, Cer 18:0;2O/16:0;O(FA 15:0), level 2) incorporating sphinganine (DS), omega-hydroxy fatty acid (O), and esterified fatty acid (E) was characterized by the same procedure as described in Cer-EOS. The ceramide (Cer-EBDS, Cer 50:1;4O, Cer 18:0;2O/17:0;(3OH)(FA 15:0), level 3) incorporating sphinganine (DS), beta-hydroxy fatty acid (B), and esterified fatty acid linked to the beta-hydroxy position was only characterized as $[M+CH_3COO]^-$ in feces samples. For the acetate adduct form of Cer 18:0;2O/17:0;(3OH)(FA 15:0), the product ion of *m/z* 241.217 (FA 15:0) and the neutral loss of Acyl 15:0;O were used to characterize the esterified fatty acid. Moreover, the product ion of *m/z* 342.3 (SPB 18:0;2O+C_2H_2O, $C_{20}H_{40}NO_3^-$), which is derived from the cleavage of the beta-hydroxy position of *N*-acyl chain as described in Cer-BDS, was used to characterize the sphingobase moiety and the existence of beta-hydroxy fatty acid.

The ceramide (Cer-NP, Cer 34:0;3O, Cer 18:0;3O/16:0, level 1) incorporating phytosphingosine (P) and normal fatty acid (N) was characterized as $[M-H]^-$ and $[M+CH_3COO]^-$. For the acetate adduct form of Cer 18:0;3O/16:0, the product ions of *m/z* 298.275 (SPB 18:0;3O-H2O, $C_{18}H_{36}NO_2^-$), *m/z* 267.232 (SPB 18:0;3O-CH_7NO, $C_{17}H_{31}O_2^-$), and *m/z* 255.232 (SPB 18:0;3O-C_2H_7NO, $C_{16}H_{31}O_2^-$) were used to characterize the acyl chain moieties. Furthermore, the product ion of *m/z* 310.274 (Acyl 16:0;O+C_3H_5NO, $C_{19}H_{36}NO_2^-$) was used as the unique ion characterizing the γ-hydroxy position in the sphingosine moiety.

The monohexosyl form[23] (HexCer) of Cer-NS, Cer-NDS, Cer-AP, Cer-HS, Cer-HDS, and Cer-EOS was characterized by the same product ions as described in the non-hexosyl forms with the confirmation of the hexosyl moiety loss (termed as "Hex" loss, $C_6H_{10}O_5$). Notably, the hydroxy position in the hydroxy fatty acid moiety was not determined because of the low sensitivity of product ions

involved with the hydroxy position in the *N*-acyl chain. In ESI(+)-MS/MS, the product ions derived from the neutral losses of Hex-H_2O and Hex-$2H_2O$ were also observed. The dihexosyl form (Hex2Cer, level 1) of Cer-NS was quantified as $[M+H]^+$ because the acyl chain moieties could only be characterized in positive ion mode. In addition to two sequential hexosyl losses, the product ions involved with SPB-H_2O, SPB-$2H_2O$, and SPB-CH_4O_2 were used to characterize the sphingobase moiety. The Hex2Cer lipid was also characterized as $[M+CH_3COO]^-$, where the sequential hexosyl losses and the product ion of *m/z* 179.056 (Hex ion, $C_6H_{12}O_6^-$) were used to characterize the lipid class: the Hex2Cer lipid in positive ion mode was always annotated as the summed form. For the trihexosyl form (Hex3Cer[56], level 2), the annotation strategy was also the same as described for Hex2Cer.

The ceramide phosphoinositol[58] (PI-Cer, PI-Cer 34:0;3O, PI-Cer 18:0;2O/16:0;O, level 2) incorporating sphingosine and fatty acid moieties was quantified in negative ion mode whereas it could be characterized in both ion modes as $[M+H]^+$ and $[M-H]^-$. In this study, the PI-Cer lipid incorporating sphingosine and hydroxy fatty acid moiety was characterized. For PI-Cer 18:0;2O/16:0;O, the product ions of *m/z* 78.959 (PO_3^-) and *m/z* 241.012 ($C_6H_{10}O_8P^-$) and the neutral loss of the inositol moiety (162.053 Da, $C_6H_{10}O_5$) were used to characterize the lipid class, and the neutral loss of 254.226 Da (Acyl 16:0;O) was used to characterize the acyl chain moiety in ESI(−)-MS/MS. Alternatively, only the lipid class was characterized by the neutral loss of $C_6H_{13}O_9P$ (260.03 Da, phosphoinositol moiety) in ESI(+)-MS/MS. The ceramide phosphoethanolamine[59] (PE-Cer, PE-Cer 36:1;2O, PE-Cer 18:1;2O/18:0, level 2) incorporating sphingosine and fatty acid was characterized only in negative ion mode in this study. For PE-Cer 18:1;2O/18:0, the product ions of *m/z* 78.959 (PO_3^-) and *m/z* 140.012 ($C_2H_7NO_4P^-$) were used for the lipid class characterization, and the Acyl 18:0 loss (266.261 Da) was used for the acyl chain characterization. The ceramide phosphoethanolamine[59] (PE-Cer+O, PE-Cer 35:0;3O, PE-Cer 18:0;2O/17:0;O, level 2) incorporating sphingosine and hydroxy fatty acid was also characterized in

negative ion mode by the same scheme as described in PE-Cer. The ceramide 1-phosphate (CerP, CerP 30:1;2O, CerP 18:1;2O/12:0, level 1) incorporating sphingosine and fatty acid moieties was quantified as $[M+H]^+$ and was characterized in both ion modes. For CerP 18:1;2O/12:0, the product ion of *m/z* 264.269 (SPB 18:1;2O-2H_2O) and the neutral loss of H_3PO_4 (97.977 Da) were used to characterize the acyl chain and lipid class characterizations, respectively. In negative ion mode, the product ions of *m/z* 78.959 (PO_3^-) and *m/z* 96.969 ($H_2PO_4^-$) were used to characterize the lipid class and the neutral loss of Acyl 12:0 (182.167 Da) was utilized for the acyl chain characterization.

For the sulfatide (SHexCer, SHexCer 36:1;2O, SHexCer 18:1;2O/18:0, level 1) incorporating sphingosine and fatty acid, the ion mode for quantifications depended on the injection volume and biological sample analyzed although the acyl chain compositions could only be determined in positive ion mode. Basically, the sensitivity of SHexCer was higher in negative ion mode and the quantification was performed by negative ion mode whereas the annotation was carried out by positive ion mode. The SHexCer lipids could be characterized as $[M+H]^+$ and $[M-H]^-$. For SHexCer 18:1;2O/18:0, the neutral loss of 260.02 Da (H_2SO_4+$C_6H_{10}O_5$) was used to characterize the lipid class and the product ions of *m/z* 282.279 (SPB 18:1;2O-H_2O, $C_{18}H_{36}NO^+$), *m/z* 264.269 (SPB 18:1;2O-2H_2O, $C_{18}H_{34}N^+$), and *m/z* 252.269 (SPB 18:1;2O-CH_4O_2, $C_{17}H_{34}N^+$) were used to characterize the acyl chain moiety in positive ion mode. Alternatively, the product ion of *m/z* 96.96 (HSO_4^-) was used for the lipid class characterization in positive ion mode. The sulfatide (SHexCer+O[51], SHexCer 36:1;3O, SHexCer 18:1;2O/18:0;O, level 2) incorporating sphingosine and hydroxy fatty acid was quantified and characterized using the same scheme as described for SHexCer. The monosialodihexosylganglioside (GM3, GM3 36:1;2O, GM3 18:1;2O/18:0, level 1) incorporating sphingosine and fatty acid was quantified as $[M-H]^-$ whereas the acyl chain composition could only be characterized by the $[M+NH_4]^+$ form. In positive ion mode, the product ion of *m/z* 292.103 ($C_{11}H_{18}NO_8^+$, *N*-acetyl-neuraminidate moiety) and the sequential neutral losses of 291.096

Da ($C_{11}H_{17}NO_8$, *N*-acetyl-neuraminidate moiety), 162.053 Da ($C_6H_{10}O_5$, galactosyl moiety), and 162.053 Da ($C_6H_{10}O_5$, glucosyl moiety) were used for the lipid class characterization. For GM3 18:1;2O/18:0, the product ions of *m/z* 282.279 (SPB 18:1;2O-H_2O, $C_{18}H_{36}NO^+$) and *m/z* 264.269 (SPB 18:1;2O-2H_2O, $C_{18}H_{34}N^+$) were used for characterizing the sphingobase moiety. In negative ion mode, the product ion of *m/z* 290.088 ($C_{11}H_{16}NO_8^-$, *N*-acetyl-neuraminidate moiety) and the neutral loss of 291.096 Da ($C_{11}H_{17}NO_8$, *N*-acetyl-neuraminidate moiety) were used to characterize the lipid class in negative ion mode. The sulfonolipid[60] (SL, SL 33:0;O, SL 18:0;O/15:0, level 2) incorporating deoxysphinganine/deoxysphingosine and fatty acid was quantified as $[M+H]^+$ and it could be characterized as $[M+H]^+$, $[M+NH_4]^+$, and $[M-H]^-$. For the ammonium adduct form of SL 18:0;O/15:0, the neutral losses of 241.241 Da (Acyl 15:0+NH_3), 259.251 Da (241.241 Da+H_2O), 255.256 Da (SPB 18:0;O+NH_3-C_2H_8N), and 273.267 Da (255.256 Da+H_2O) were used to characterize the acyl chain moieties whereas the product ion of *m/z* 124.006 ($C_2H_6NO_3S^+$) was used for the lipid class characterization. For the proton loss form of SL 18:0;O/16:0 in negative ion mode, the neutral loss of Acyl 16:0 (238.229 Da) and the product ion of 79.957 (HSO_3^-) were used to characterize the acyl chain moiety and the lipid class, respectively. The sulfonolipid[60] (SL+O, SL 33:1;2O, SL 17:0;O/16:1;O, level 2) incorporating deoxysphinganine/deoxysphingosine and hydroxy fatty acid was quantified as [M+H]+, and it could be characterized as $[M+H]^+$, $[M+NH_4]^+$, and $[M-H]^-$. For the proton adduct form of SL 17:0;O/16:1h in positive ion mode, the product ion of *m/z* 253.216 ($C_{16}H_{29}O_2^+$, Acyl 16:1;O^+) and the neutral loss of 270.22 Da (Acyl 16:1;O+H_2O) were used to characterize the acyl chains with the same product ion of *m/z* 124.006 being used for the lipid class annotation. The same diagnostic ions were used in negative ion mode as described for the normal SL lipid.

Annotations in LipidMAPS Sterol Lipids [ST]. The annotation of cholesterol (level 1) should be performed by checking the retention time of the internal standard, and it was quantified as $[M\text{-}H_2O+H]^+$ because of the highest sensitivity compared to other adduct forms whereas it could also be detected as $[M+H]^+$, $[M+NH_4]^+$, and $[M+Na]^+$. Although MS-DIAL 4 exports the annotation as "cholesterol" as default, the terminology should be changed to ST 27:1;O as recommended in LSI where ST and O denote the sterol backbone and oxygen-atom added to the normal ST moiety, respectively, if no standard is available. For other sterols, the structural backbone for brassicasterol, campesterol, sitosterol, and stigmasterol were described as ST 28:2;O, ST 28:1;O, ST 29:1;O, and ST 29:2;O, respectively. The cholesteryl ester (CE, level 1) was quantified as $[M+NH_4]^+$ and characterized by the product ion of *m/z* 369.349 (ST 27:1$^+$, $C_{27}H_{45}^+$). The other sterol esters[61] including brassicasteryl ester (BRSE, level 2), campesteryl ester (CASE, level 2), sitosteryl ester (SISE, level 2), and stigmasteryl ester (STSE, level 2) were quantified as $[M+NH_4]^+$ and characterized by the product ions of *m/z* 381.341 (ST 28:2$^+$, $C_{28}H_{45}^+$), *m/z* 383.376 (ST 28:1$^+$, $C_{28}H_{47}^+$), *m/z* 397.386 (ST 29:1$^+$, $C_{29}H_{49}^+$), and *m/z* 395.363 (ST 29:2$^+$, $C_{29}H_{47}^+$), respectively, where the annotations were based on the species levels of SE 28:2/18:1, SE 28:1/18:1, SE 29:1/18:1, and SE 29:2/18:1, respectively, for oleate ester description.

The sulfate conjugate[62] to sterols (SSulfate, level 2) were characterized as $[M\text{-}H]^-$ by the product ion of *m/z* 96.96 (HSO_4^-) and annotated as ST 27:1;O;S for cholesterol sulfate. The hexosyl conjugate, known as sterolglycosides[61] (SHex, level 2), were quantified as $[M+NH_4]^+$ and could also be characterized as the $[M\text{-}H]^-$ form. For example, the stigmasterol hexoside was annotated as ST 29:2;O;Hex with the confirmation of the product ions of *m/z* 395.367 (ST 29:2$^+$, $C_{29}H_{47}^+$) and *m/z* 179.0561 (hexose moiety, $C_6H_{11}O_6^-$) in positive and negative ion mode, respectively. The acylhexosyl sterols[63], also known as acylsterolglycosides, including acylhexosyl- cholesterol (AHexCS, level 2), brassicasterol (AHexBRS, level 2), campesterol (AHexCAS, level 2), sitosterol (AHexSIS, level 2), and stigmasterol (AHexSTS,

level 2) were quantified as $[M+NH_4]^+$ and also characterized as $[M-H]^-$ and $[M+CH_3COO]^-$, where the annotations were performed according to the species levels of ST 27:1;O;Hex;FA 18:1, ST 28:2;O;Hex;FA 18:1, ST 28:1;O;Hex;FA 18:1, ST 29:1;O;Hex;FA 18:1, and ST 29:2;O;Hex;FA 18:1, respectively, for oleate ester description. The characterizations for AHexCS, AHexBRS, AHexCAS, AHexSIS, and AHexSTS were performed in positive ion mode by the product ions of *m/z* 369.349 (ST $27:1^+$, $C_{27}H_{45}^+$), *m/z* 381.341 (ST $28:2^+$, $C_{28}H_{45}^+$), *m/z* 383.376 (ST $28:1^+$, $C_{28}H_{47}^+$), *m/z* 397.386 (ST $29:1^+$, $C_{29}H_{49}^+$), and *m/z* 395.363 (ST $29:2^+$, $C_{29}H_{47}^+$), respectively, whereas the FA ions derived from the ester acyl chain moiety were used for the lipid annotations in negative ion mode.

The annotation of bile acids (level 1) was ideally performed by matching the retention time and MS/MS spectrum of authentic standards. Otherwise, the annotations for e.g. cholic acid, glycodeoxycholic acid, and taurodeoxycholic acid were described as ST 24:1;O5, ST 24:1;O4;G, and ST 24:1;O4;T, respectively. The quantification was performed by the proton loss form in negative ion mode. The sulfate conjugate[62] (BASulfate, level 2) was quantified and characterized as $[M-H]^-$ by the product ion of *m/z* 96.96 (HSO_4^-) and was annotated as ST 24:1;O5;S for cholic acid sulfate. Bile acid esters such as deoxycholic acid ester (DCAE, level 3) were quantified as $[M+NH_4]^+$ and also characterized by $[M-H]^-$, where the annotation was performed according to the species level as ST 24:1;O4/18:1 for oleate ester description. For DCAE lipid, the product ion of *m/z* 357.274 ($C_{24}H_{37}O_2^+$, ST $24:1;O2^+$) and the FA ion derived from the ester chain moiety were used for the lipid characterizations in positive- and negative ion mode, respectively. Only one lipid, calcidiol, for Vitamin D (level 1) was characterized as $[M+H]^+$ in this study by the sequential H_2O losses from the precursor *m/z* value.

Annotations in LipidMAPS Prenol Lipids [PR]. Three phenol lipids including coenzyme Q (CoQ, level 1), vitamin A fatty acid ester (VAE, level 1), and vitamin E (tocopherol, level 1) were incorporated in

MS-DIAL 4. The CoQ lipid was annotated as $[M+H]^+$ by the product ion of *m/z* 197.081 ($C_{10}H_{13}O_4^+$): CoQ8, 9, and 10 were characterized in this study. The VAE lipid was characterized as $[M+H]^+$ and $[M+Na]^+$, and the sodium adduct form was utilized for quantification because of higher sensitivity than that of the proton adduct form in our experimental condition. The product ions of *m/z* 269.226 ($C_{20}H_{29}^+$) and *m/z* 119.086 ($C_9H_{11}^+$) were used for the diagnostic ions. The tocopherol lipid was characterized as $[M-H]^-$ and $[M+CH_3COO]^-$ and quantified by the proton loss form. The product ion of *m/z* 163.075 ($C_{10}H_{11}O_2^-$) was used for the characteristic ion.

Reference (Supplementary Note 2)

48. Dührkop, K. *et al. Nat. Methods* **16**, 299–302 (2019).

49. Tsugawa, H. *et al. Metabolites* **9**, 119 (2019).

50. Tadano-Aritomi, K., Matsuda, J., Fujimoto, H., Suzuki, K. & Ishizuka, I. *J. Lipid Res.* **44**, 1737–1743 (2003).

51. Han, X. Part II characterization of lipids. In Lipidomics: Comprehensive Mass Spectrometry of Lipids 459, https://doi.org/10.1002/9781119085263 (2016)

52. Xu, F., Zou, L., Lin, Q., & Ong, C. N. *Rapid Commun. Mass Spectrom.* **23**, 3243–3254 (2009).

53. Kim, J. & Hoppel, C. L. *J. Lipid Res.* **52**, 389–392 (2011).

54. Lee, H. C., Simon, G. M. & Cravatt, B. F. *Biochemistry* **54**, 2539–2549 (2015).

55. Chen, W. W., Chao, Y. J., Chang, W. H., Chan, J. F. & Hsu, Y. H. H. *Sci. Rep.* **8**, 1–14 (2018).

56. Calvano, C.D., Glaciale, M., Palmisano, F. & Cataldi, T.R. *Electrophoresis* 39, 1634–1644 (2018)

57. Hirabayashi, T. *et al. Nat. Commun.* **8**, 14609 (2017).

58. Lorenzen, W., Bozhüyük, K. A. J., Cortina, N. S. & Bode, H. B. *J. Lipid Res.* **55**, 2620–2633 (2015).

59. Guschina, I. A. *et al. J. Eukaryot. Microbiol.* **56**, 52–57 (2009).

60. Walker, A. *et al. Sci. Rep.* **7**, 1–10 (2017).

61. Hailat, I. & Helleur, R. *Int. J. Mass Spectrom.* **362**, 24–31 (2014).

62. Nuzzo, G. *et al. Mar. Drugs* **17**, 1–10 (2019).

63. Schrick, K., Shiva, S., Arpin, J.C., Delimont, N., Isaac, G., Tamura, P. & Welti, R. *Lipids* **47**, 185–193 (2012).

Supplementary Fig. 1 | Details of tandem mass spectrometry (MS/MS) characterization of 117 lipid subclasses categorized as LipidMAPS Fatty Acyls [FA], Glycerolipids [GL], Glycerophospholipids [GP], Sphingolipids [SP], Sterol Lipids [ST], and Prenol Lipids [PR]. The important fragment ions and neutral losses for characterizing the lipid subclass at the molecular species level are described. The details of fragment descriptions are provided in **Supplementary Note 2**.

Fatty Acyls [FA]

ESI(+)-MS/MS for Fatty Acyls [FA]: CAR, NAGly, NAGlySer, NAOrn, NAE

CAR 18:1 as $[M]^+$

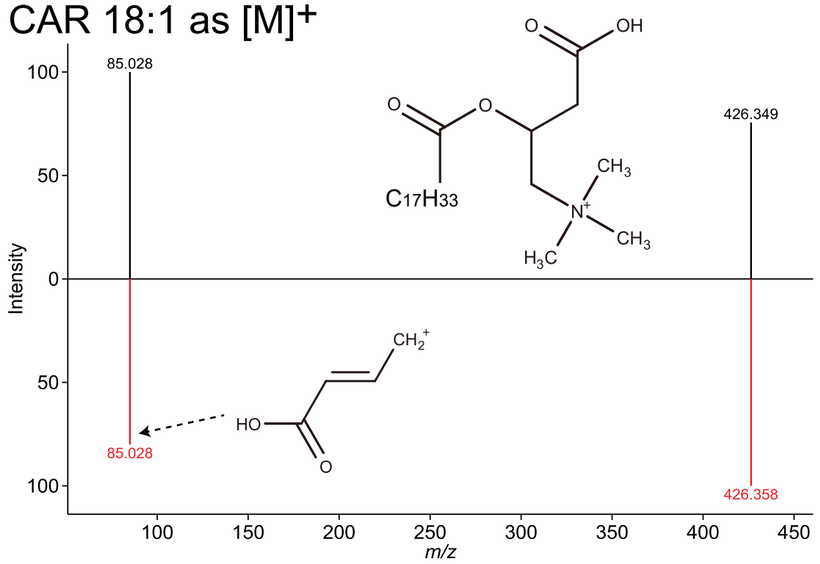

NAGly 15:0/16:0 as $[M+NH_4]^+$

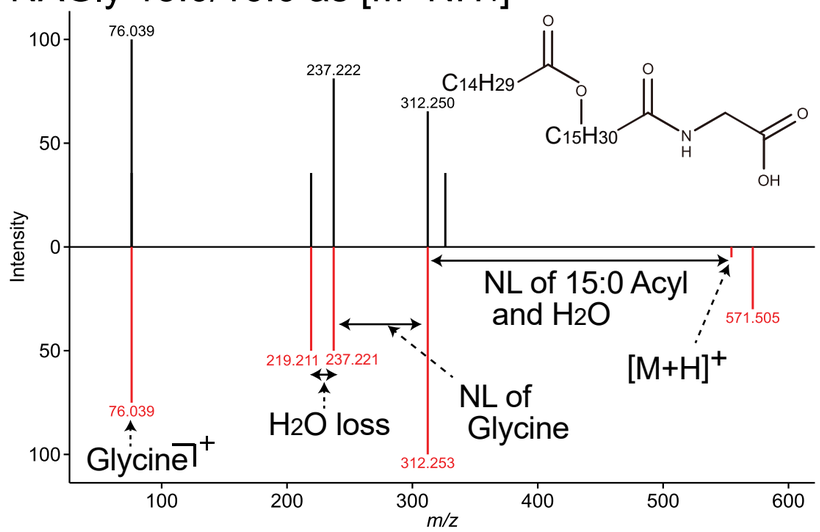

NAGlySer 15:0/16:0 as $[M+NH_4]^+$

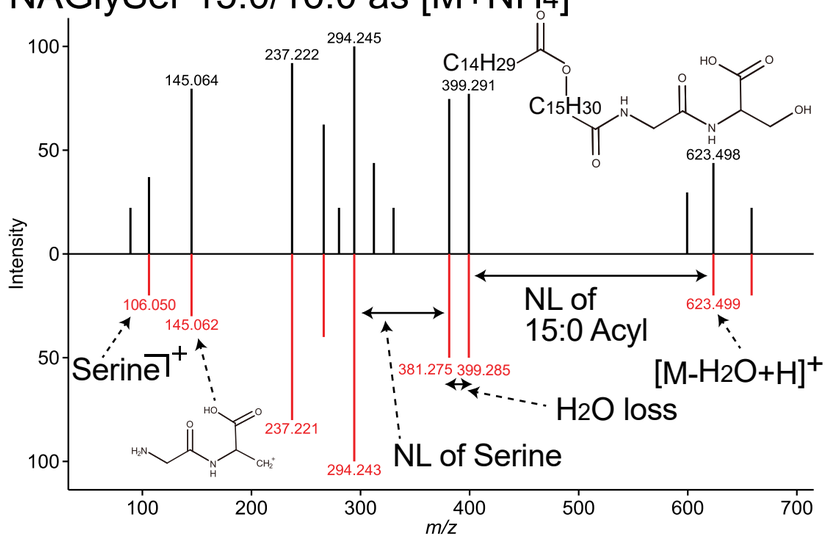

NAOrn 15:0/17:0 as $[M+H]^+$

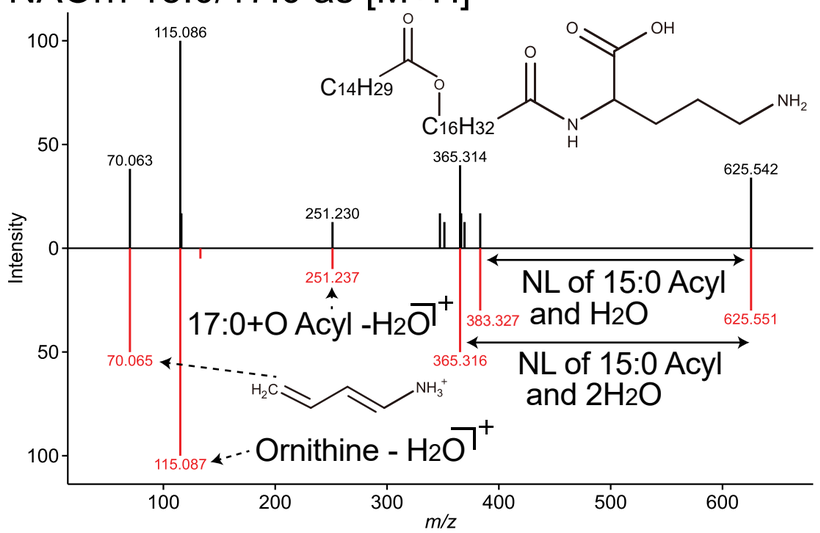

NAE 20:4 as $[M+H]^+$

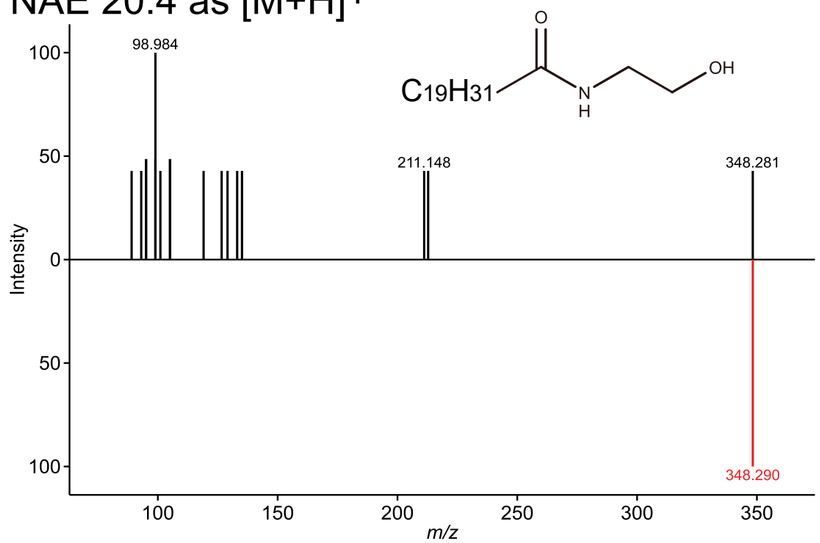

ESI(-)-MS/MS for Fatty Acyls [FA]: FA, FAHFA, NAGly, NAGlySer

FA 18:1 as [M-H]-

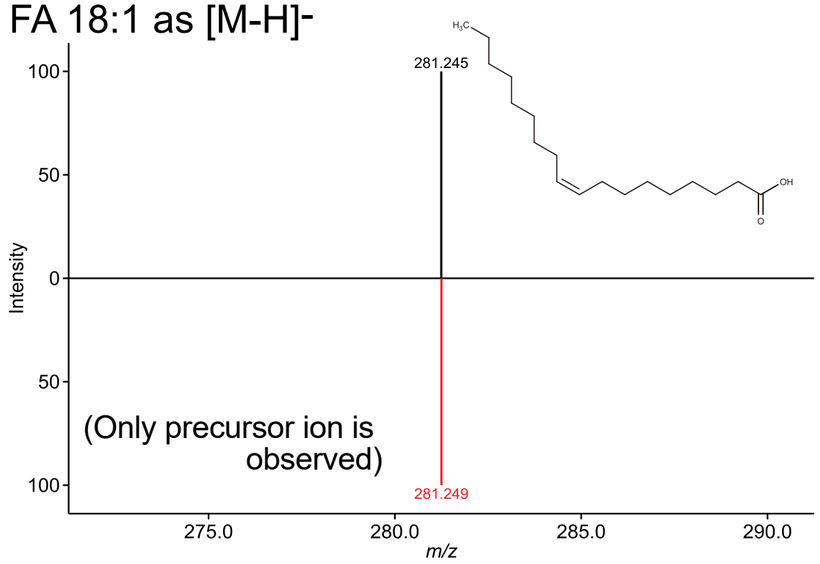

FAHFA 16:0/18:1 as [M-H]-

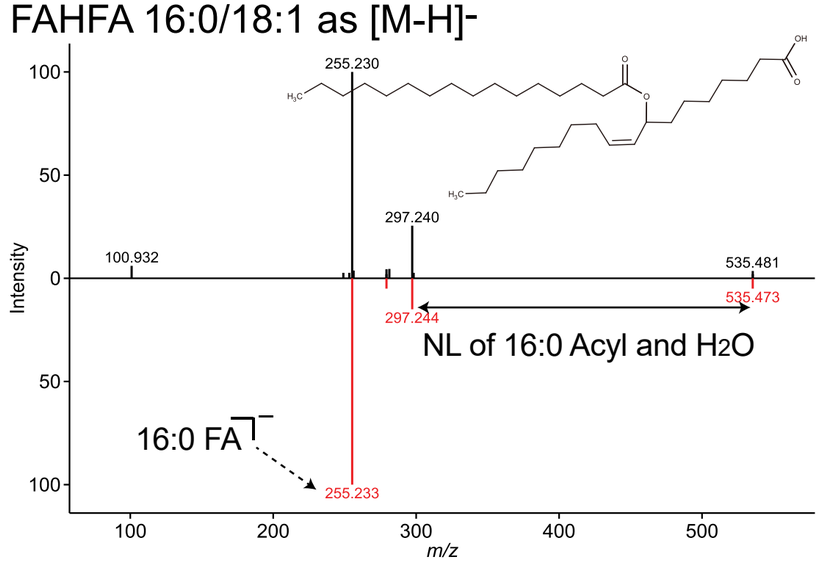

NAGly 15:0/16:0 as [M-H]-

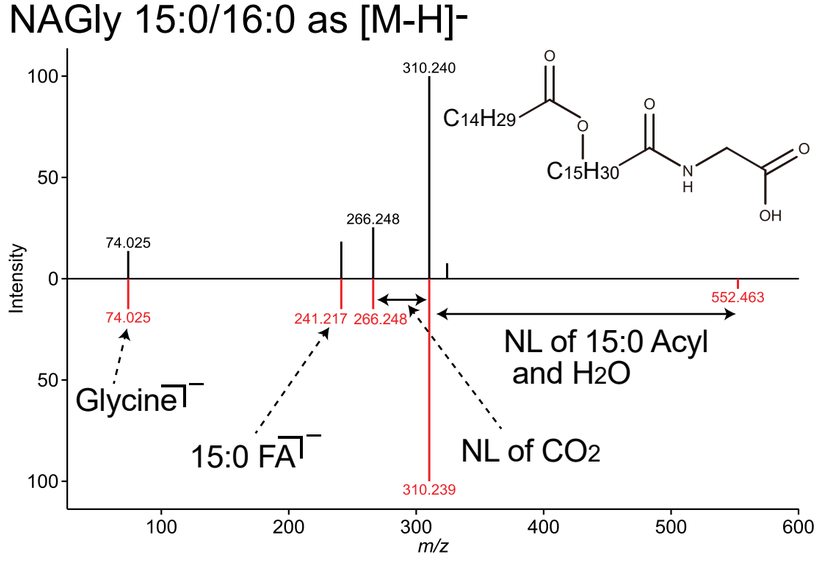

NAGlySer 15:0/17:0 as [M-H]-

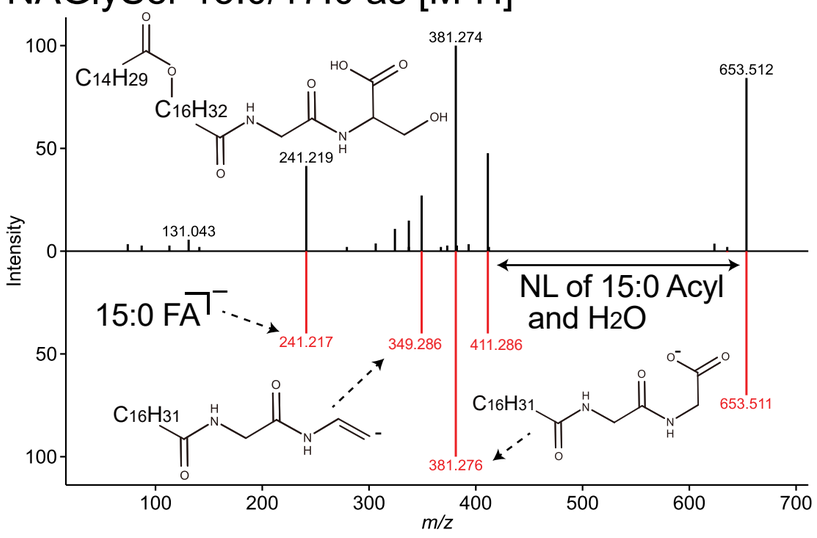

Glycerolipids [GL]

ESI(+)-MS/MS for Glycerolipids [GL]: ADGGA, DGGA, SQDG, MGDG, Ether MGDG, DGDG, LDGCC, DGCC, LDGTS

ADGGA (O-16:0)16:0_18:2 as $[M+NH_4]^+$

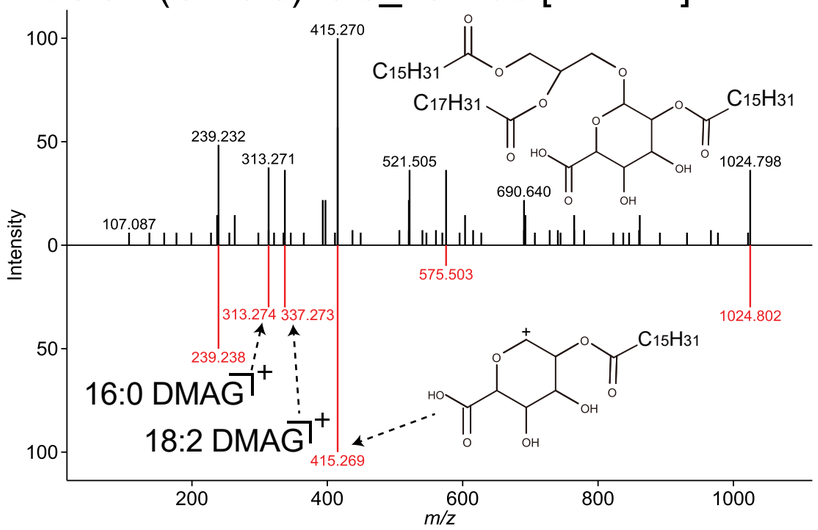

DGGA 16:0_18:2 as $[M+NH_4]^+$

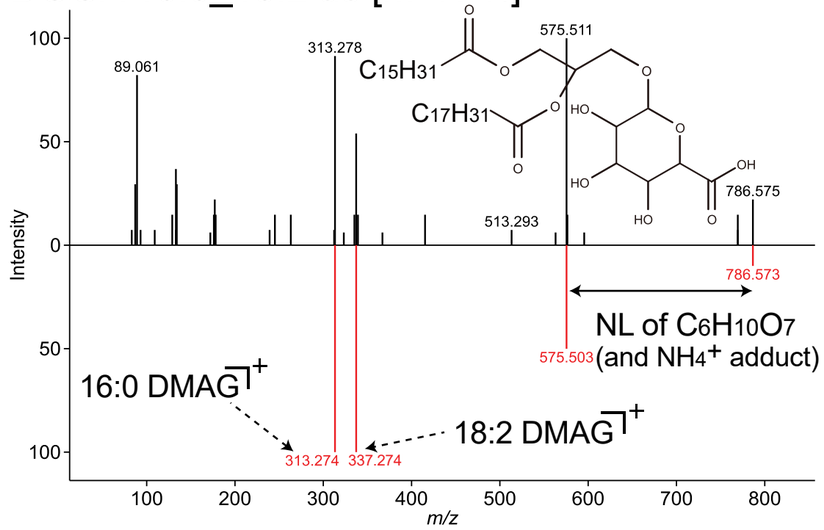

SQDG 16:0_18:1 as $[M+NH_4]^+$

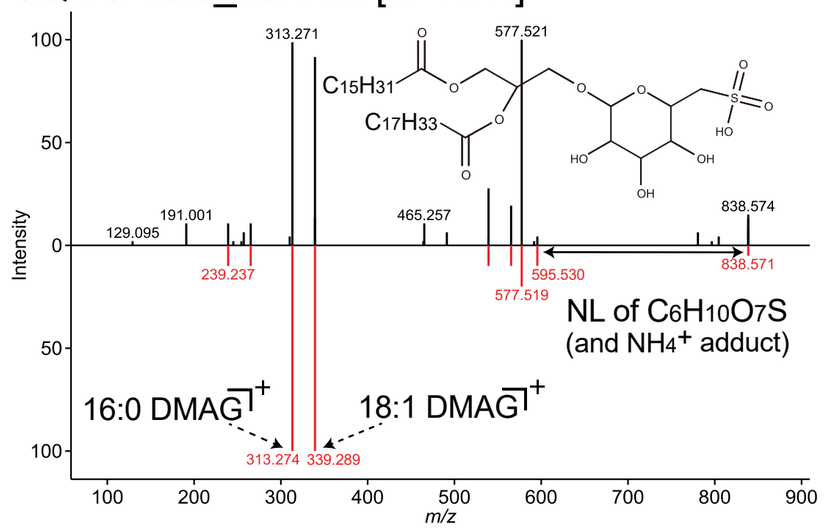

MGDG 16:0_18:1 as $[M+NH_4]^+$

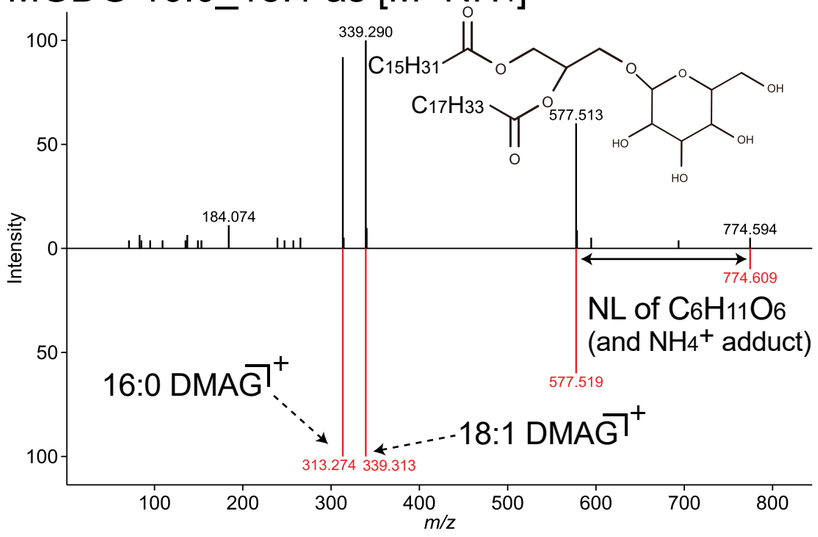

MGDG O-16:0_16:0 as $[M+NH_4]^+$

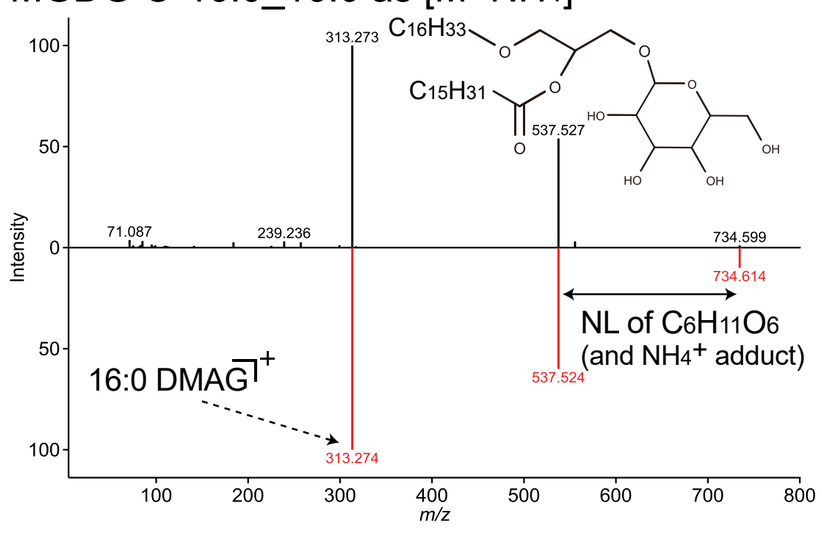

DGDG 16:0_18:1 as $[M+NH_4]^+$

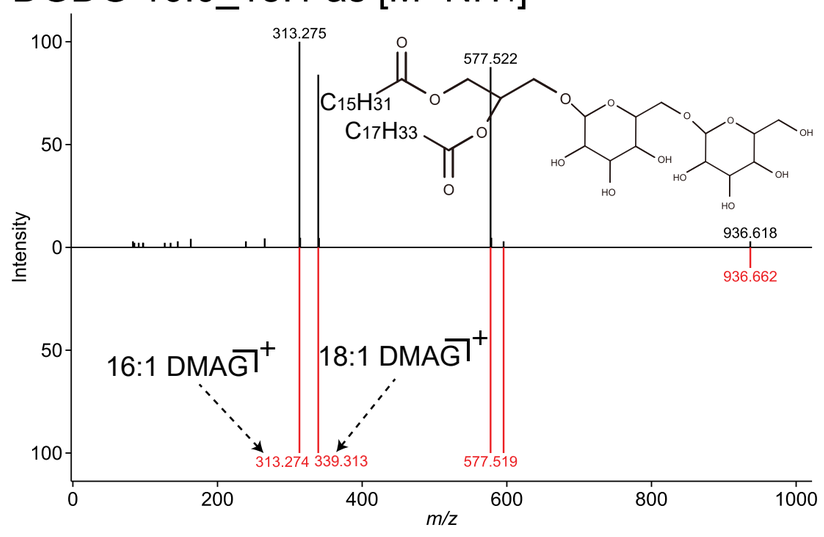

LDGCC 16:0 as $[M+H]^+$

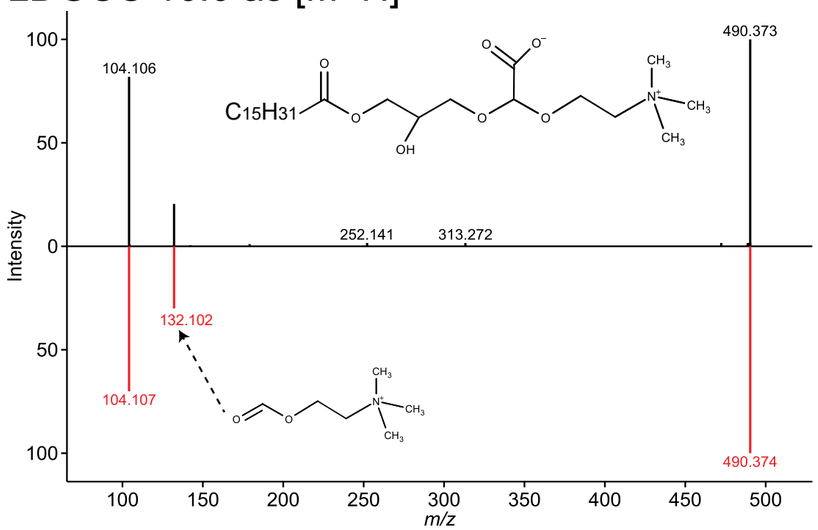

DGCC 16:0_18:1 as $[M+H]^+$

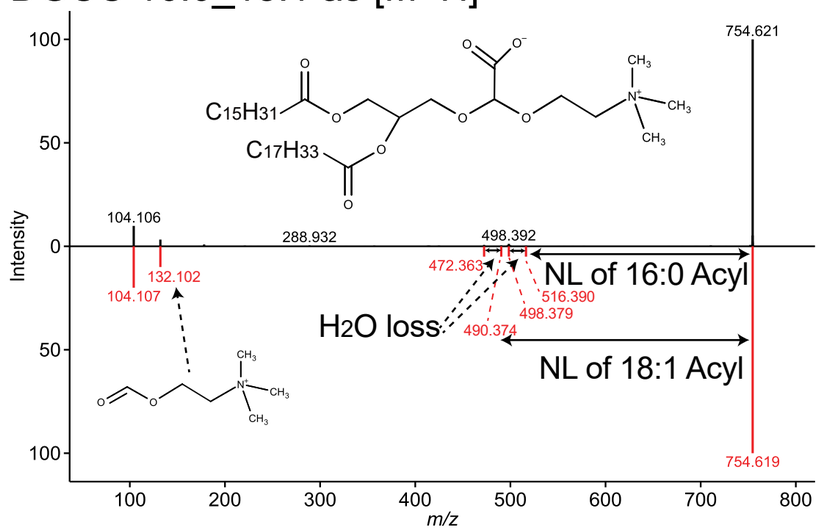

LDGTS 18:1 as $[M+H]^+$

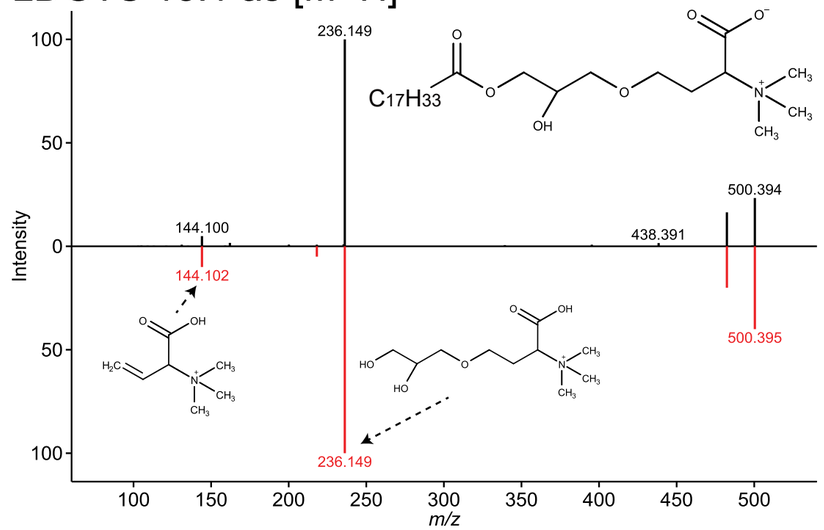

ESI(+)-MS/MS for Glycerolipids [GL]: DGTS, MG, DG, Ether DG, TG, Ether TG

DGTS 16:0_18:1 as $[M+H]^+$

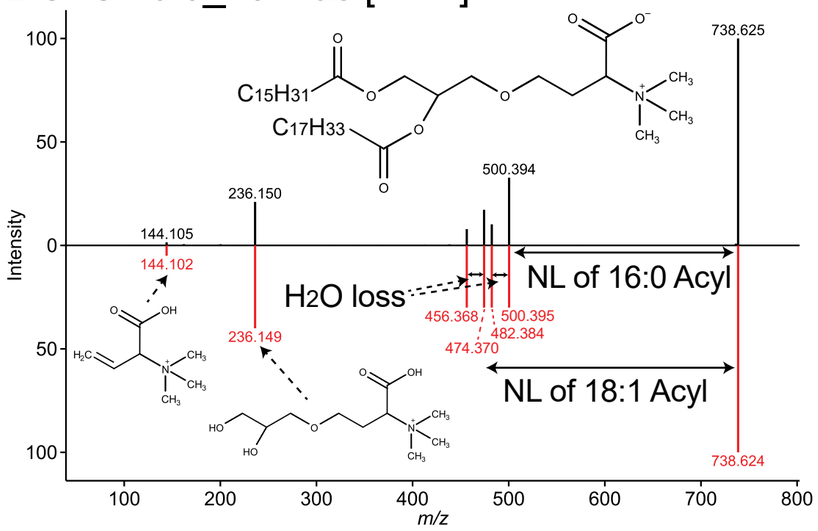

MG 18:0 as $[M+NH_4]^+$

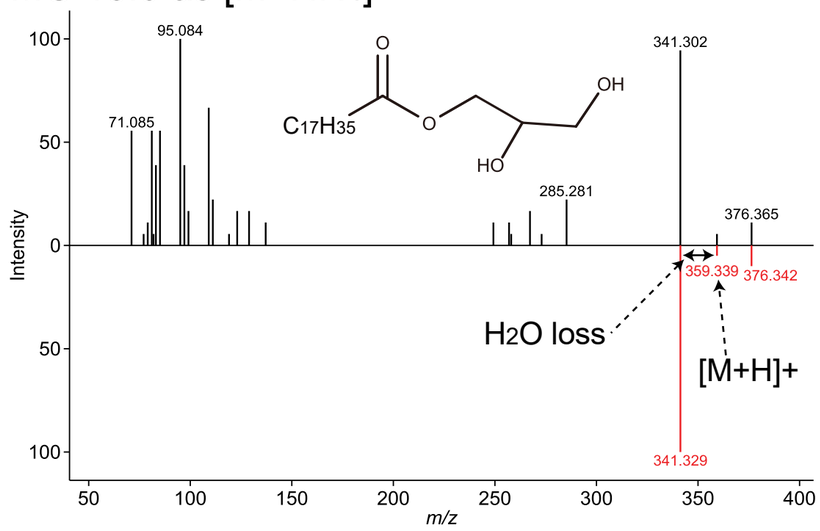

DG 18:0_20:4 as $[M+NH_4]^+$

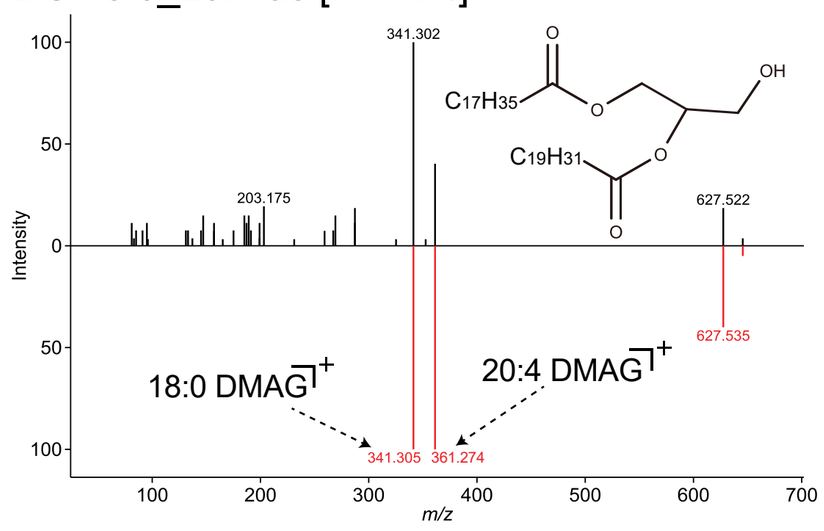

DG O-16:0_18:1 as $[M+NH_4]^+$

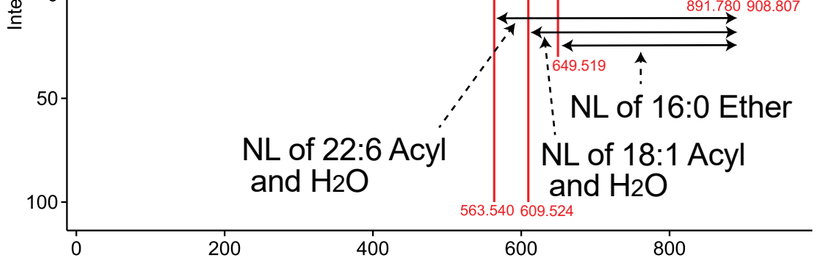

TG 16:0_18:2_22:6 as $[M+NH_4]^+$

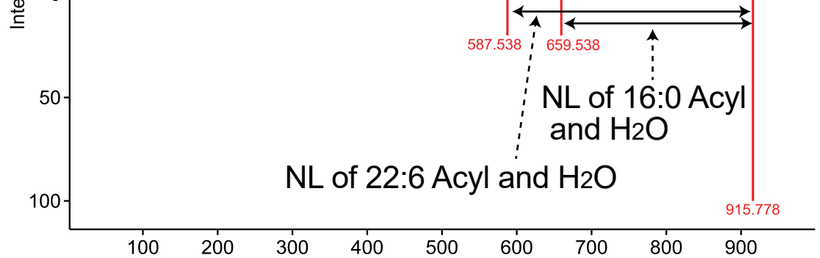

TG 16:0_18:2_22:6 as $[M+Na]^+$

TG O-16:0_18:1_22:6 as $[M+NH_4]^+$

TG O-18:0_16:0_22:6 as $[M+Na]^+$

ESI(-)-MS/MS for Glycerolipids [GL]: ADGGA, DGGA, SQDG, MGDG, Ether MGDG, DGDG, Ether DGDG, Ether SMGDG

ADGGA 16:0_16:0_18:2 as [M-H]⁻

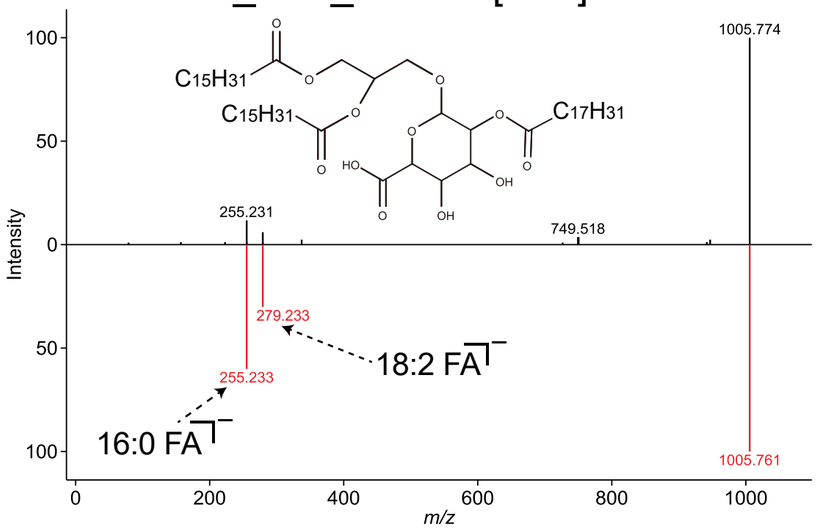

DGGA 16:0_18:2 as [M-H]⁻

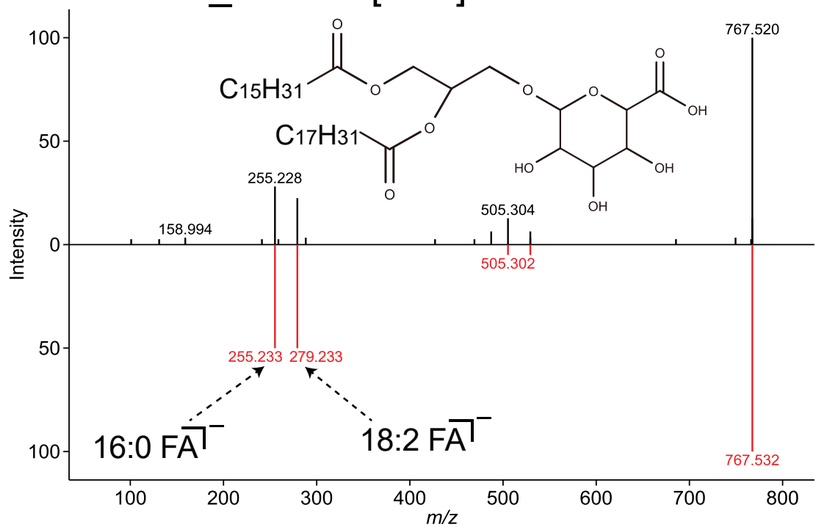

SQDG 16:0_16:0 as [M-H]⁻

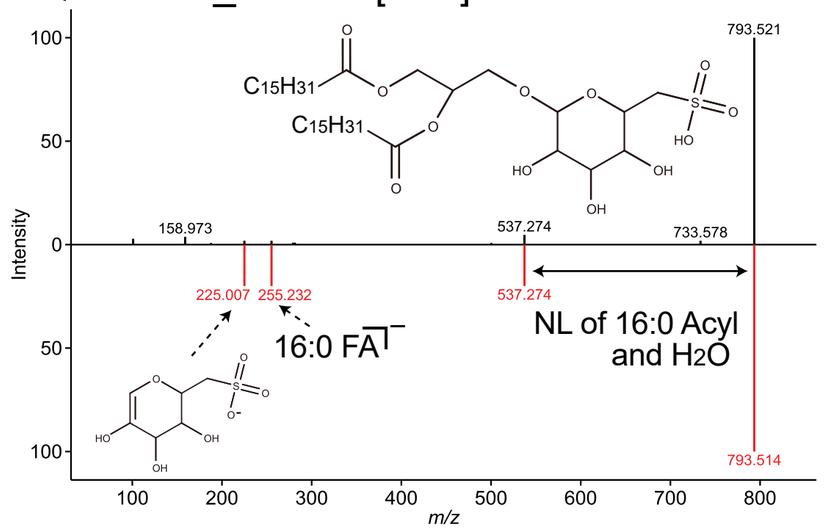

MGDG 16:0_18:1 as [M+CH3COO]⁻

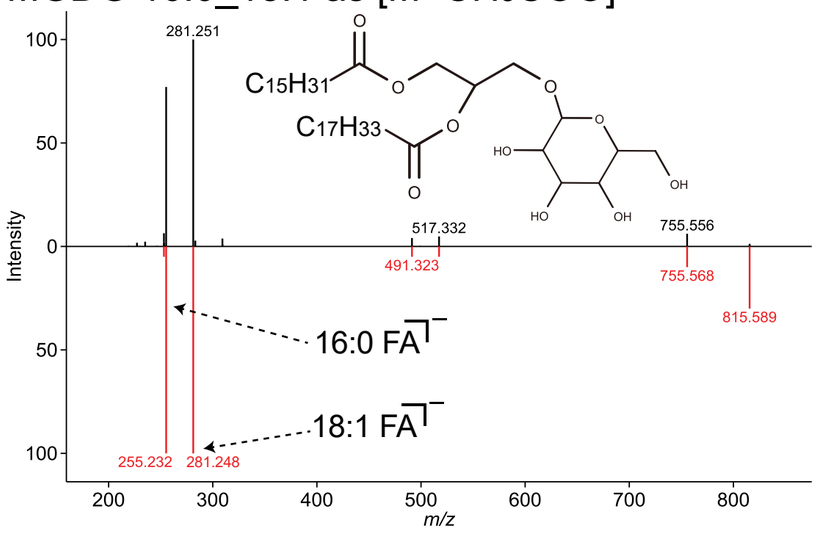

MGDG O-16:0_18:1 as [M+CH3COO]⁻

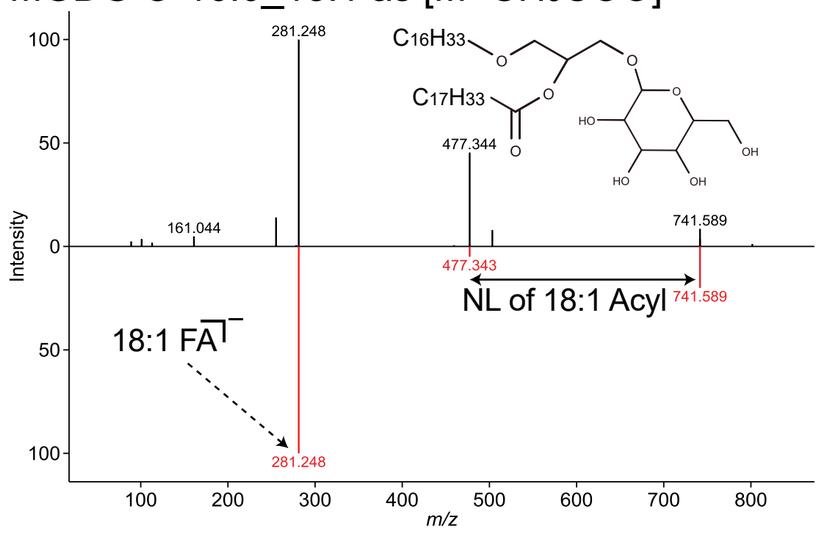

DGDG 16:0_18:1 as [M+CH3COO]⁻

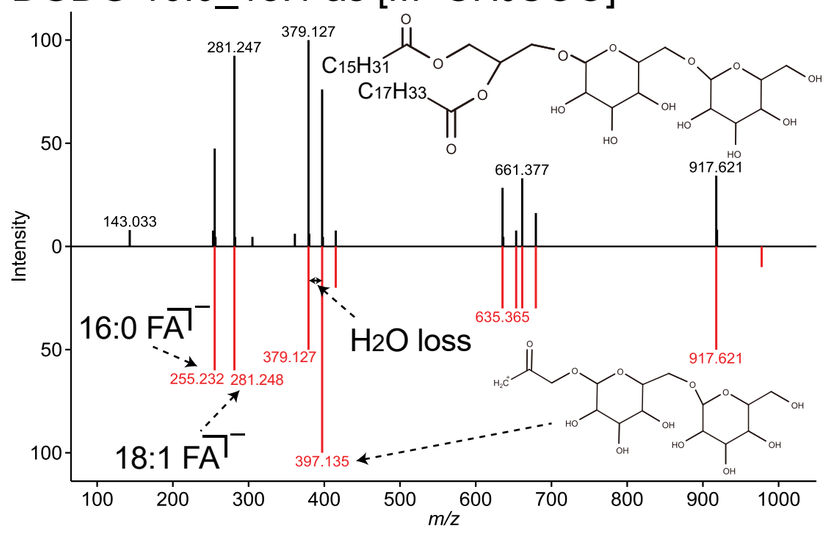

DGDG O-18:2_16:0 as [M+CH3COO]⁻

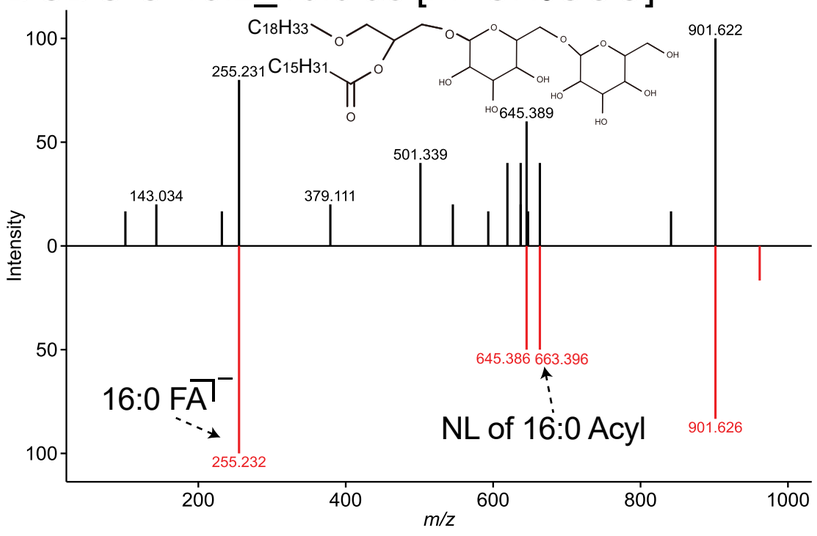

SMGDG O-16:0_14:0 as [M-H]⁻

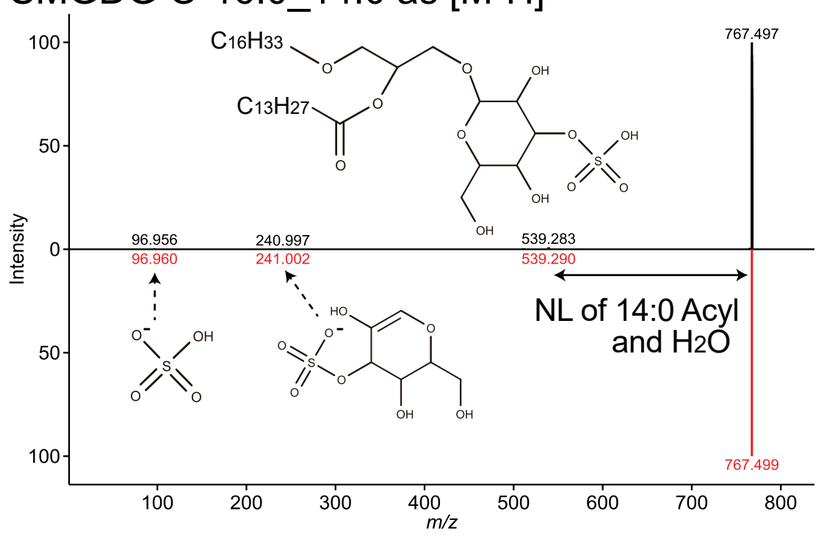

Glycerophospholipids [GP]

ESI(+)-MS/MS for Glycerophospholipids [GP]: BMP, CL, LPC, Ether LPC, LPE, Ether LPE,

BMP 18:1_22:4 as $[M+NH_4]^+$

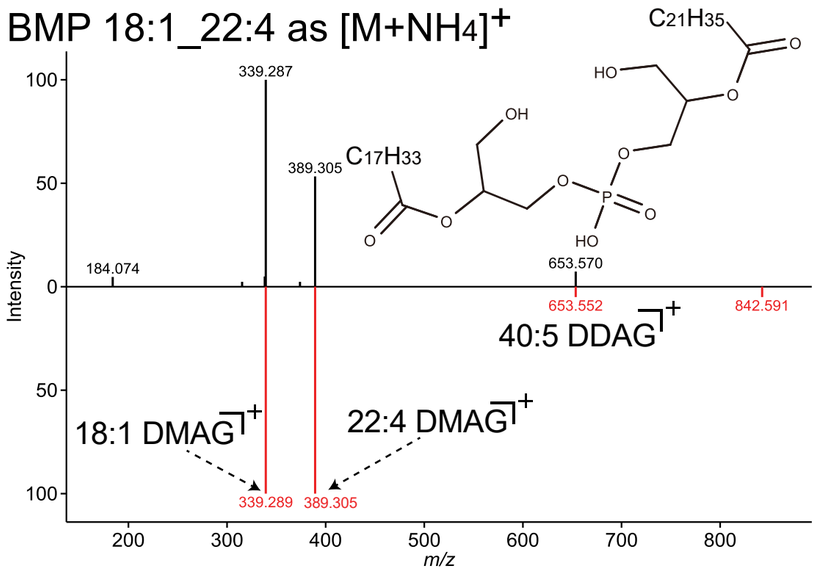

CL 34:1_36:3 as $[M+NH_4]^+$

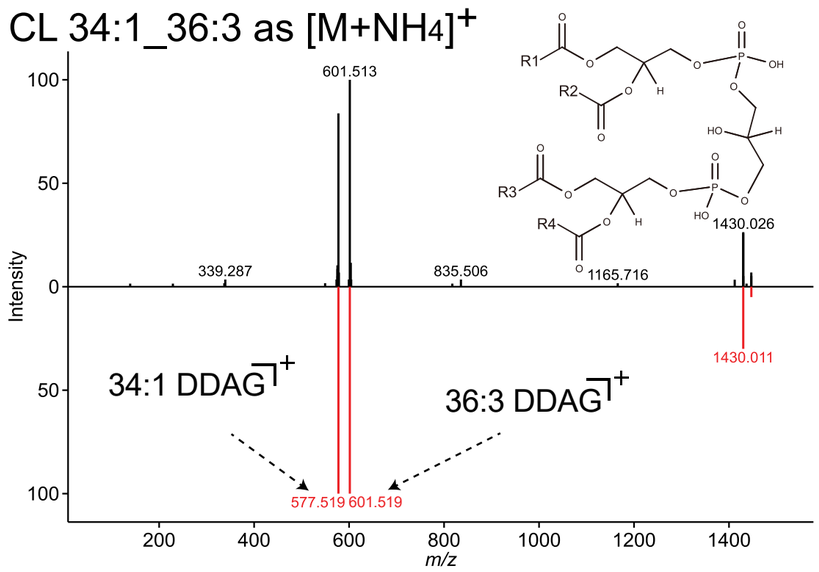

LPC 18:1/0:0 as $[M+H]^+$

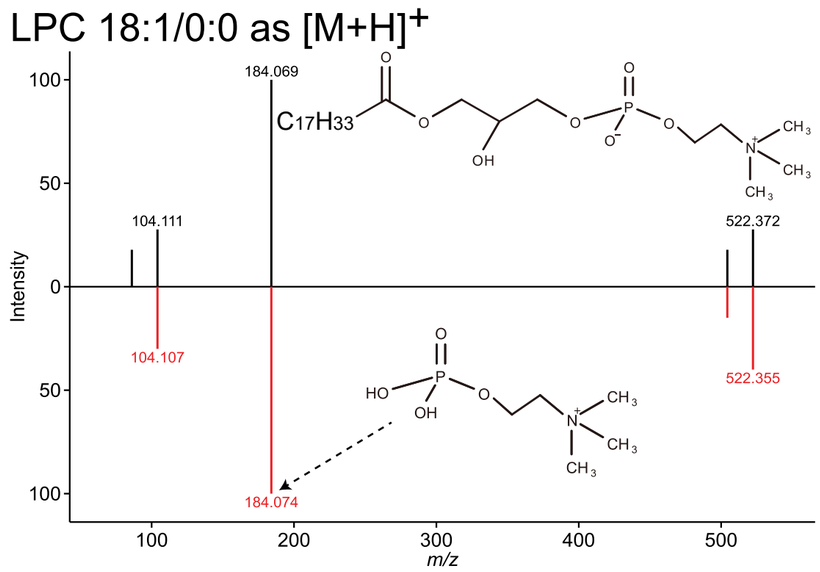

LPC 18:1 as $[M+Na]^+$

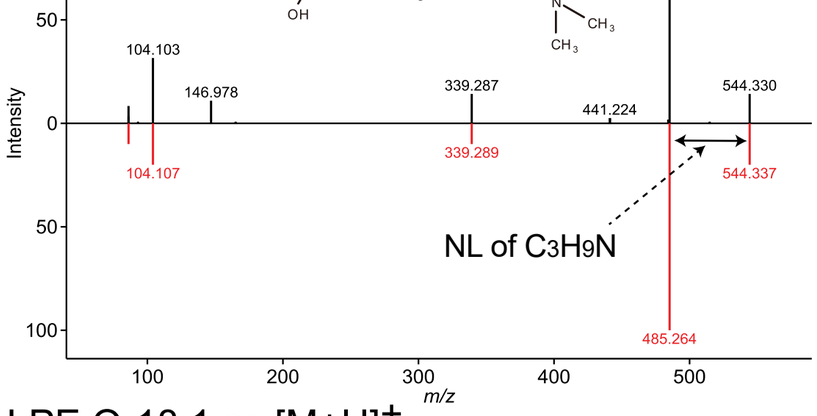

LPC O-18:1 as $[M+H]^+$

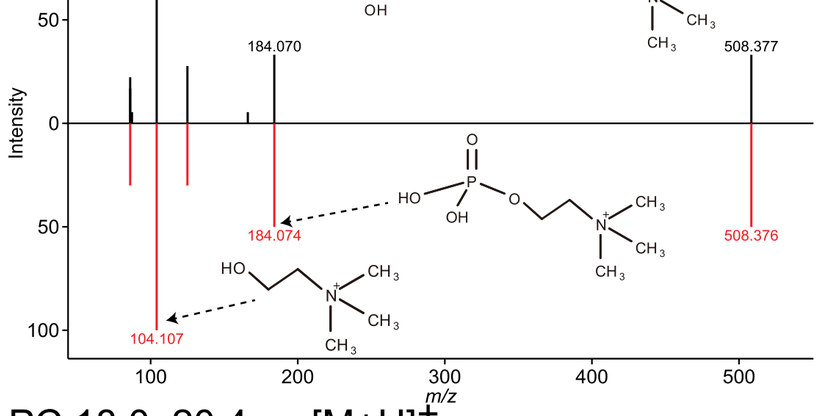

LPE 18:1 as $[M+H]^+$

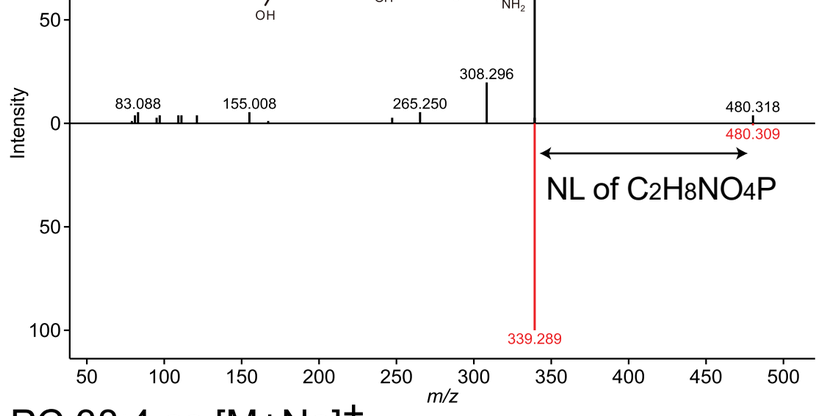

LPE O-18:1 as $[M+H]^+$

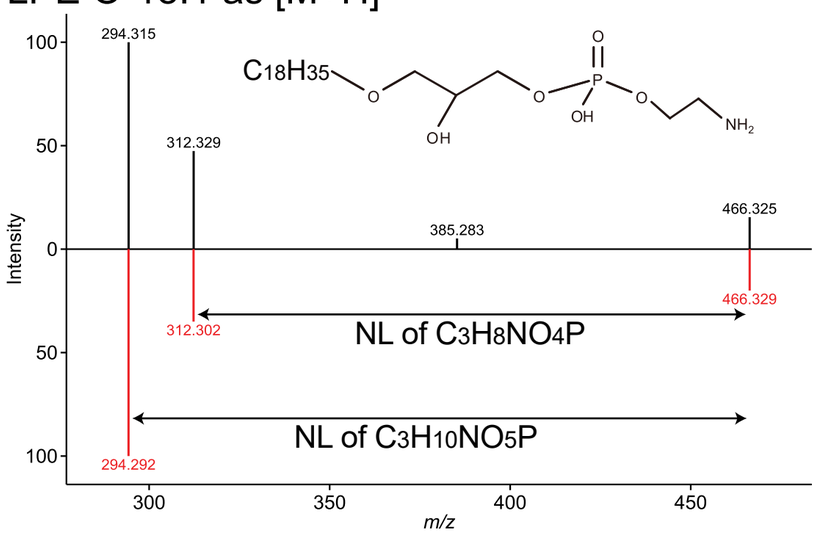

PC 18:0_20:4 as $[M+H]^+$

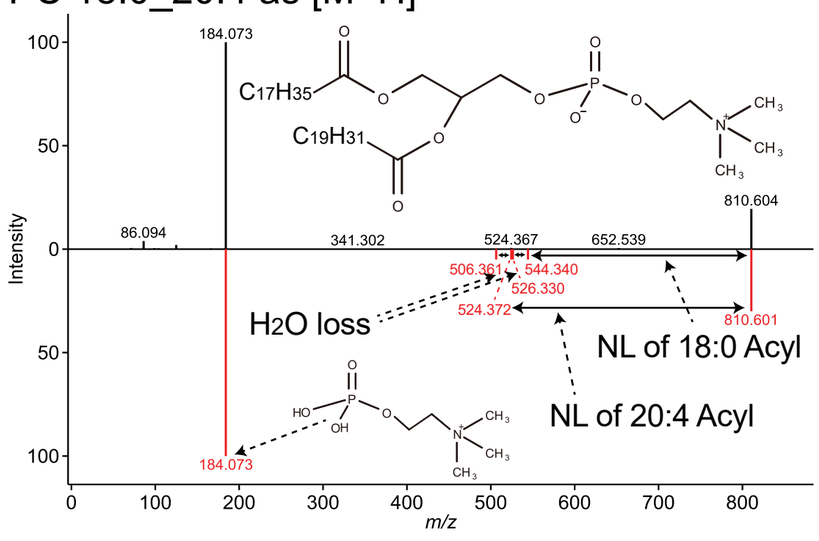

PC 38:4 as $[M+Na]^+$

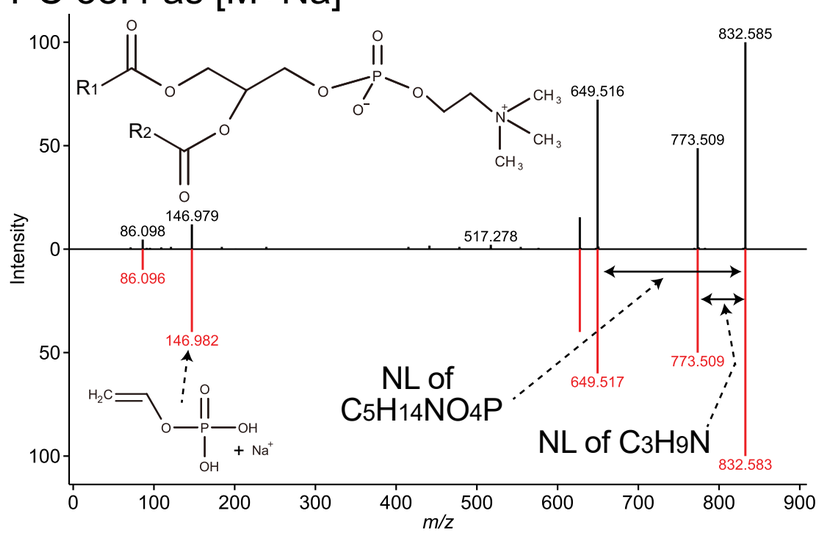

ESI(+)-MS/MS for Glycerophospholipids [GP]: Ether PC, PE, Ether PE_P, PG, PI, PS

PC O-38:4 as $[M+H]^+$

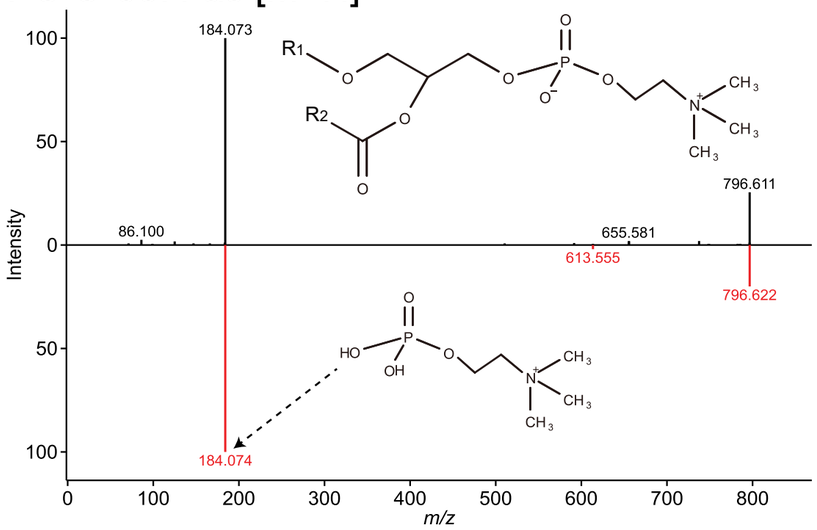

PE 18:0_20:4 as $[M+H]^+$

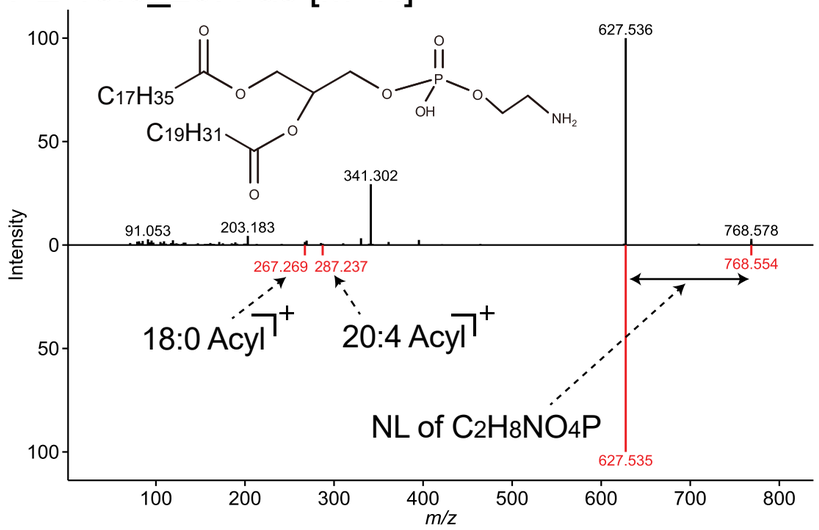

PE 38:4 as $[M+Na]^+$

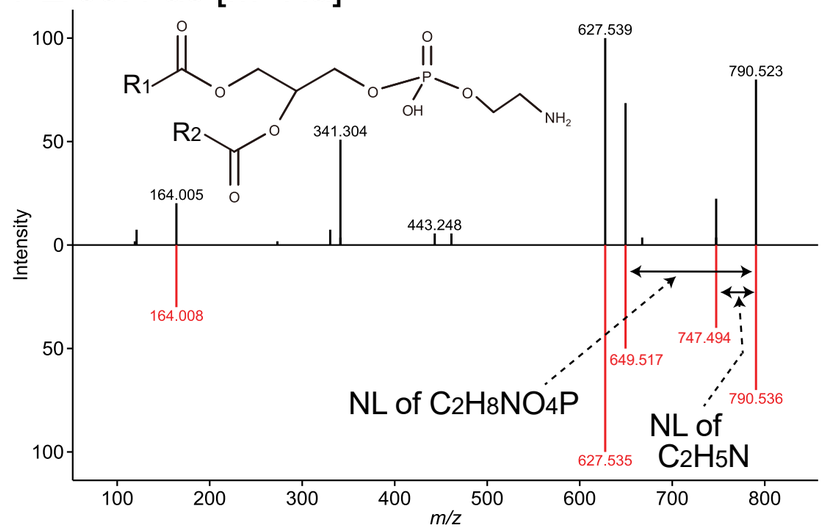

PE P-18:0_20:3 as $[M+H]^+$

PG 18:0_20:4 as $[M+NH_4]^+$

PI 38:4 as $[M+NH_4]^+$

PI 38:4 as $[M+Na]^+$

PS 18:0_20:4 as $[M+H]^+$

PS 38:4 as $[M+Na]^+$

ESI(+)-MS/MS for Glycerophospholipids [GP]: HBMP, Ether PE_O

HBMP 18:1/16:1_18:1 as $[M+NH_4]^+$

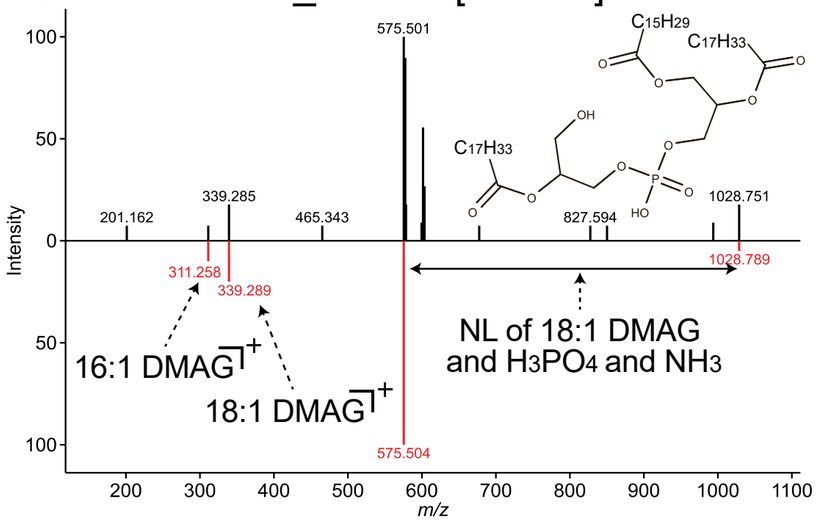

PE O-16:0_18:1 as $[M+H]^+$

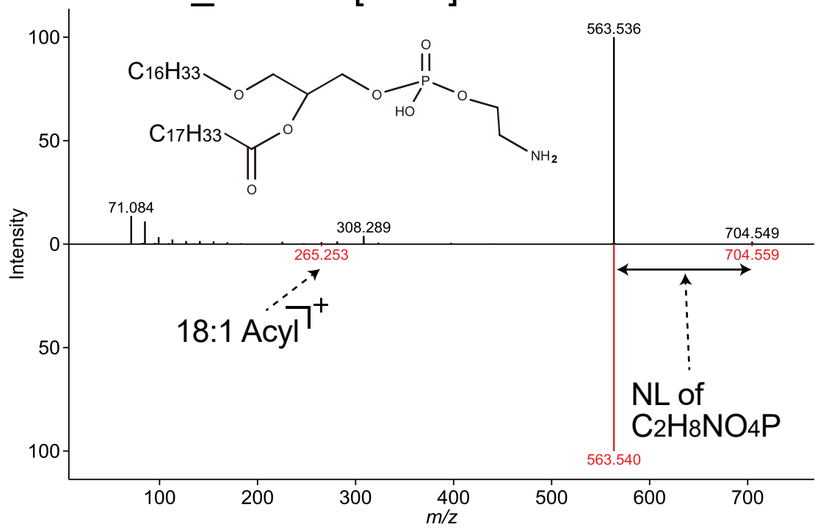

ESI(-)-MS/MS for Glycerophospholipids [GP]: CL, MLCL, DLCL, LNAPE, LNAPS, LPA, LPC, Ether LPC, LPE

CL 16:0_18:1_18:2_18:2 as $[M-H]^-$

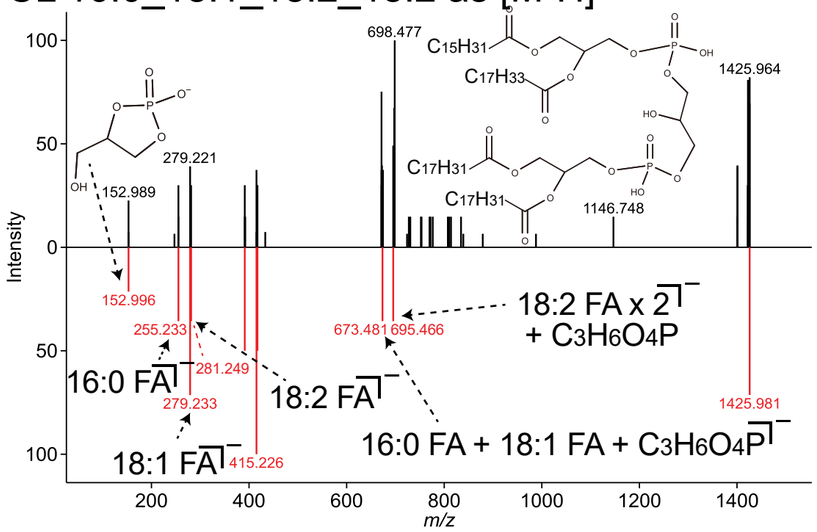

MLCL 16:0_16:0_16:0 as $[M-H]^-$

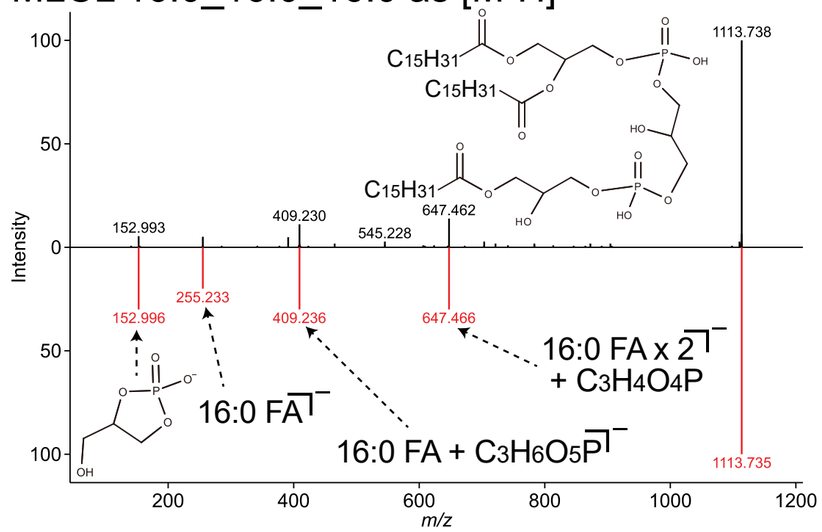

DLCL 16:0_18:2 as $[M-H]^-$

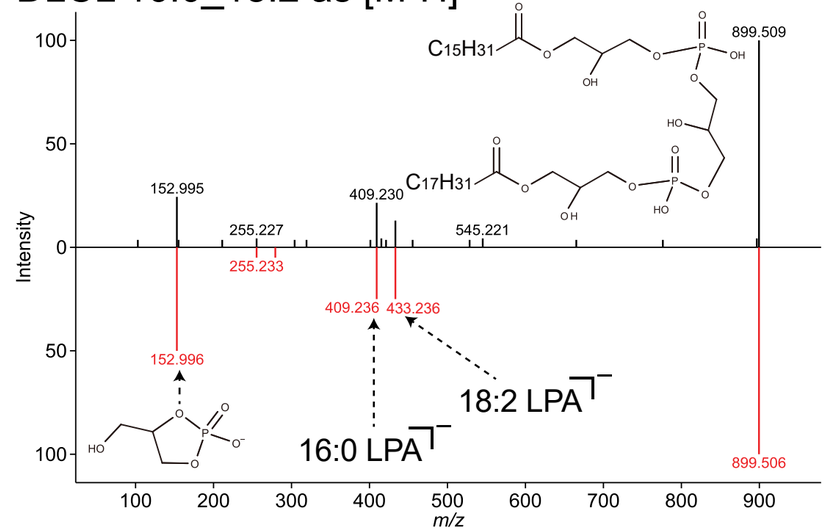

LNAPE 16:0/N-18:2 as $[M-H]^-$

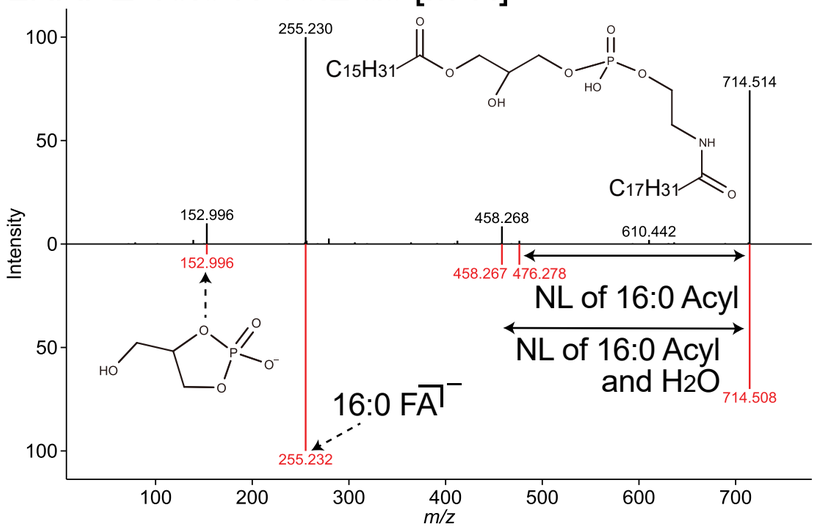

LNAPS 18:0/N-16:0 as $[M-H]^-$

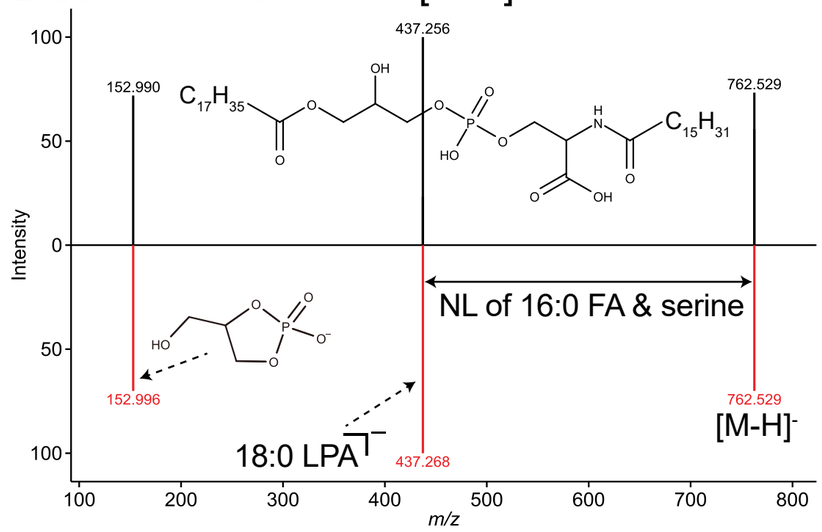

LPA 16:0 as $[M-H]^-$

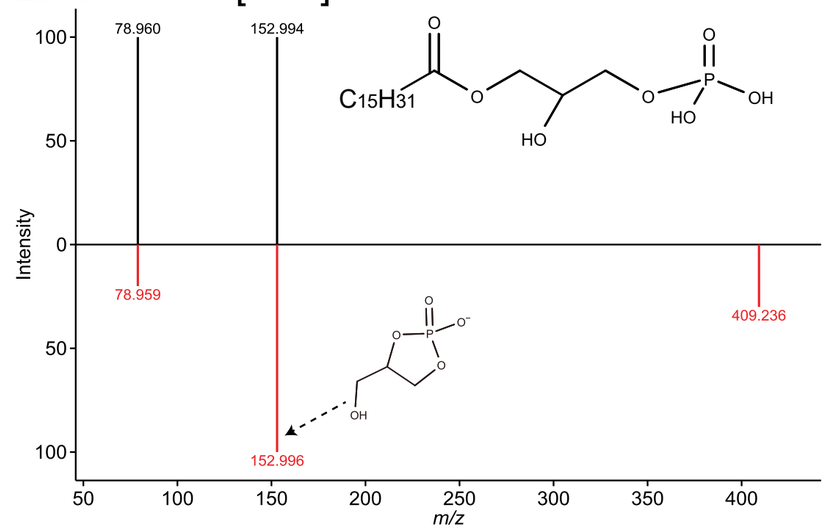

LPC 18:1 as $[M+CH_3COO]^-$

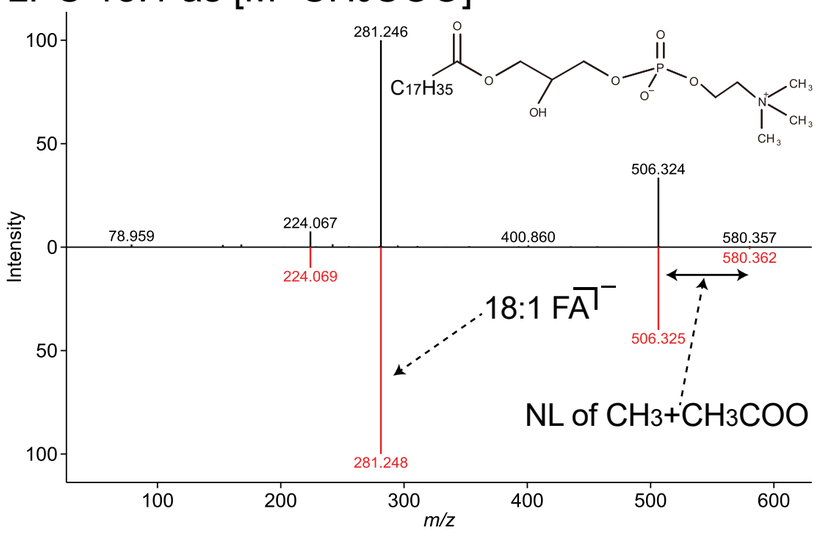

LPC O-18:1 as $[M+CH_3COO]^-$

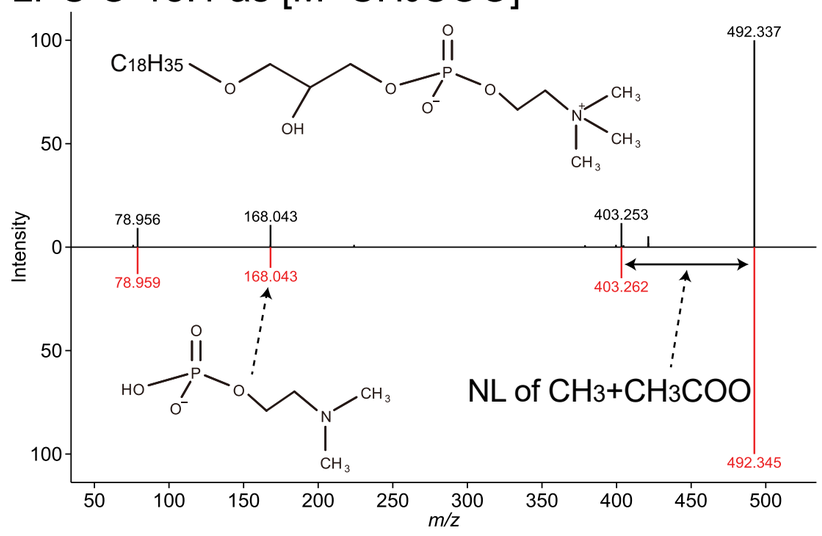

LPE 18:1 as $[M-H]^-$

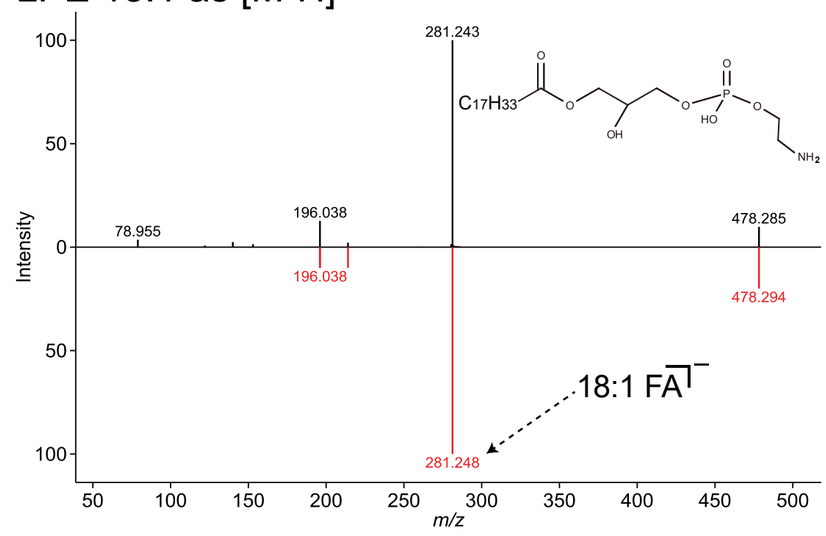

ESI(-)-MS/MS for Glycerophospholipids [GP]: Ether LPE, LPG, Ether LPG, LPI, LPS, PA, PC, Ether PC, PE

LPE O-18:1 (LPE P-18:0) as [M-H]$^-$

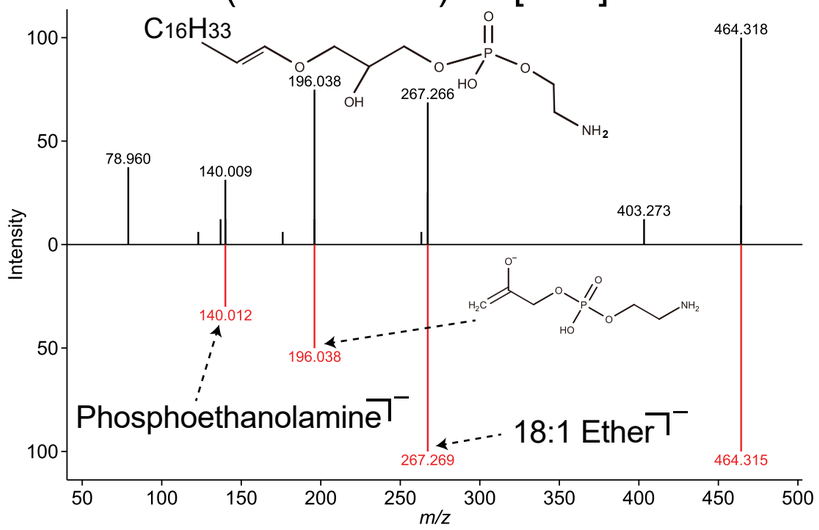

LPG 18:1 as [M-H]$^-$

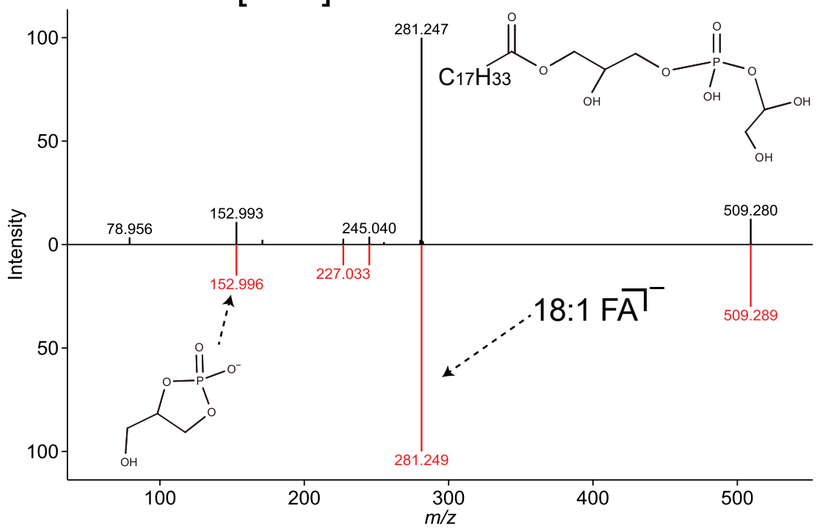

LPG O-18:1 as [M-H]$^-$

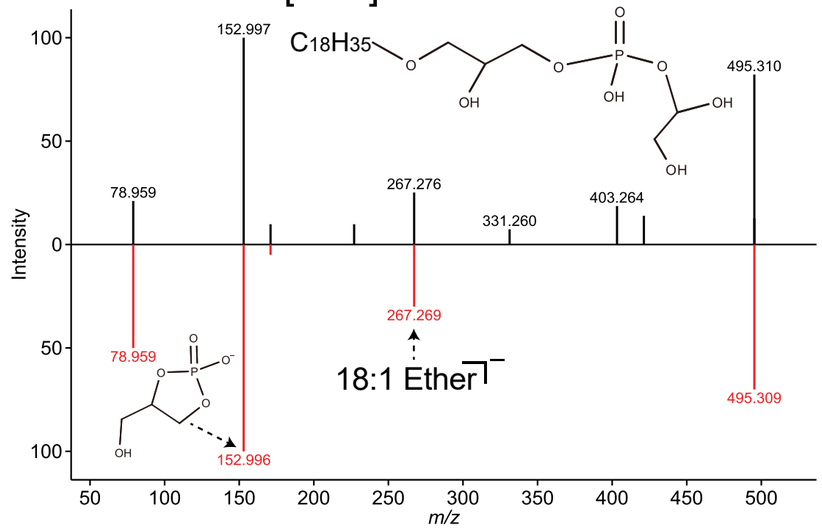

LPI 18:1 as [M-H]$^-$

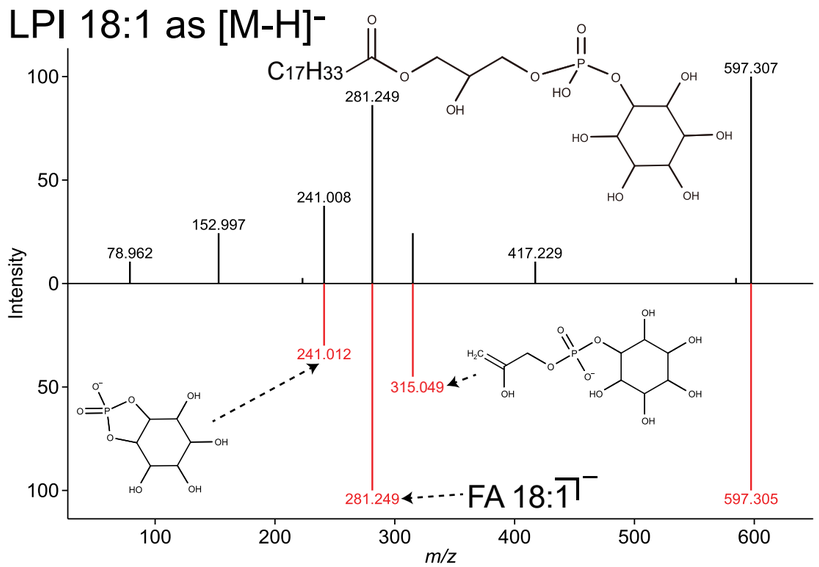

LPS 18:0 as [M-H]$^-$

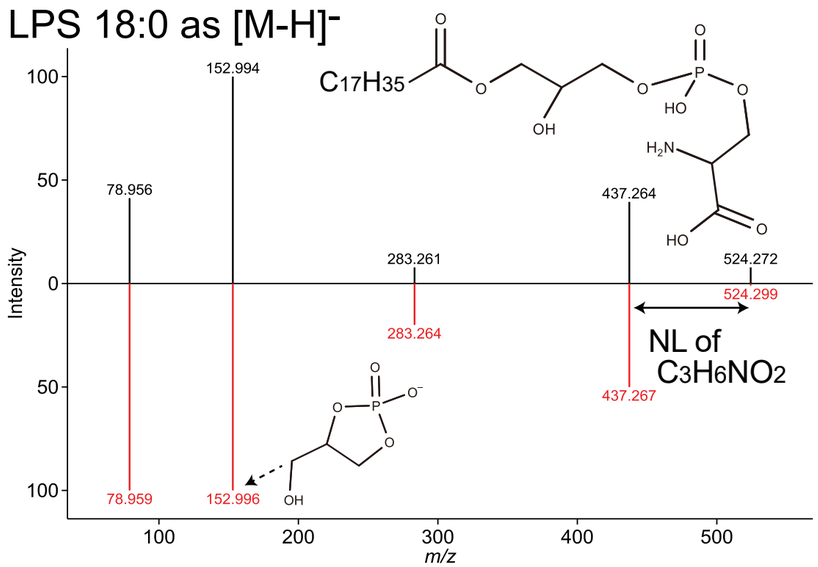

PA 16:0_18:1 as [M-H]$^-$

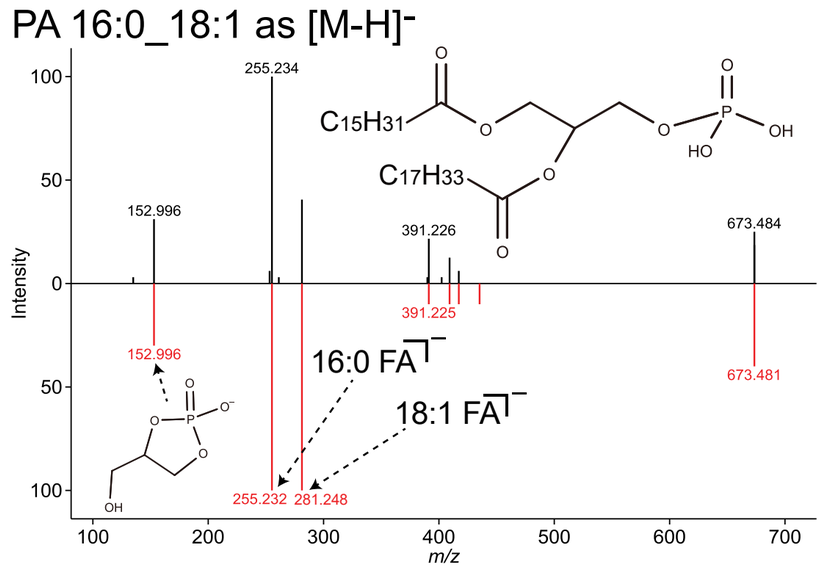

PC 18:0_20:4 as [M+CH3COO]$^-$

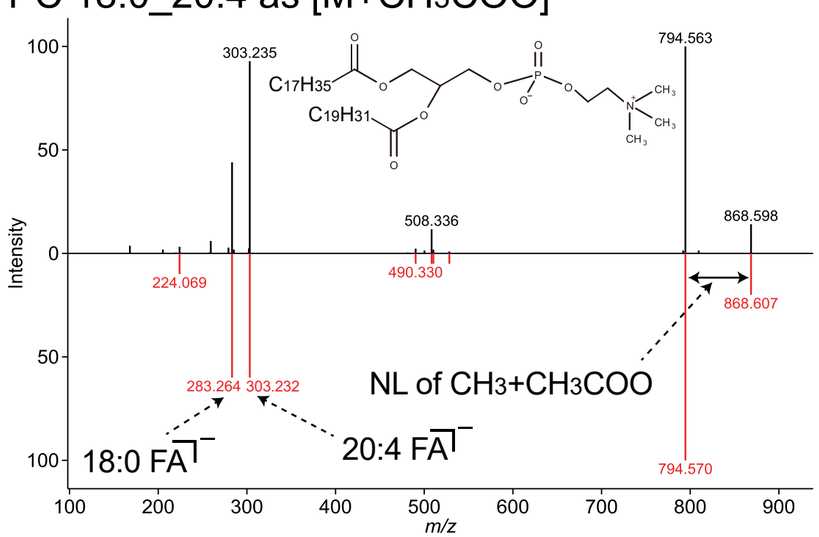

PC O-18:0_20:4 as [M+CH3COO]$^-$

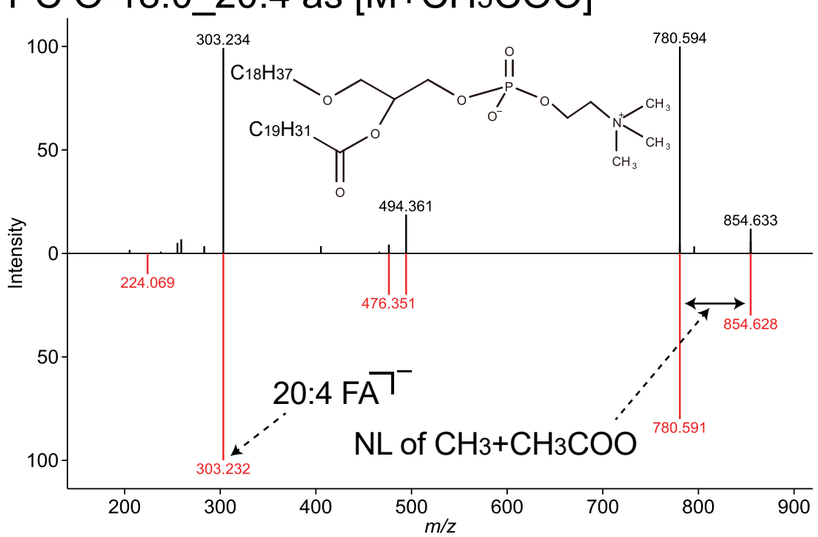

PE 18:0_20:4 as [M-H]$^-$

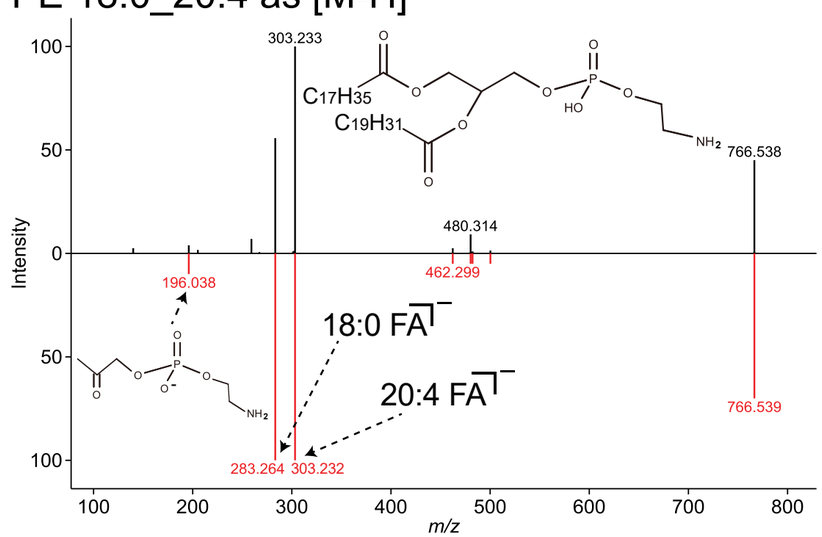

ESI(-)-MS/MS for Glycerophospholipids [GP]: Ether PE, PG, Ether PG, PI, Ether PI, PS, Ether PS, PMeOH, PEtOH

PE O-16:0_18:1 as [M-H]-

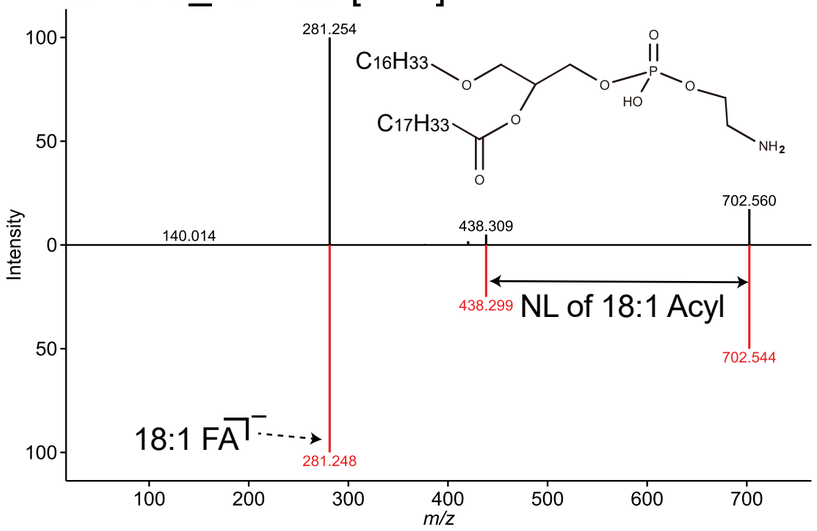

PG 18:0_20:4 as [M-H]-

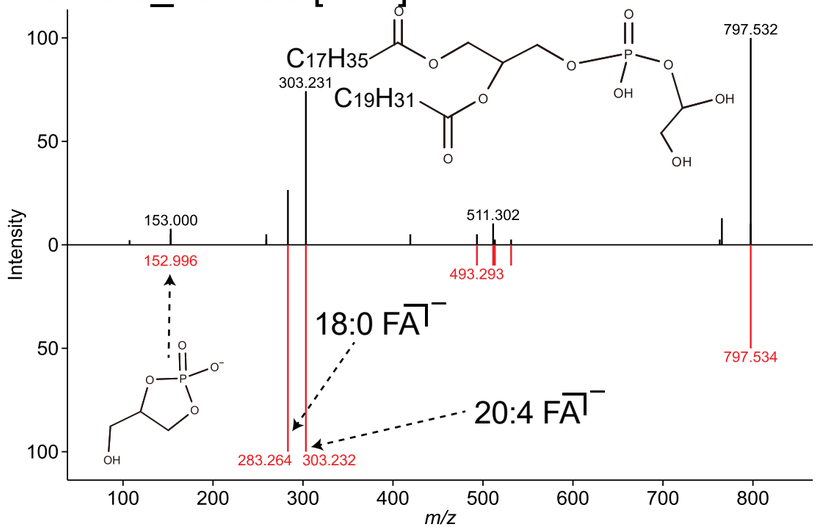

PG O-18:1_16:0 as [M-H]-

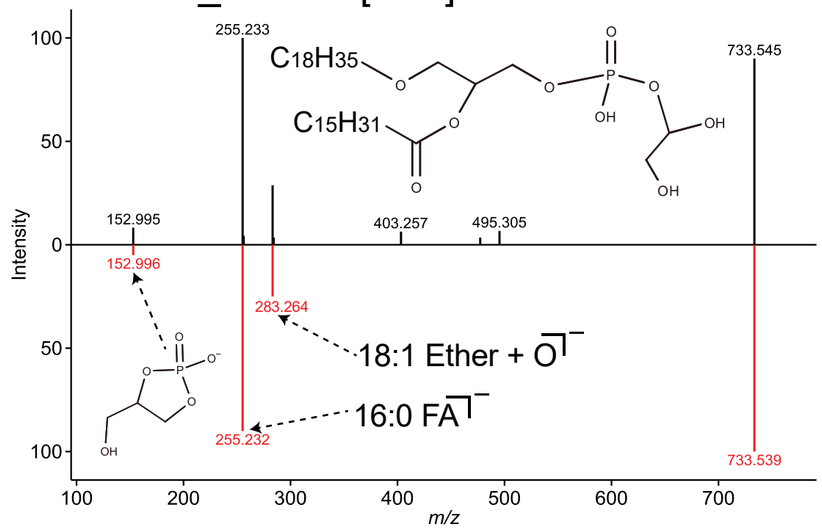

PI 18:0_20:4 as [M-H]-

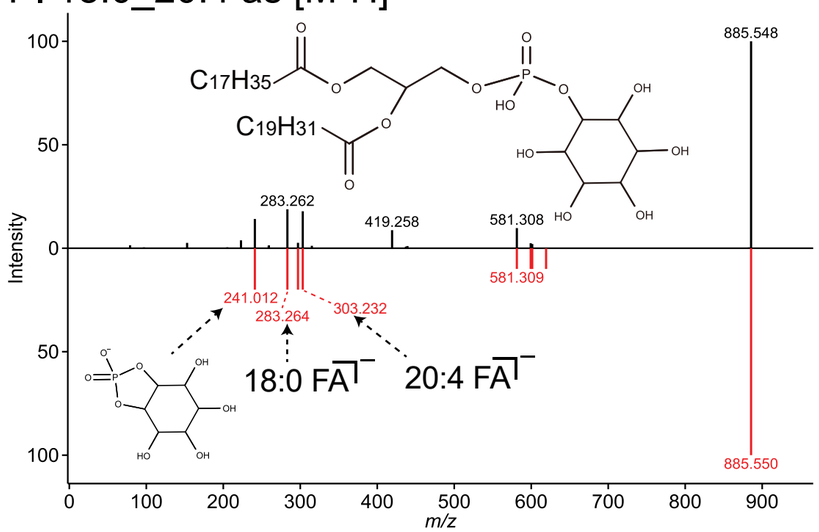

PI O-16:0_20:4 as [M-H]-

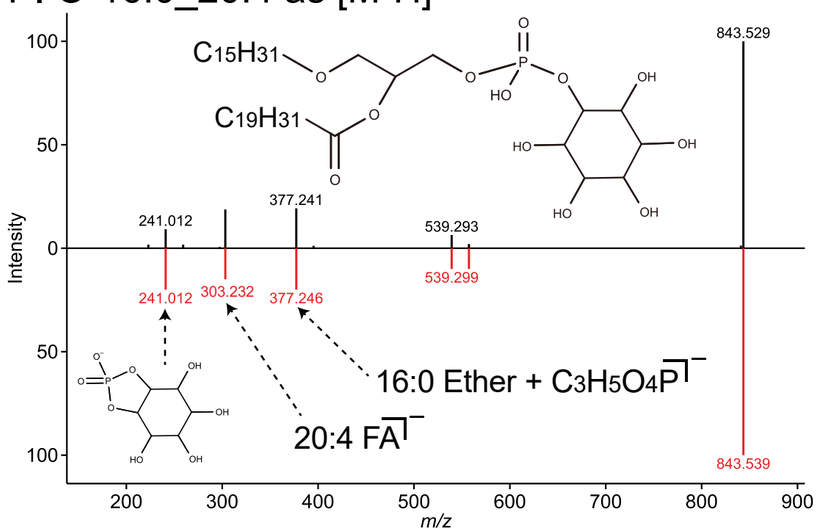

PS 18:0_20:4 as [M-H]-

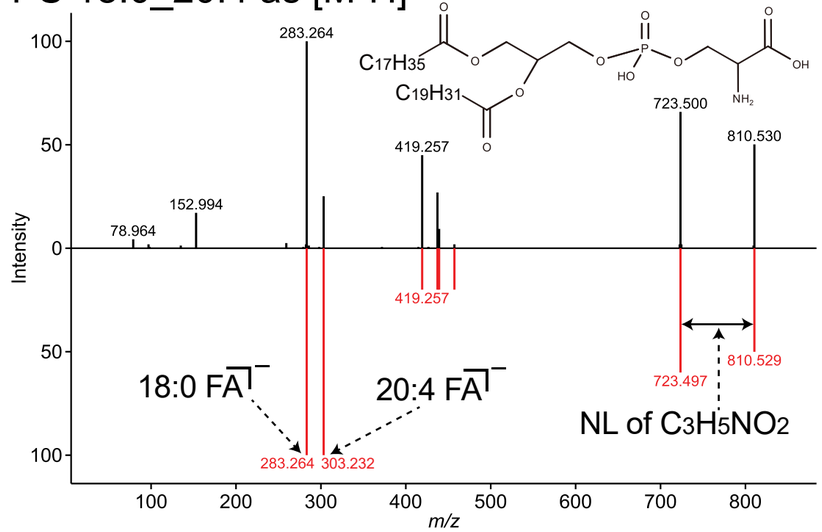

PS O-16:0_22:6 as [M-H]-

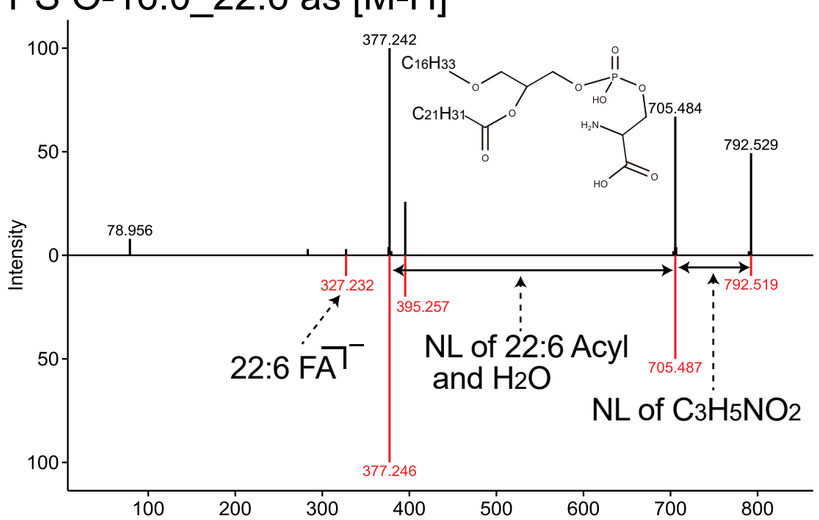

PMeOH 16:0_18:2 as [M-H]-

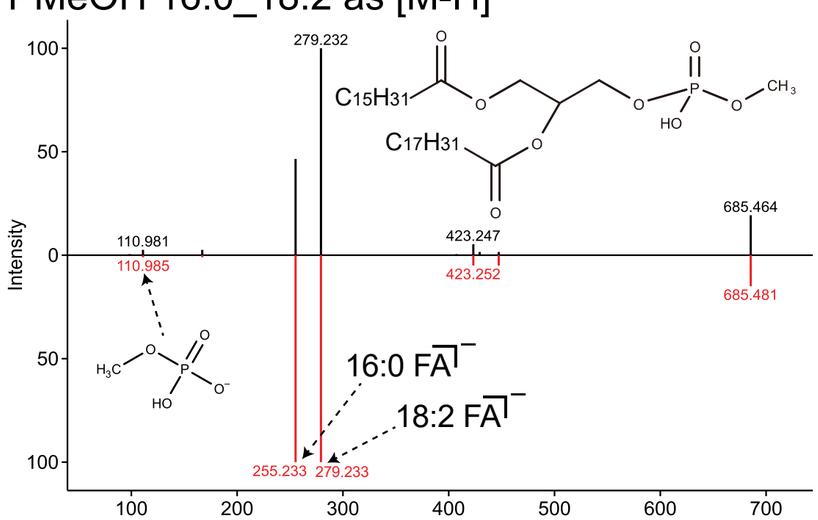

PEtOH 18:0_20:4 as [M-H]-

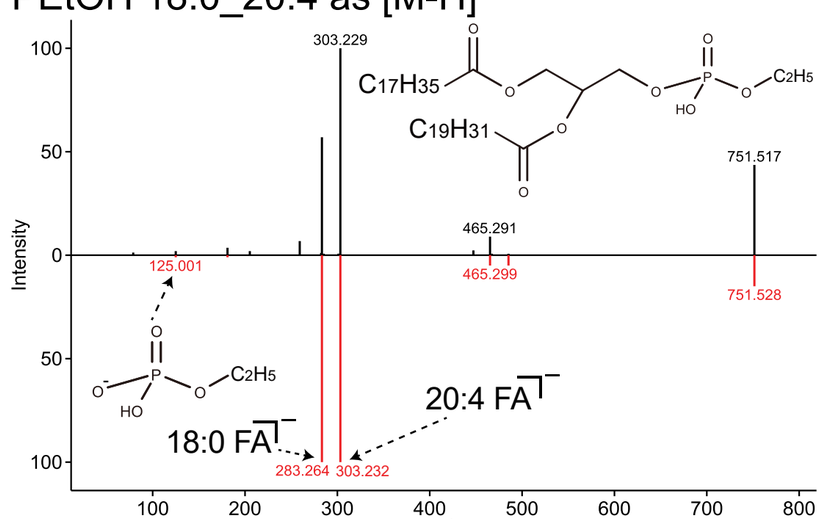

ESI(-)-MS/MS for Glycerophospholipids [GP]: OxPC, OxPE, Ether OxPE, OxPG, OxPI, OxPS, HBMP

(OxPC) PC 16:0_18:2;O as $[M+CH_3COO]^-$

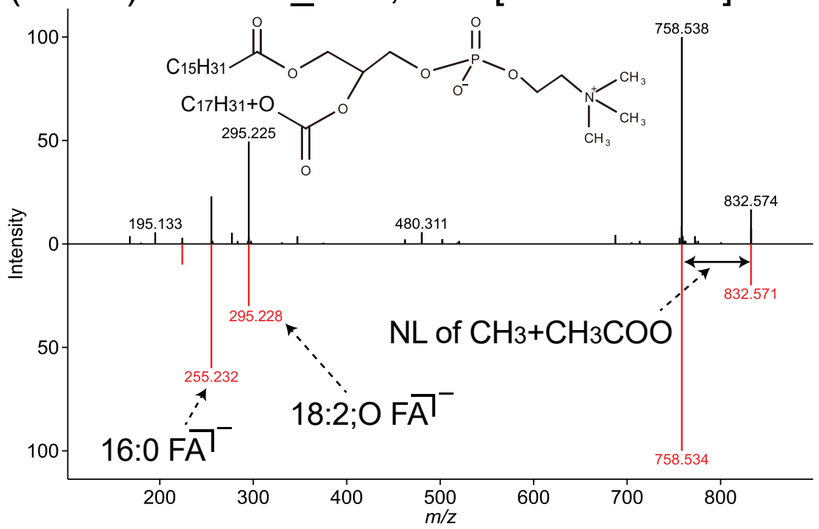

(OxPE) PE 18:0_20:4;4O as $[M-H]^-$

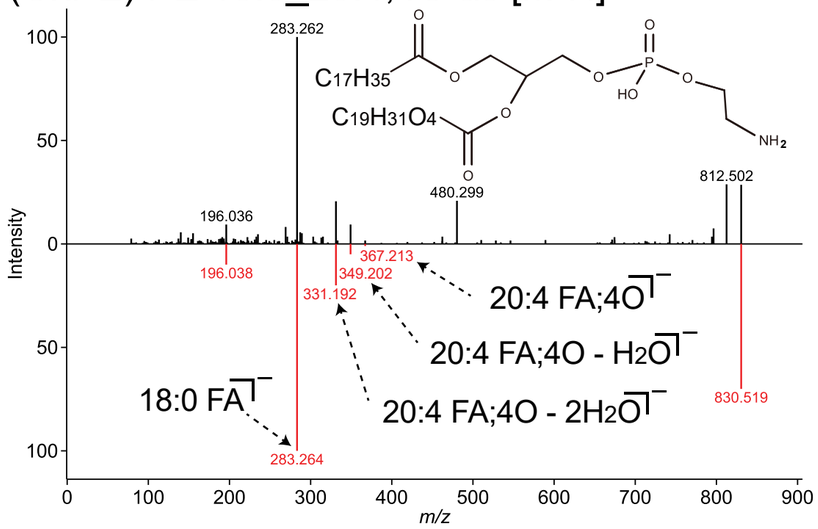

(Ether OxPE) PE O-16:0_22:6;O as $[M-H]^-$

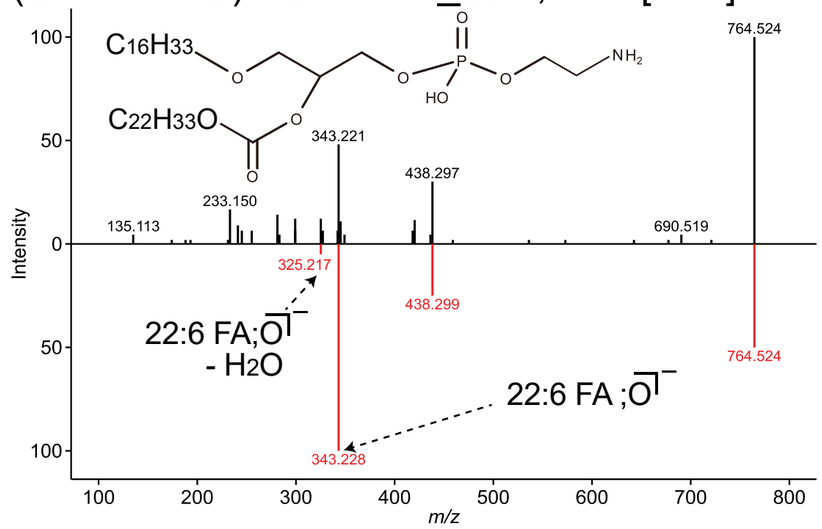

(OxPG) PG 16:0_18:3;O as $[M-H]^-$

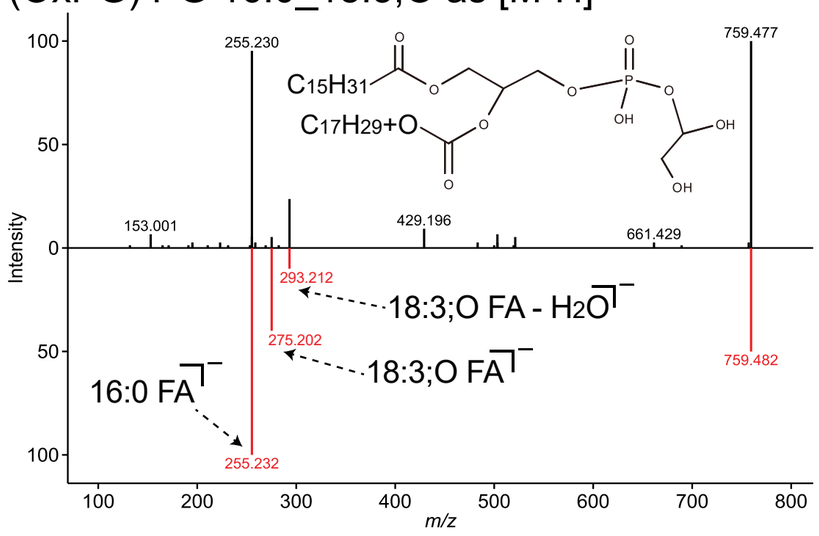

(OxPI) PI 18:0_20:4;4O as $[M-H]^-$

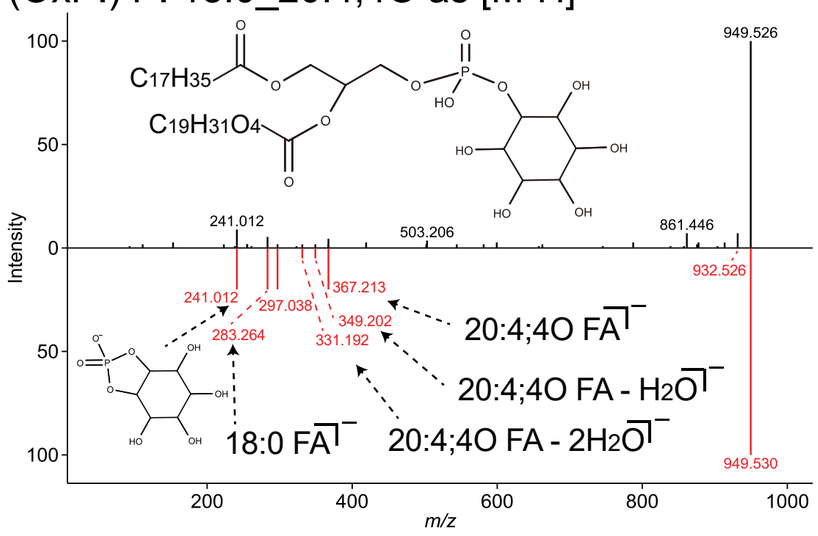

(OxPS) PS 18:0_20:4;4O as $[M-H]^-$

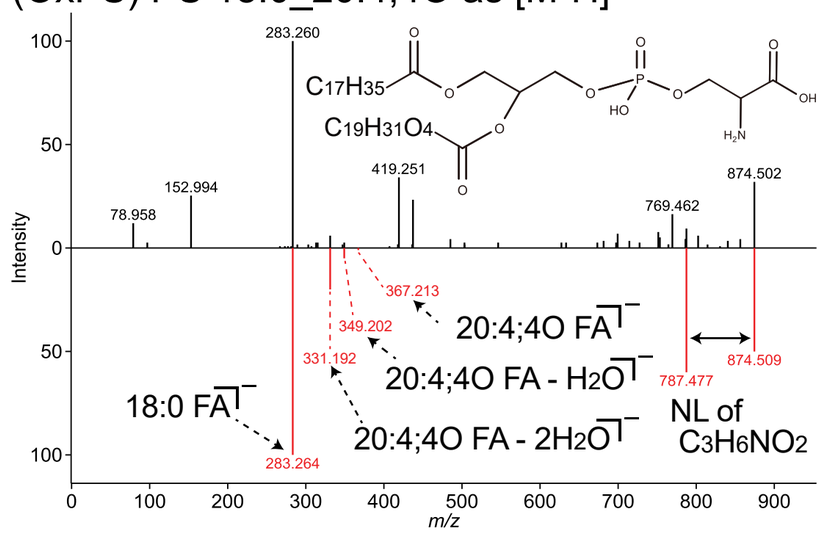

HBMP 16:0/16:0_18:2 as $[M-H]^-$

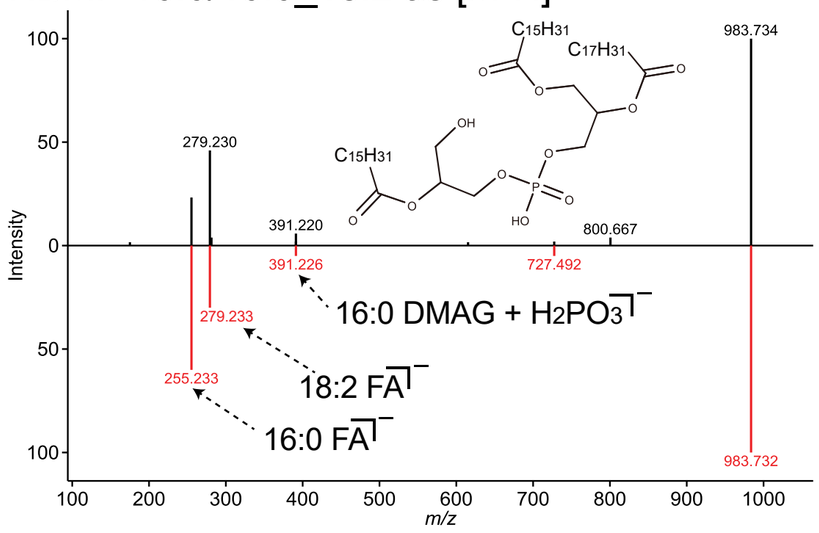

Sphingolipids [SP]

ESI(+)-MS/MS for Sphingolipids [SP]: Cer-AP, Cer-EOS, Cer-HDS, Cer-HS, Cer-NDS, Cer-NS, CerP, SM

(Cer-AP) Cer 18:1;3O/24:0;(2OH) as $[M+H]^+$

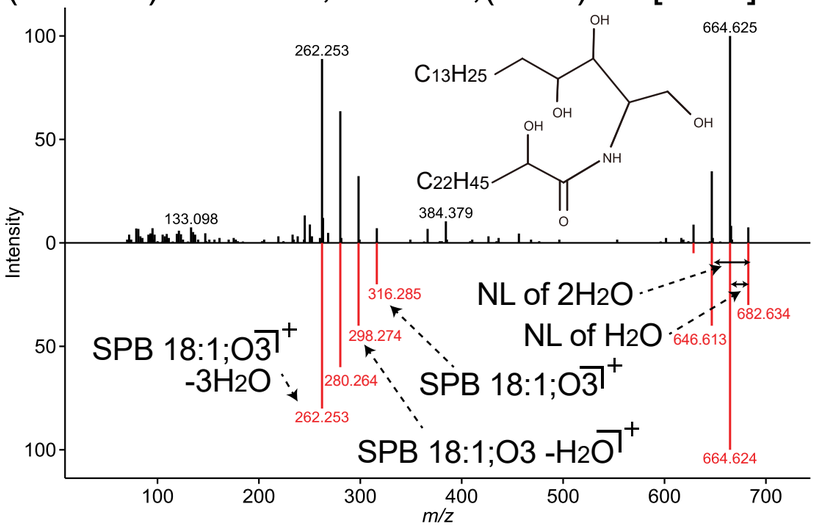

(Cer-EOS) Cer 18:1;2O/52:3 as $[M+H]^+$

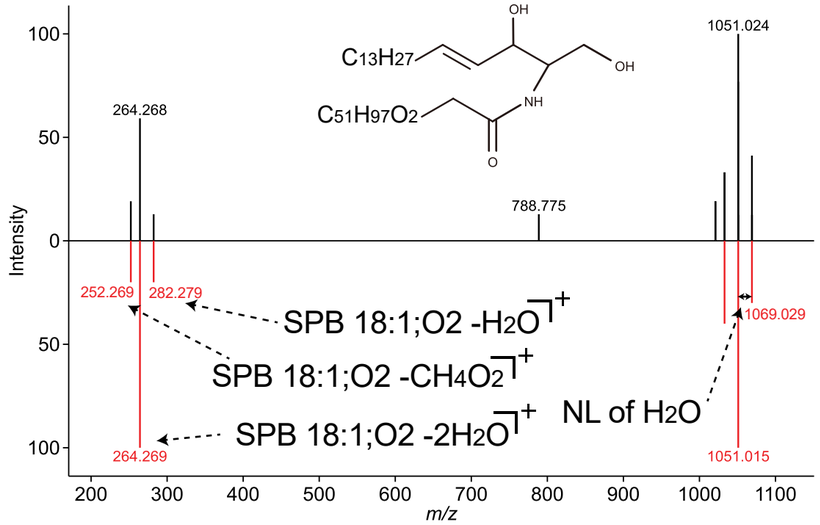

(Cer-HDS) Cer 19:0;2O/17:0;O as $[M+H]^+$

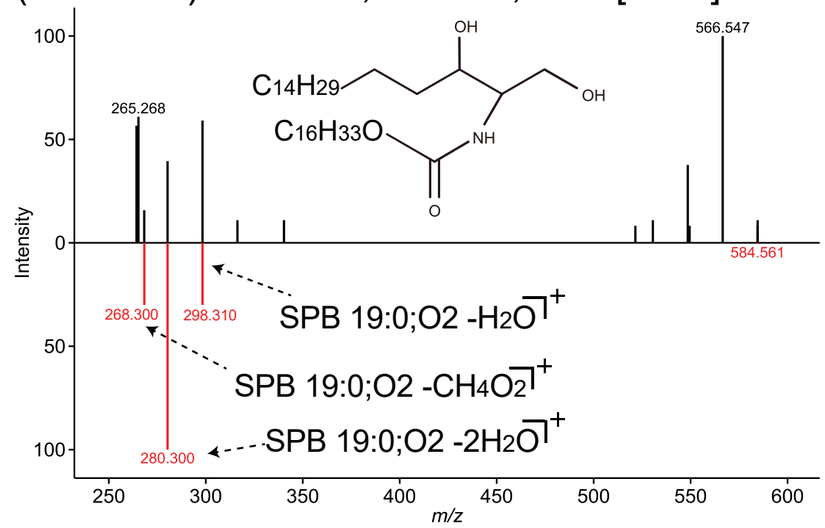

(Cer-HS) Cer 20:1;2O/24:0;O as $[M+H]^+$

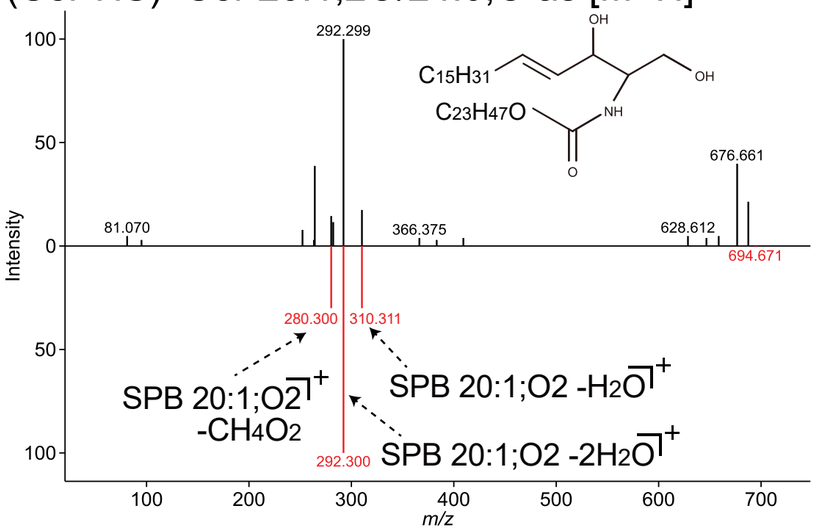

(Cer-NDS) Cer 18:0;2O/26:0 as $[M+H]^+$

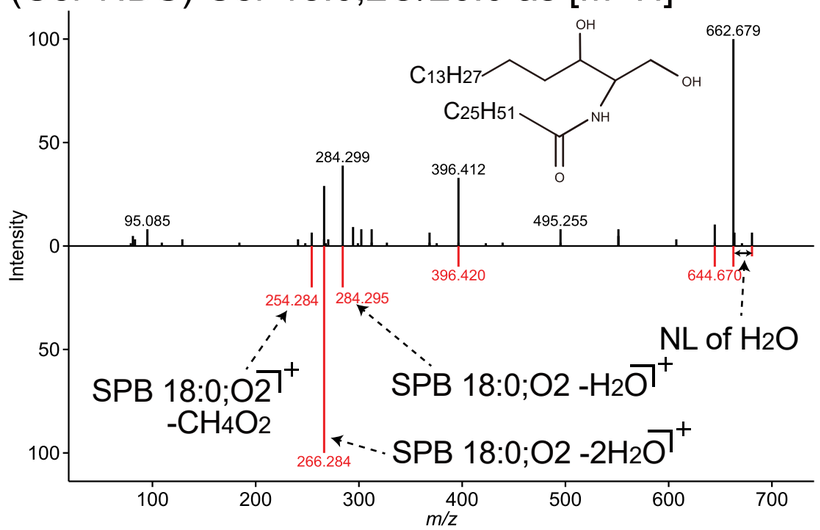

(Cer-NS) Cer 18:1;2O/24:0 as $[M+H]^+$

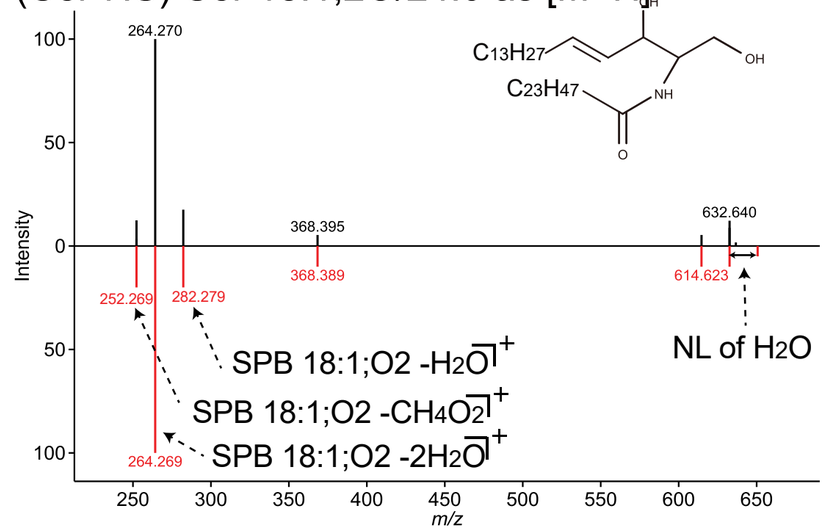

CerP 18:1;2O/12:0 as $[M+H]^+$

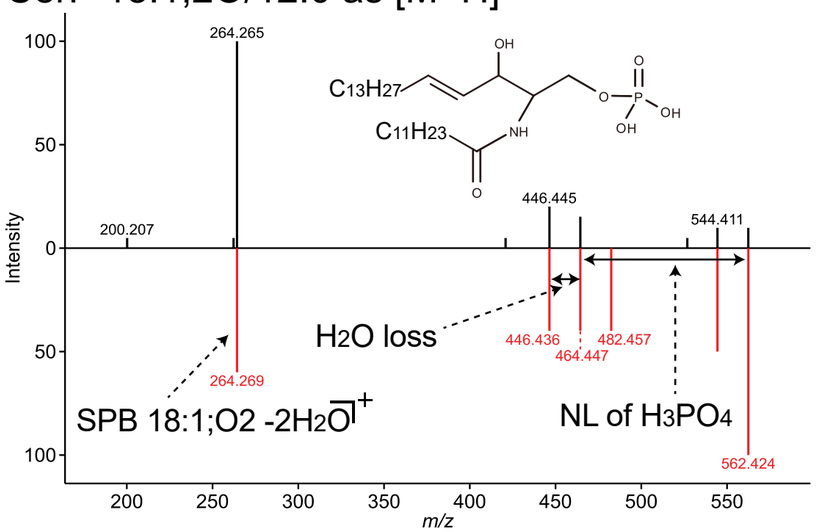

SM 18:1;2O/16:0 as $[M+H]^+$

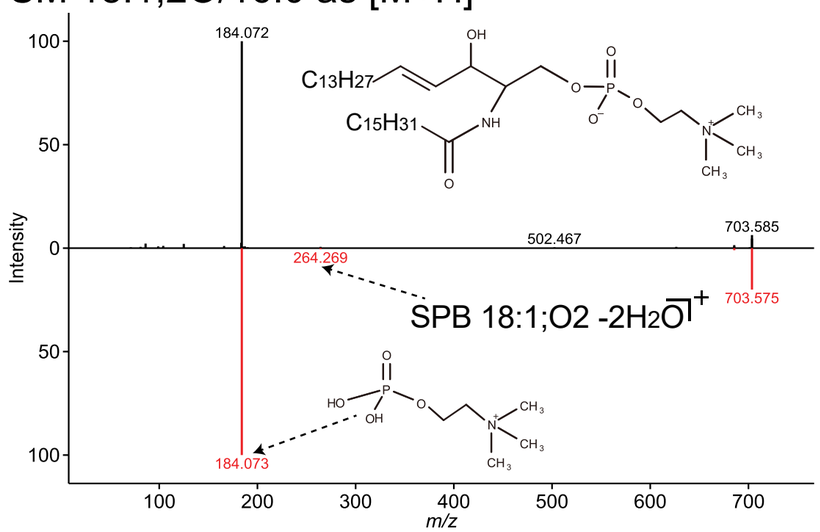

SM 34:1;2O as $[M+Na]^+$

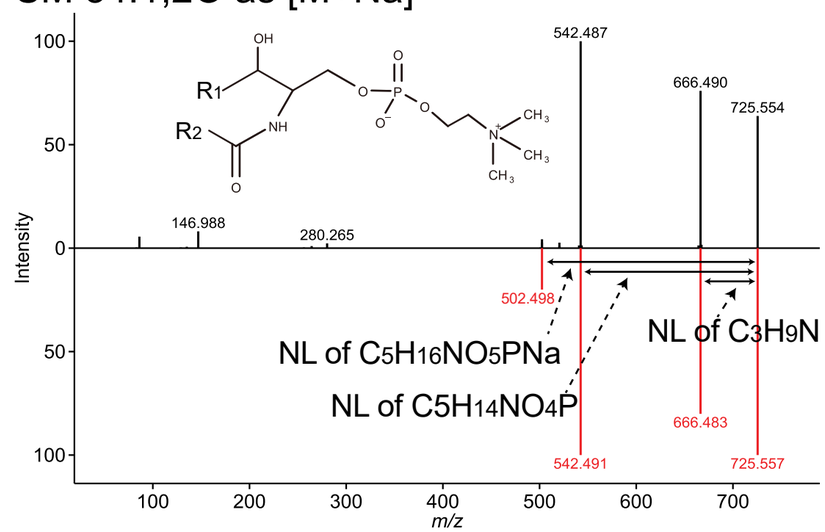

ESI(+)-MS/MS for Sphingolipids [SP]: SM+O, Sphinganine, Sphingosine, Phytosphingosine, HexCer-AP, HexCer-EOS, HexCer-HDS, HexCer-HS, HexCer-NDS

SM 34:1;3O as $[M+H]^+$

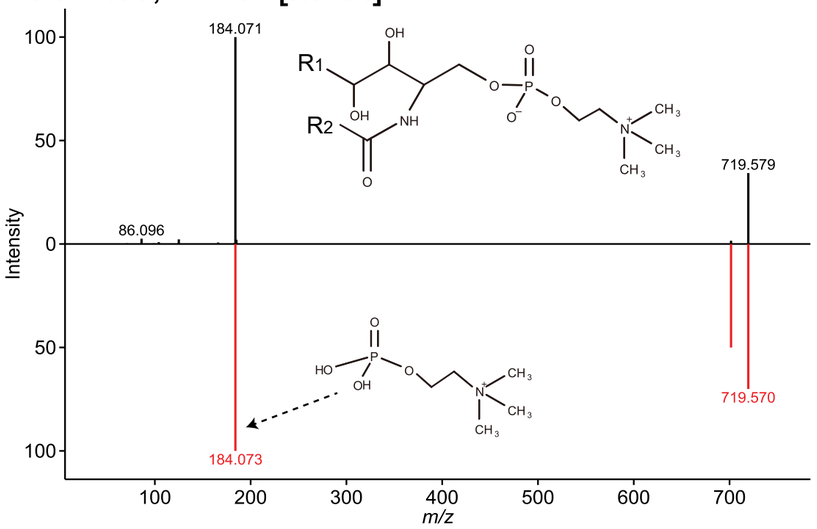

(DHSph) SPB 17:0;2O as $[M+H]^+$

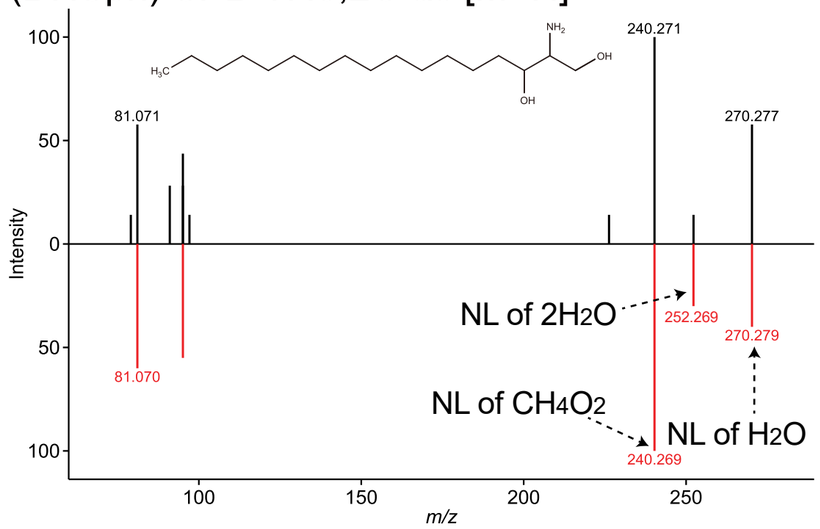

(Sph) SPB 18:1;2O as $[M+H]^+$

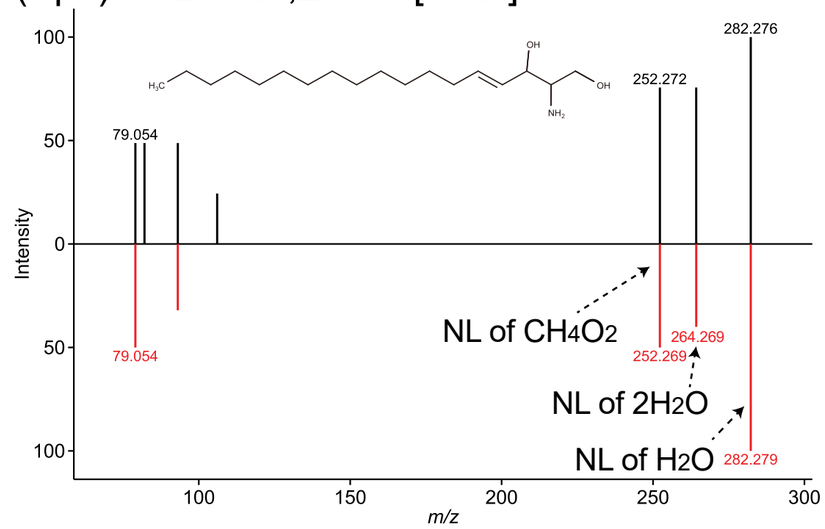

(PhytoSph) SPB 18:0;3O as $[M+H]^+$

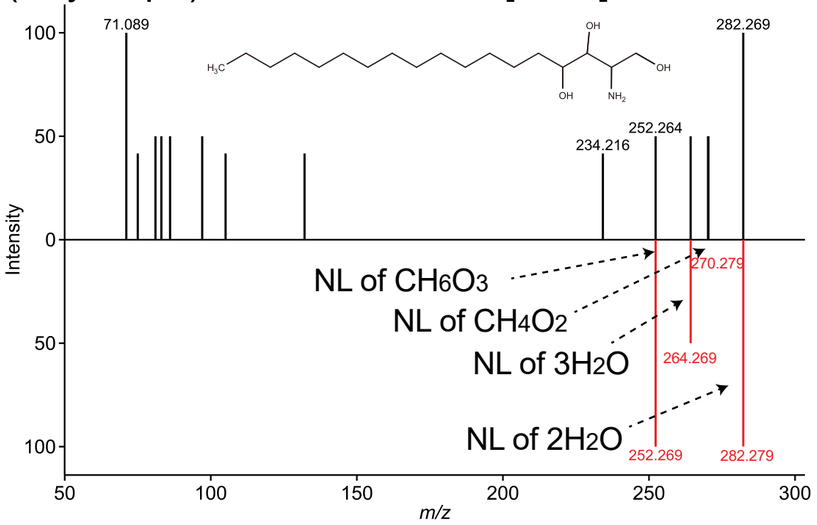

(HexCer-AP) HexCer 18:0;3O/24:0;(2OH) as $[M+H]^+$

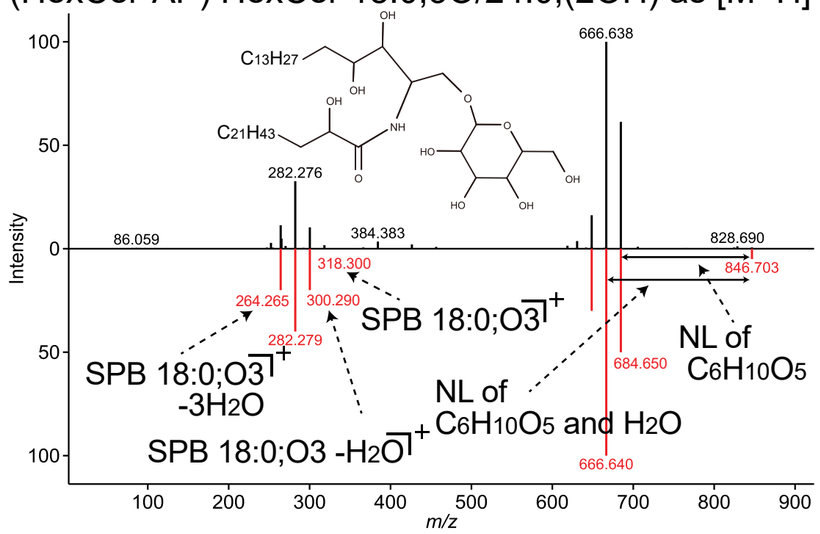

(HexCer-EOS) HexCer 17:1;2O/52:4 as $[M+H]^+$

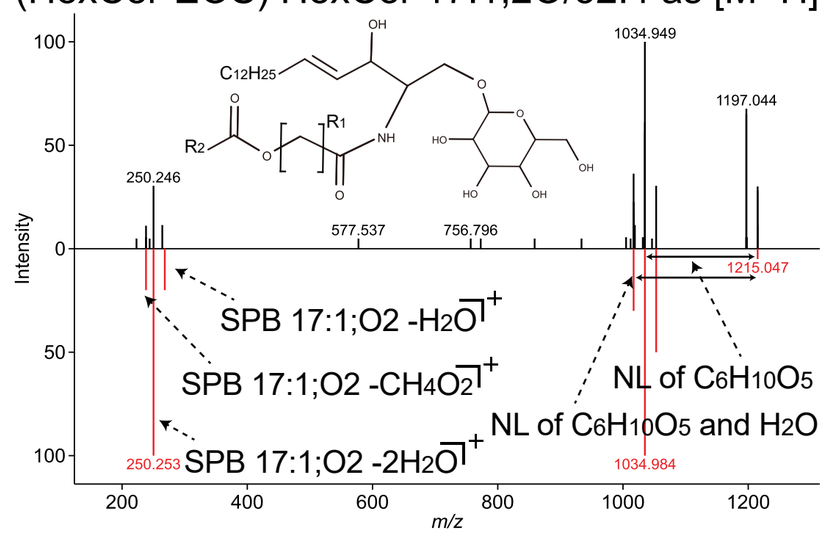

(HexCer-HDS) HexCer 18:0;2O/16:0;O as $[M+H]^+$

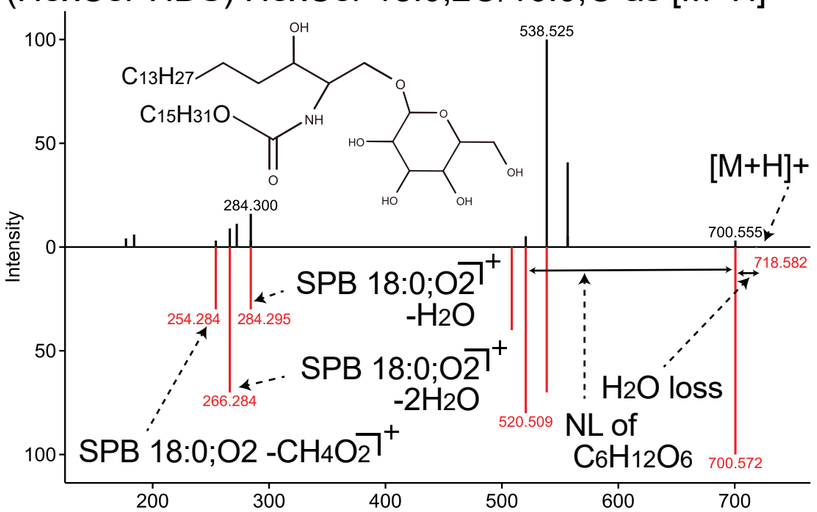

(HexCer-HS) HexCer 18:1;2O/24:1;O as $[M+H]^+$

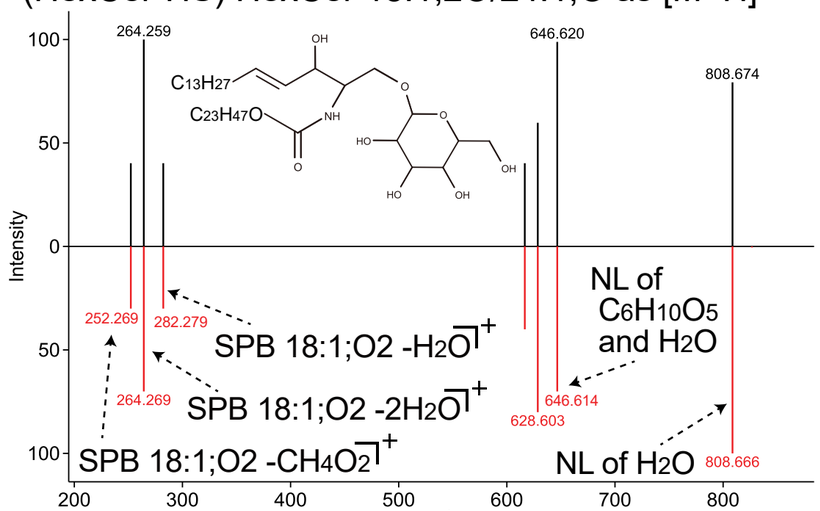

(HexCer-NDS) HexCer 18:0;2O/22:0 as $[M+H]^+$

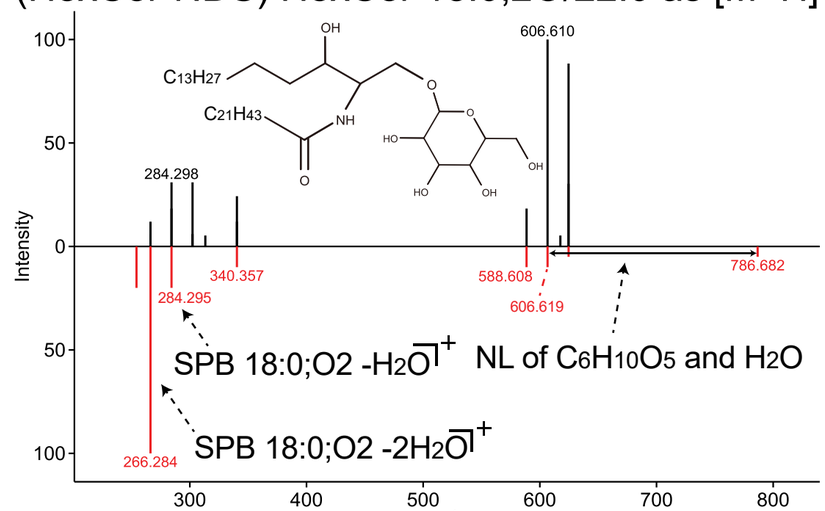

ESI(+)-MS/MS for Sphingolipids [SP]: HexCer-NS, Hex2Cer, Hex3Cer, PI-Cer+O, SHexCer, SHexCer+O, SL, SL+O, GM3

(HexCer-NS) HexCer 18:1;2O/24:0 as $[M+H]^+$

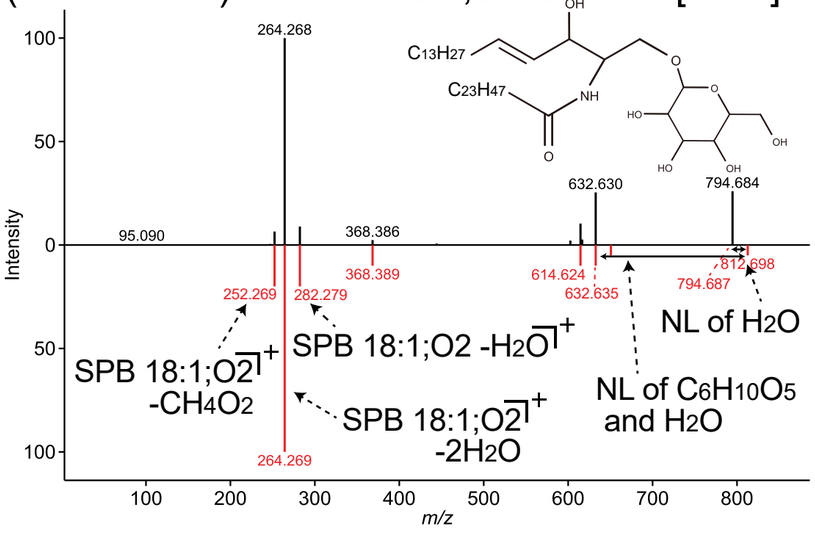

Hex2Cer 18:1;2O/16:0 as $[M+H]^+$

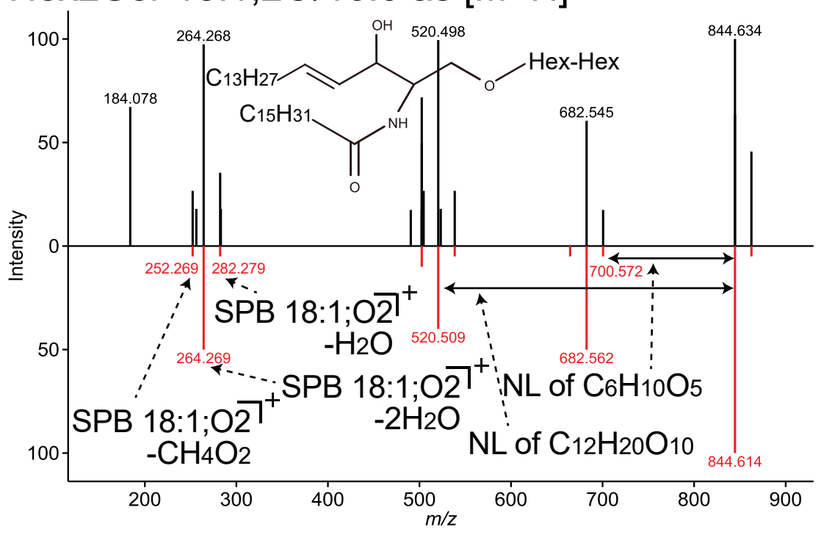

Hex3Cer 18:1;2O/16:0; $[M+H]^+$

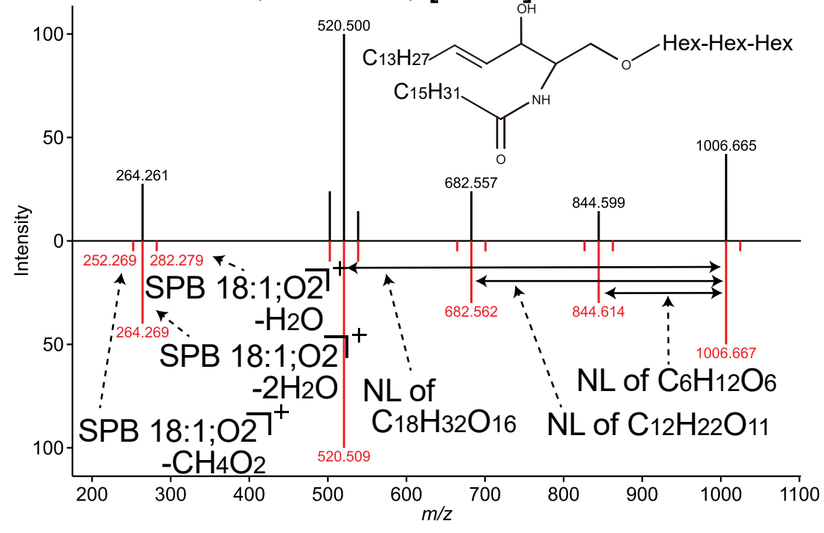

PI-Cer 34:0;3O as $[M+H]^+$

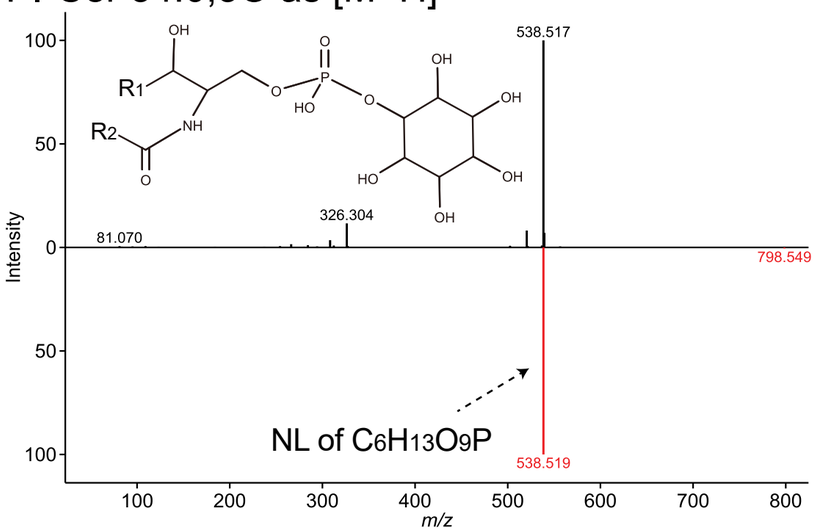

SHexCer 18:1;2O/18:0 as $[M+H]^+$

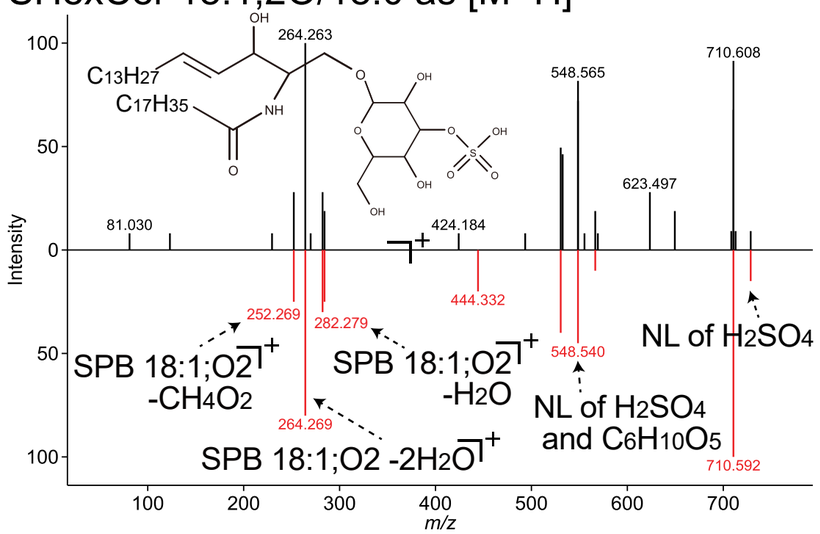

SHexCer 18:1;2O/18:0;O as $[M+H]^+$

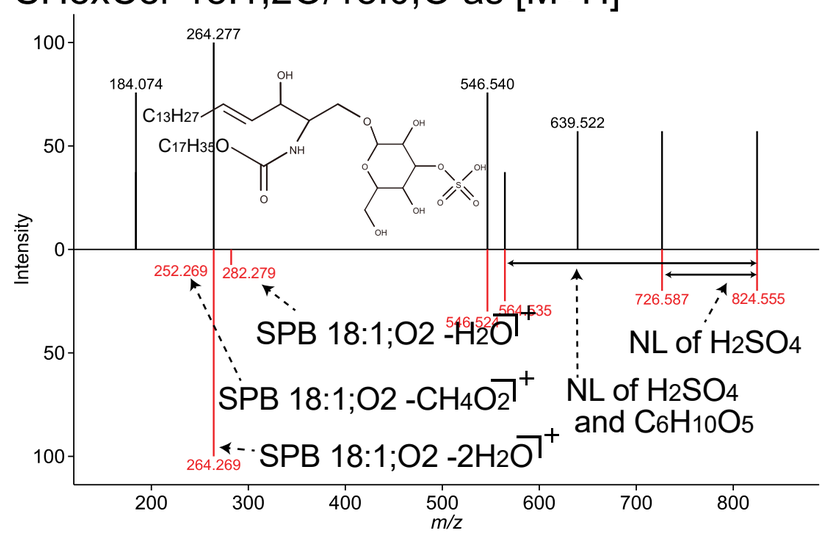

SL 18:0;O/15:0 as $[M+NH_4]^+$

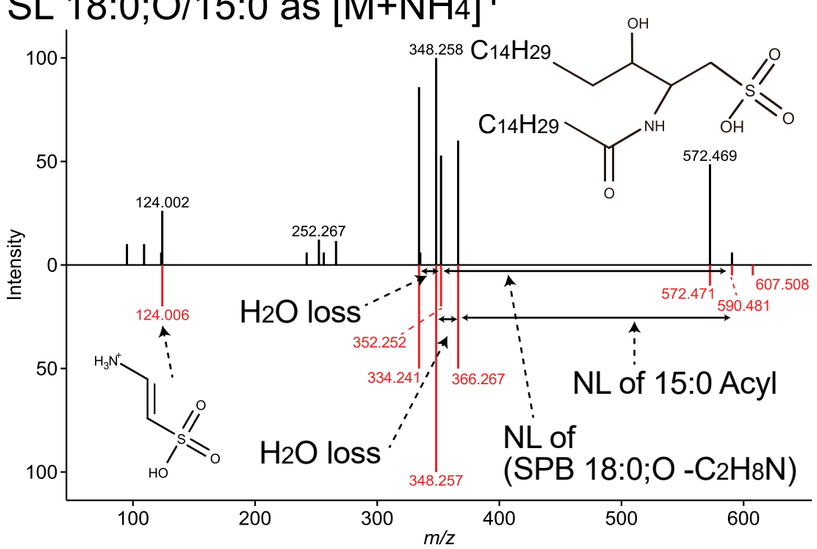

SL 17:0;O/16:1;O as $[M+H]^+$

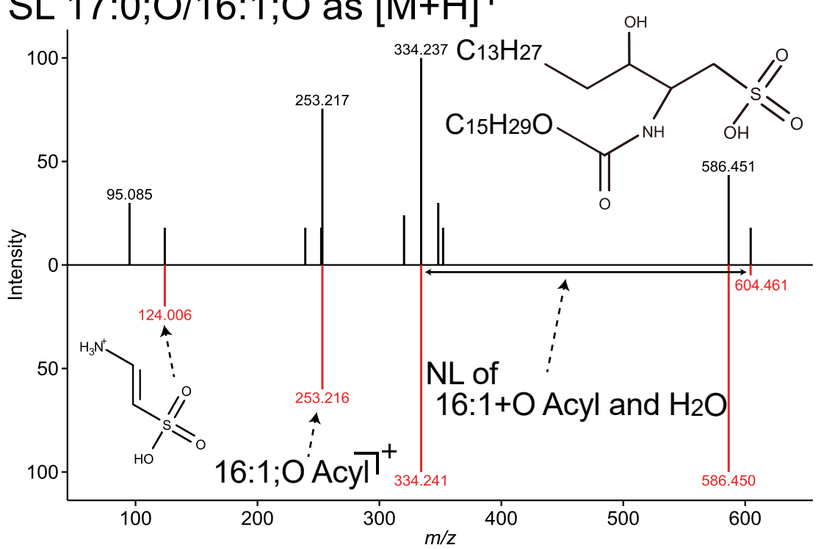

GM3 18:1;2O/18:0 as $[M+NH_4]^+$

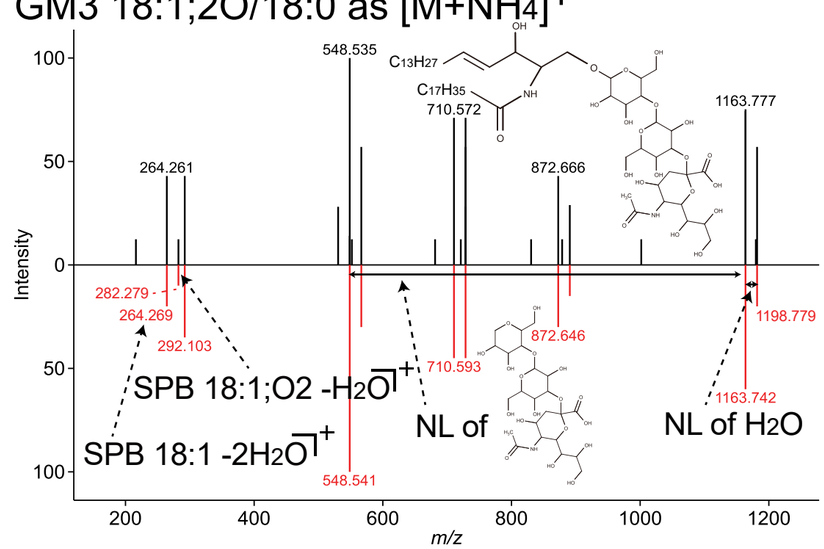

ESI(+)-MS/MS for Sphingolipids [SP]: AHexCer, ASM

AHexCer (O-16:0)18:1;2O/22:0;O as $[M+H]^+$

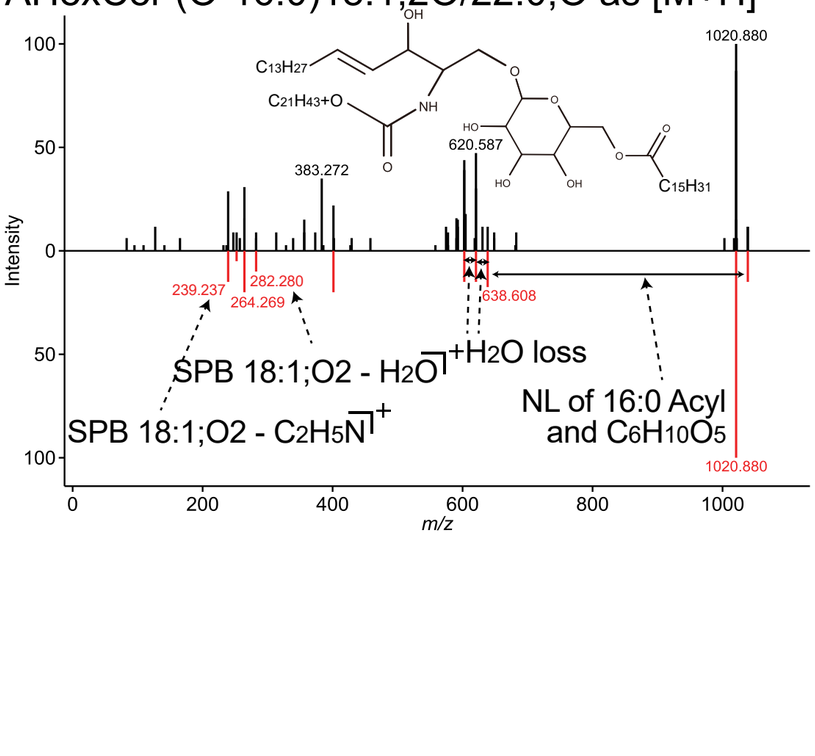

(ASM) SM 34:1;2O(FA 18:0) as $[M+H]^+$

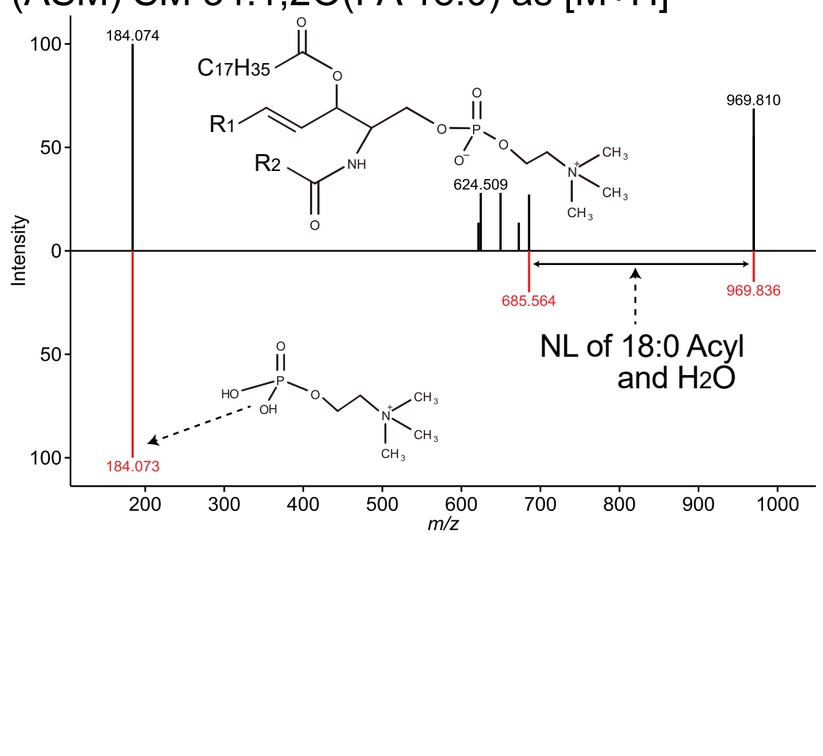

ESI(-)-MS/MS for Sphingolipids [SP]: Cer-ADS, Cer-AS, Cer-BDS, Cer-BS, Cer-AP, Cer-HS, Cer-EOS, Cer-EODS, Cer-EBDS

(Cer-ADS) Cer 18:0;2O/16:0;(2OH) as $[M+CH_3COO]^-$

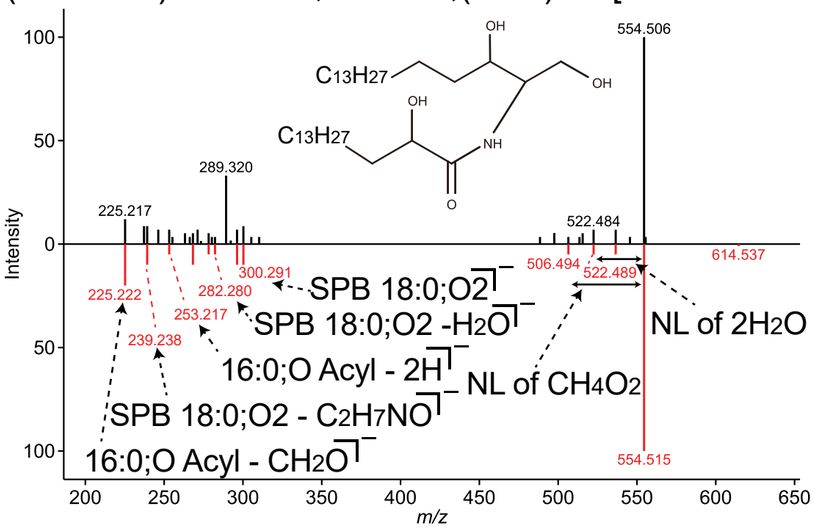

(Cer-AS) Cer 18:1;2O/16:0;(2OH) as $[M+CH_3COO]^-$

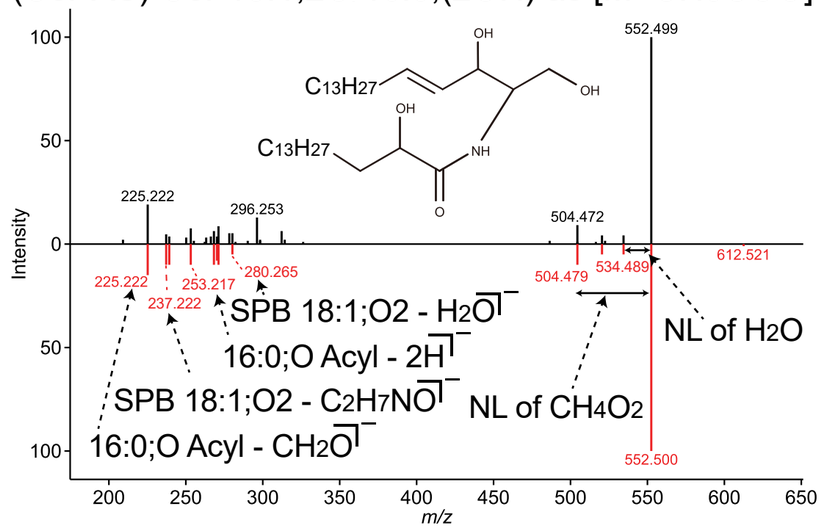

(Cer-BDS) Cer 18:0;2O/16:0;(3OH) as $[M-H]^-$

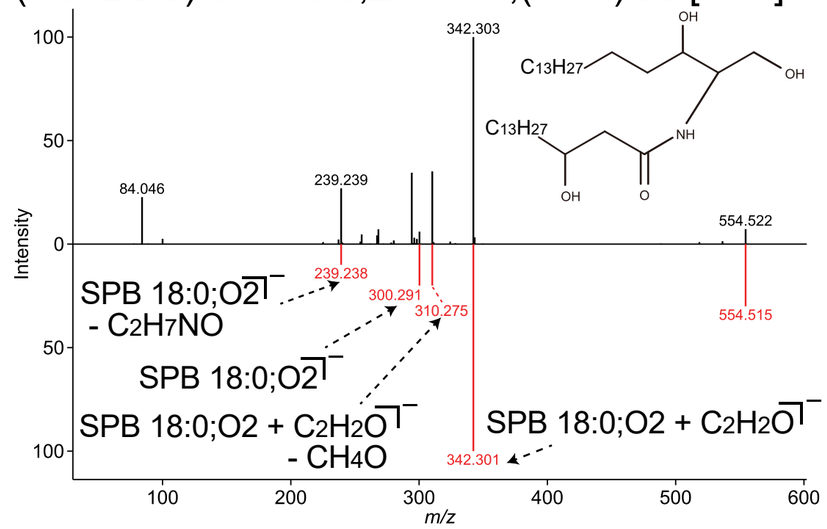

(Cer-BS) Cer 16:1;2O/24:0;(3OH) as $[M-H]^-$

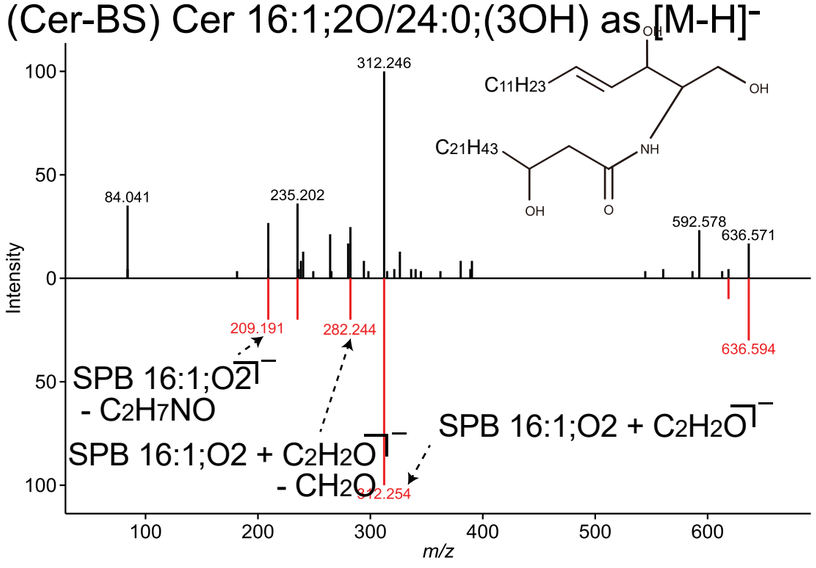

(Cer-AP) Cer 18:0;3O/20:0;(2OH) as $[M+CH_3COO]^-$

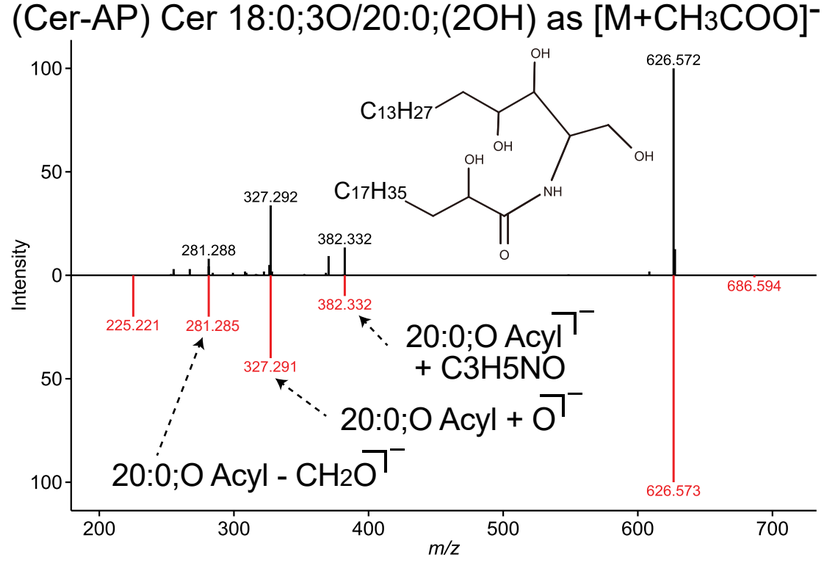

(Cer-HS) Cer 18:1;2O/22:0;O as $[M+CH_3COO]^-$

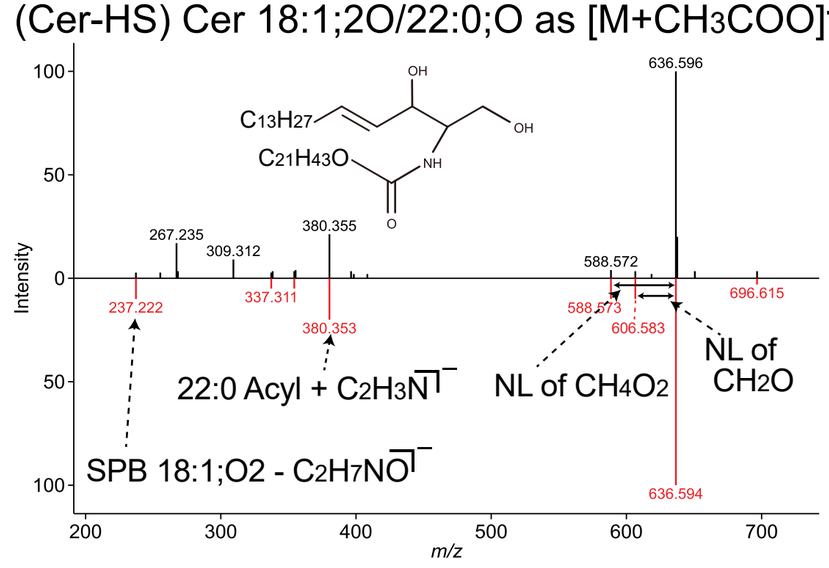

(Cer-EOS) Cer 18:1;2O/32:0;O(FA 18:2) as $[M+CH_3COO]^-$

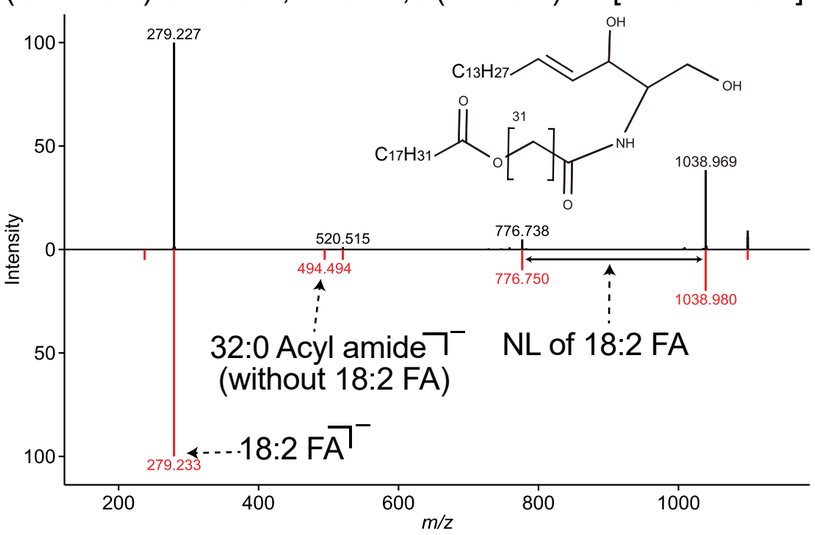

(Cer-EODS) Cer 18:0;2O/16:0;O(FA 15:0) as $[M-H]^-$

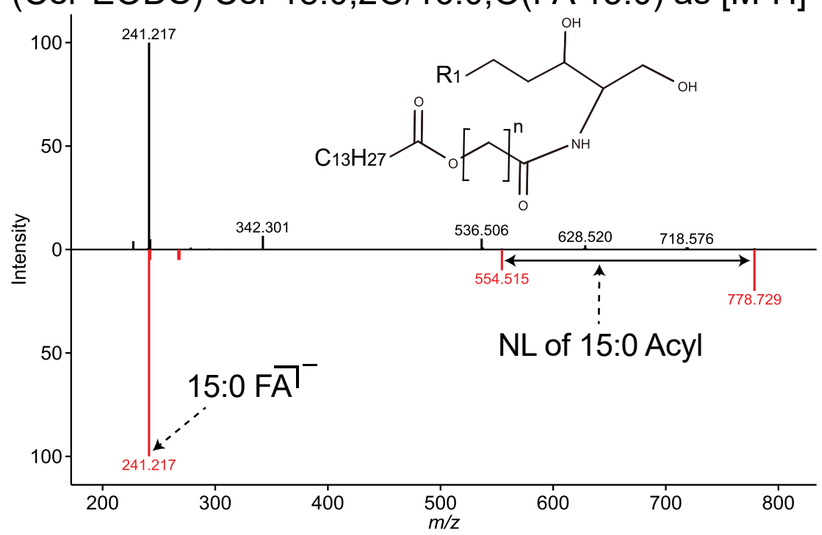

(Cer-EBDS) Cer 18:0;2O/17:0;(3OH)(FA 15:0) as $[M+CH_3COO]^-$

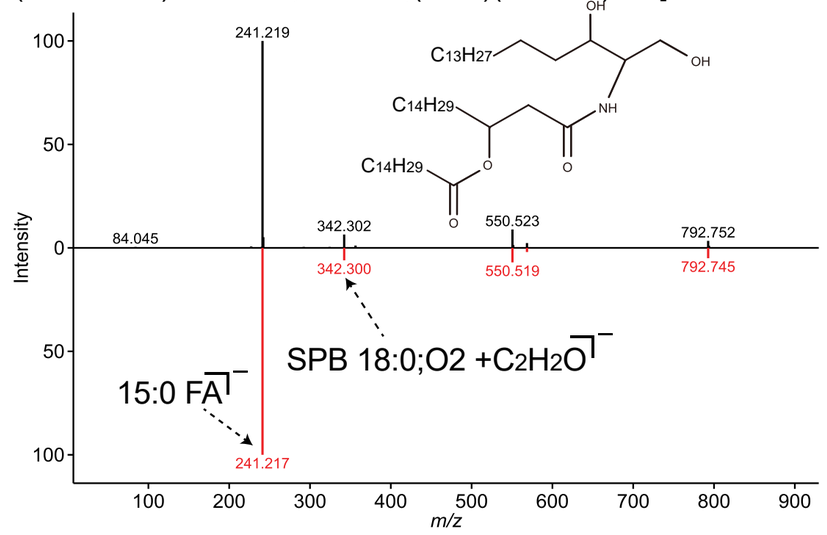

ESI(-)-MS/MS for Sphingolipids [SP]: Cer-NDS, Cer-NP, Cer-NS, CerP, SM, SM+O, HexCer-AP, HexCer-EOS, HexCer-HDS

(Cer-NDS) Cer 18:0;2O/16:0 as $[M+CH_3COO]^-$

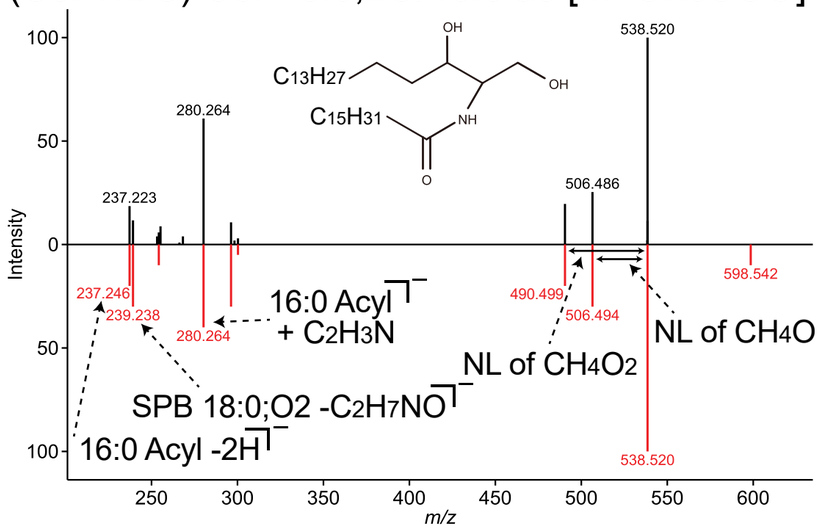

(Cer-NP) Cer 18:0;3O/16:0 as $[M+CH_3COO]^-$

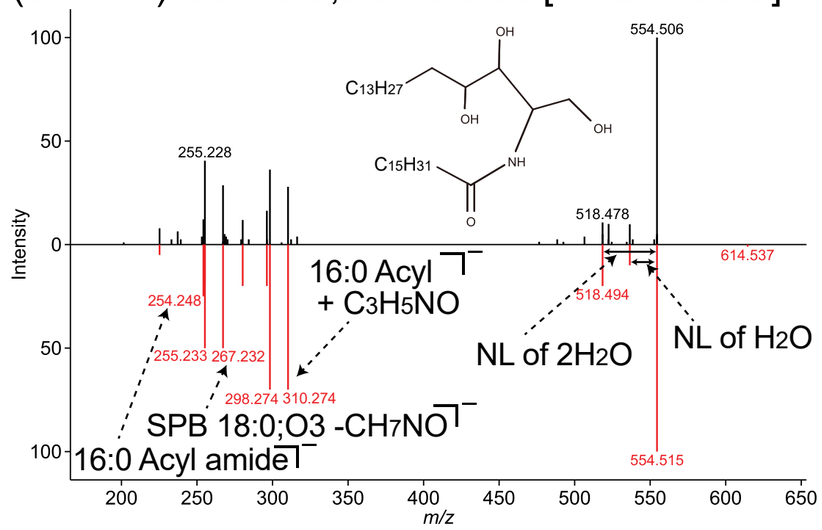

(Cer-NS) Cer 18:1;2O/16:0 as $[M+CH_3COO]^-$

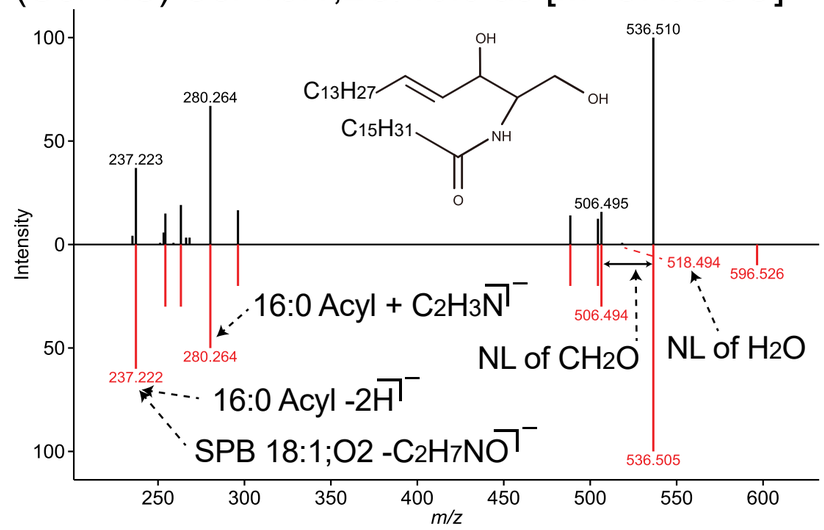

CerP 18:1;2O/12:0 as $[M-H]^-$

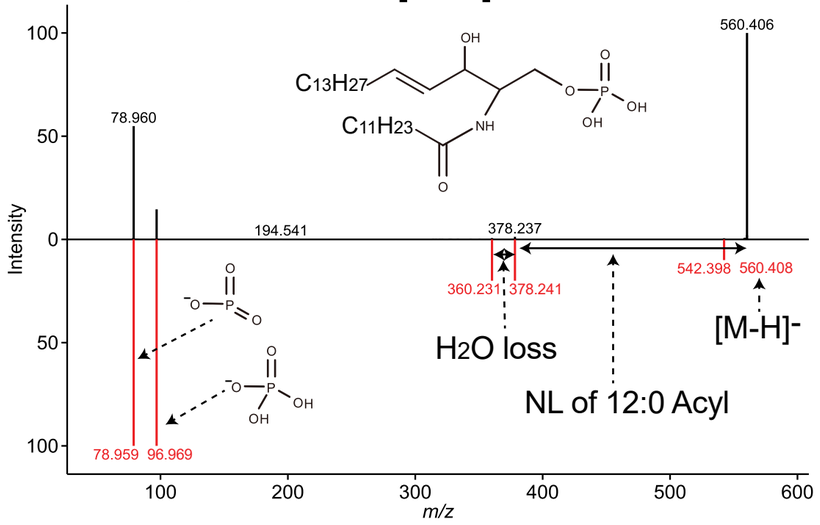

SM 18:1;2O/20:0 as $[M+CH_3COO]^-$

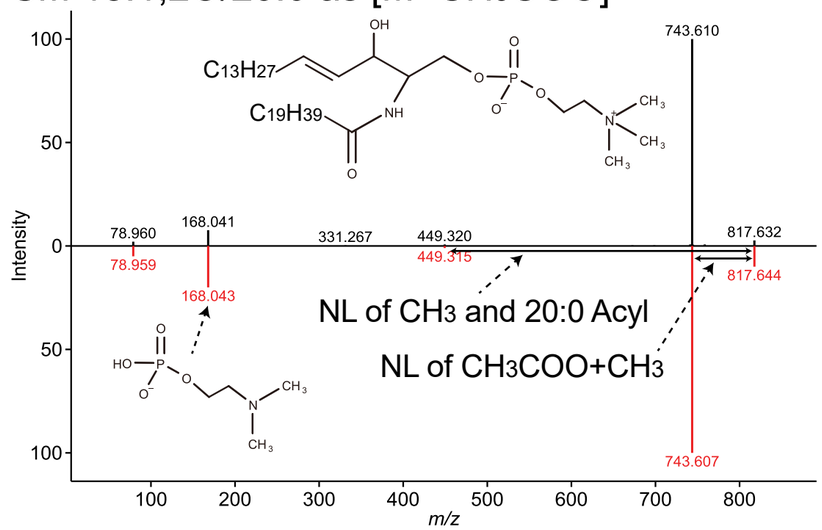

SM 34:1;3O as $[M+CH_3COO]^-$

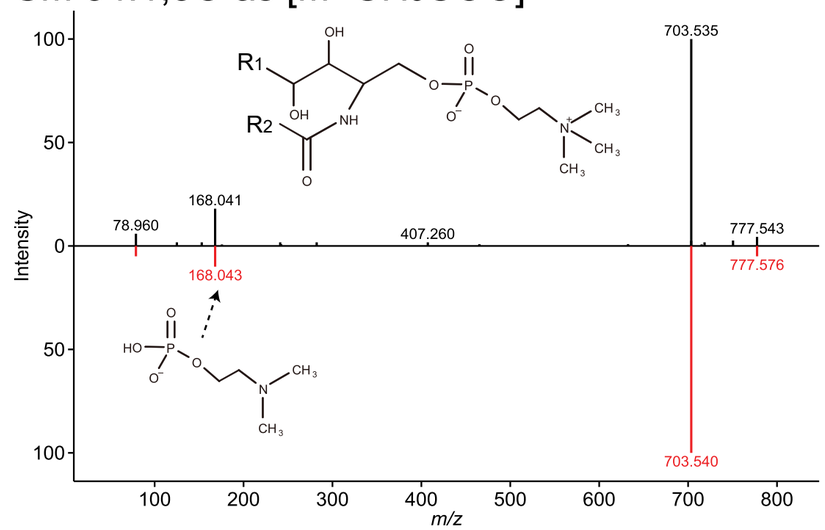

(HexCer-AP) HexCer 18:0;3O/16:0;(2OH) as $[M+CH_3COO]^-$

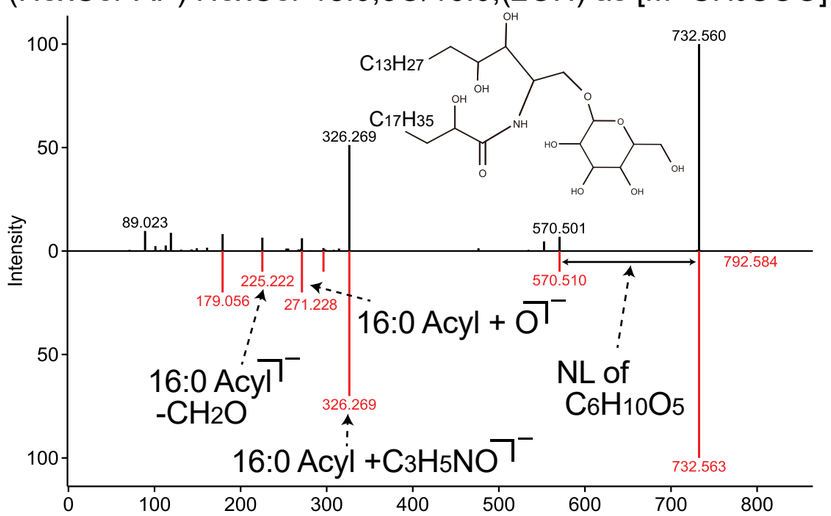

(HexCer-EOS) HexCer 18:1;2O/32:0;O(FA 18:2) as $[M+CH_3COO]^-$

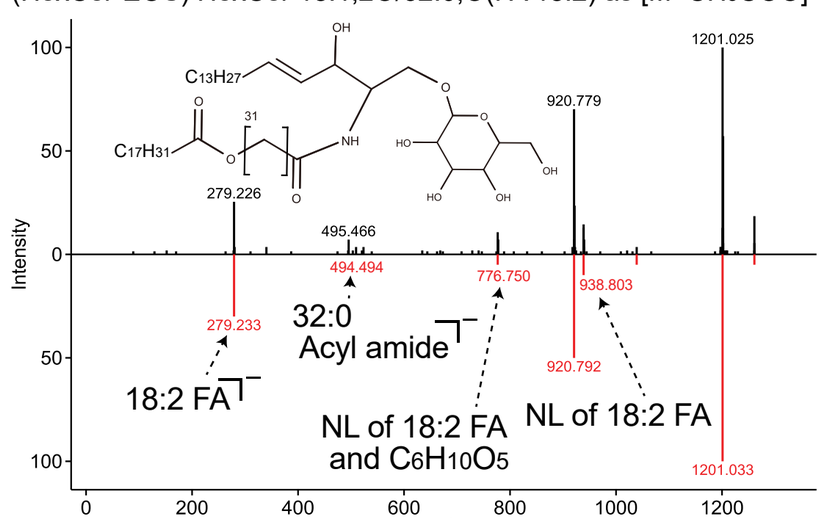

(HexCer-HDS) HexCer 34:0;3O as $[M+CH_3COO]^-$

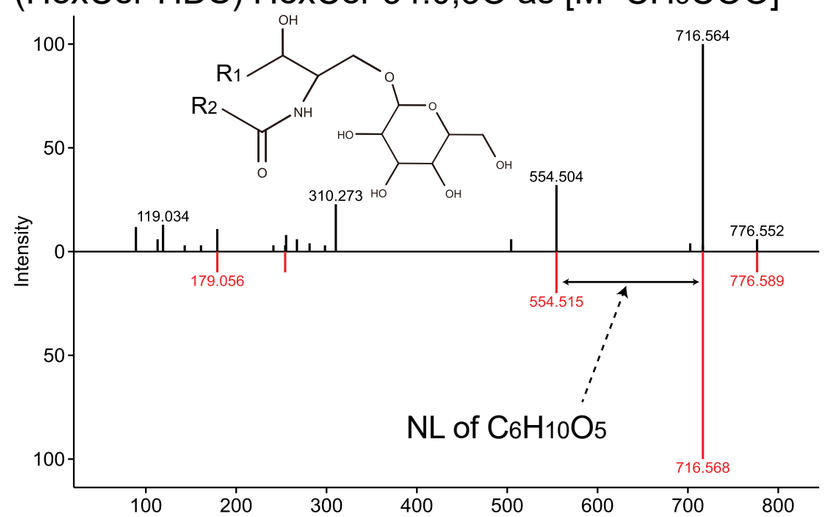

ESI(-)-MS/MS for Sphingolipids [SP]: HexCer-HS, HexCer-NDS, HexCer-NS, Hex2Cer, Hex3Cer, PE-Cer, PE-Cer+O, PI-Cer+O, GM3

(HexCer-HS) HexCer 16:1;2O/26:1;O as $[M+CH_3COO]^-$

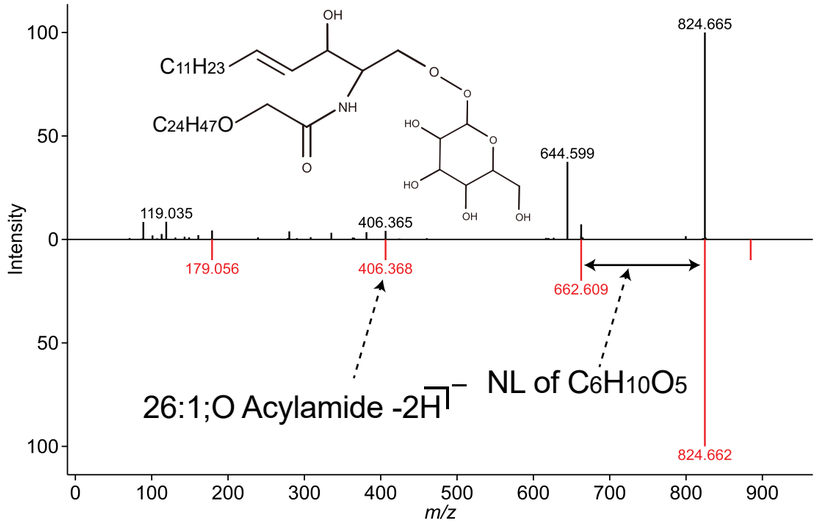

(HexCer-NDS) HexCer 18:0;2O/16:0 as $[M+CH_3COO]^-$

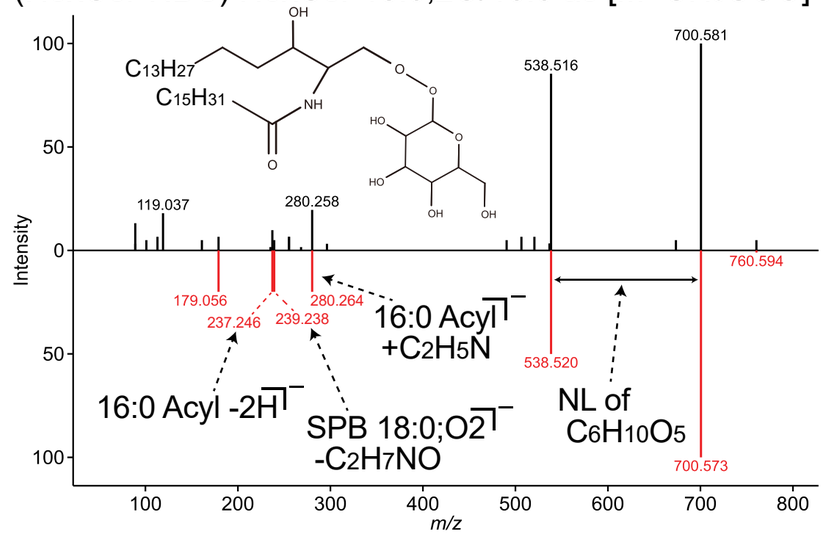

(HexCer-NS) HexCer 18:1;2O/20:0 as $[M+CH_3COO]^-$

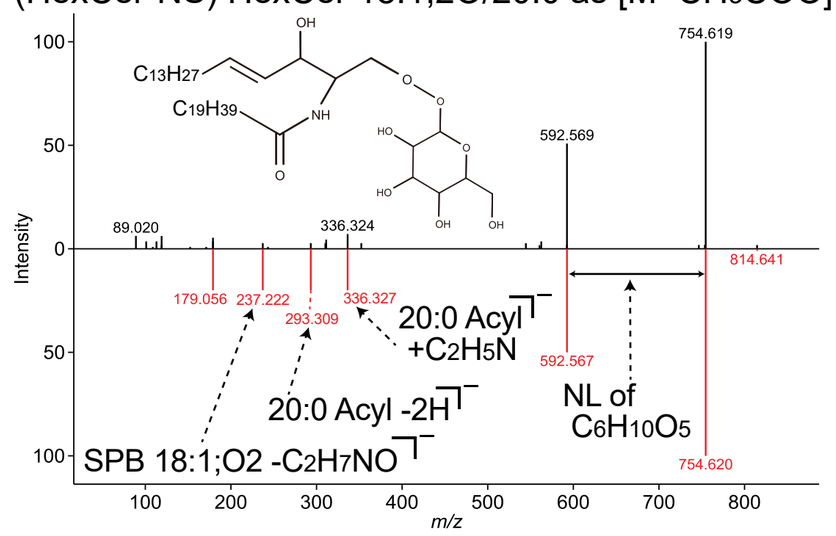

Hex2Cer 34:1;2O as $[M+CH_3COO]^-$

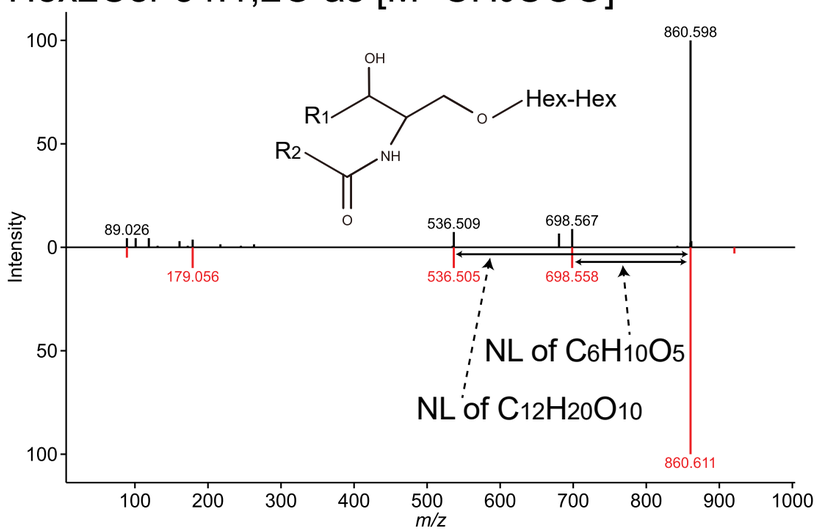

Hex3Cer 42:1;2O as $[M+CH_3COO]^-$

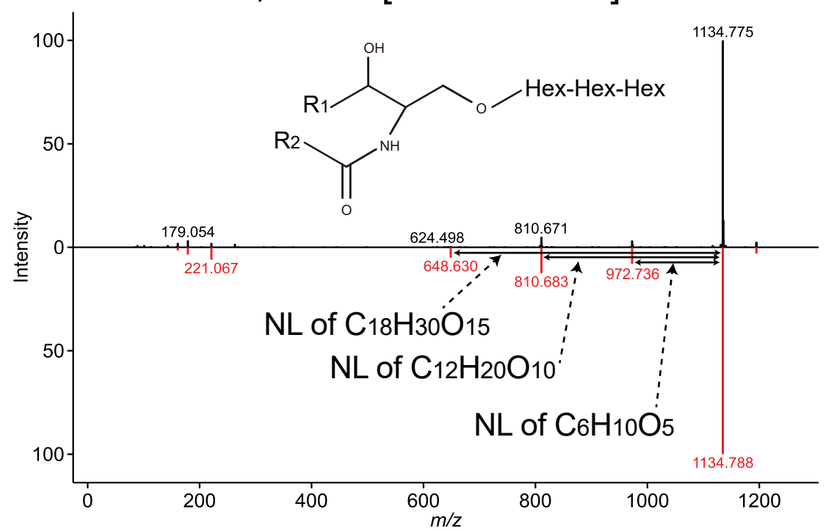

PE-Cer 18:1;2O/18:0 as $[M-H]^-$

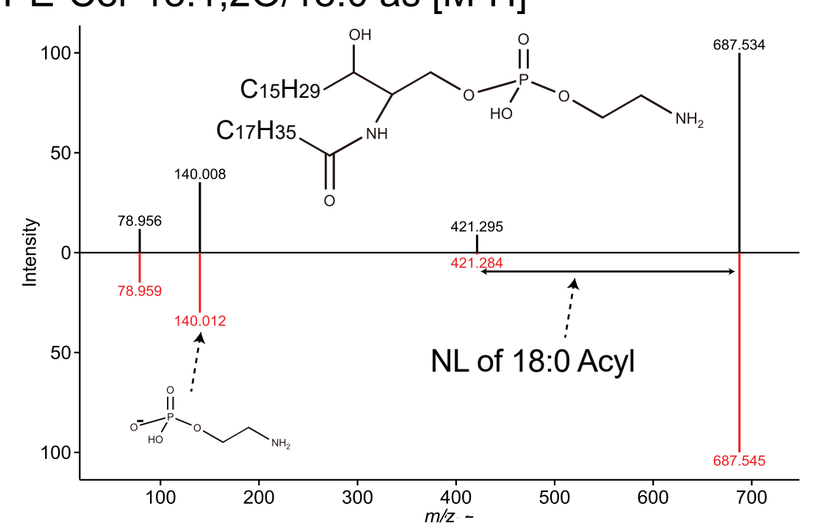

PE-Cer 18:0;2O/17:0;O as $[M-H]^-$

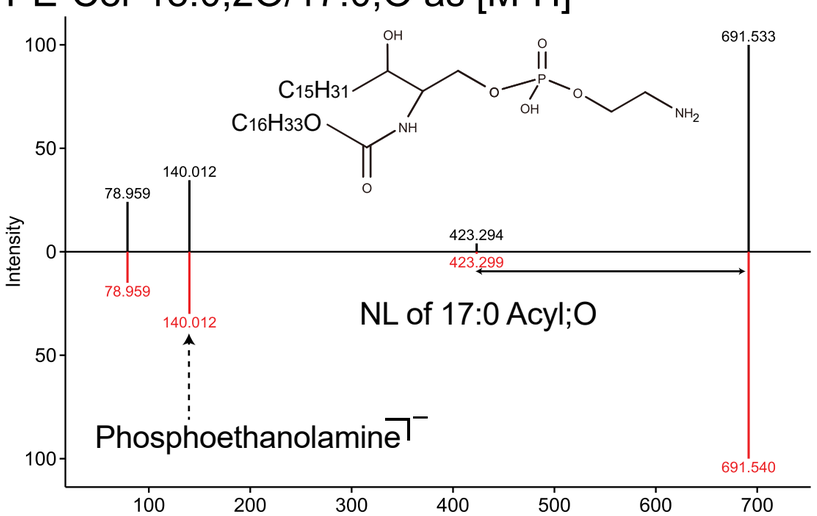

PI-Cer 18:0;2O/16:0;O as $[M-H]^-$

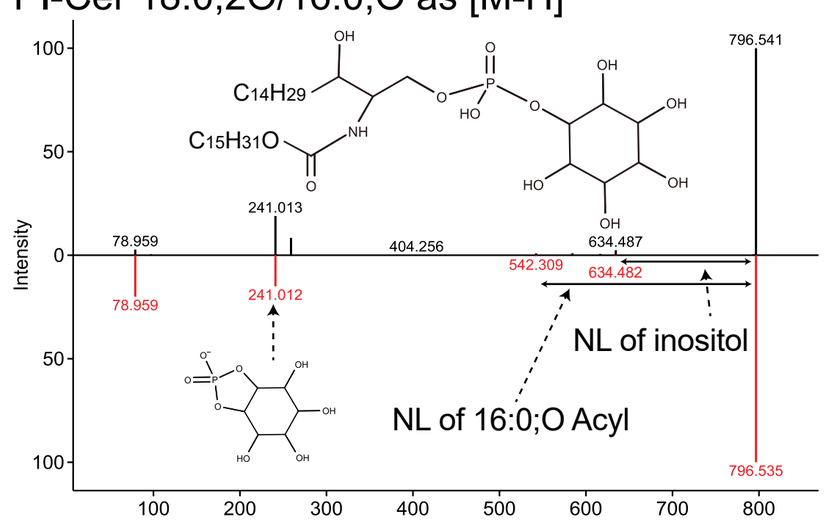

GM3 34:1;2O as $[M-H]^-$

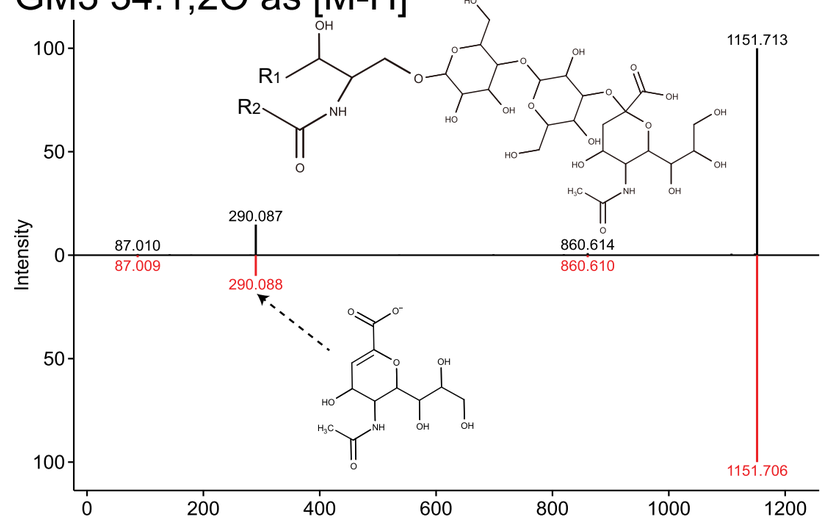

ESI(-)-MS/MS for Sphingolipids [SP]: AHexCer, ASM, SHexCer, SHexCer+O, SL, SL+O

AHexCer (O-16:0)18:1;2O/22:0;O as $[M+CH_3COO]^-$

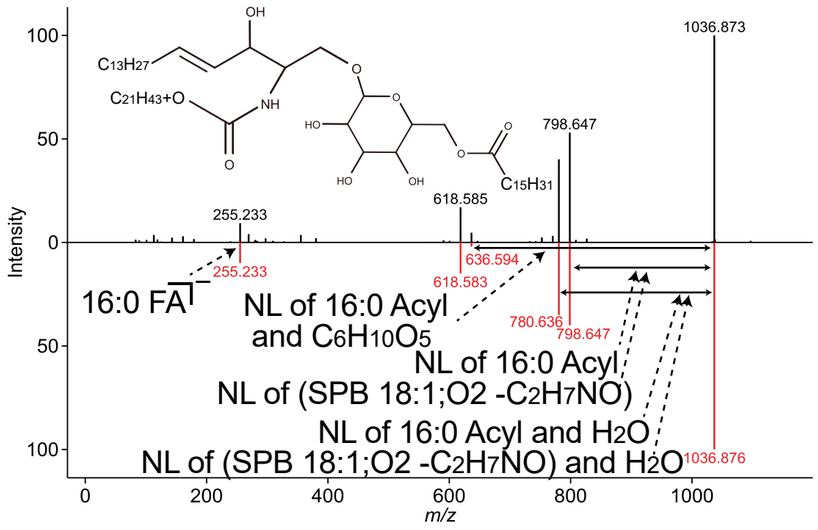

(ASM) SM 34:1;2O(FA 18:0) as $[M+CH_3COO]^-$

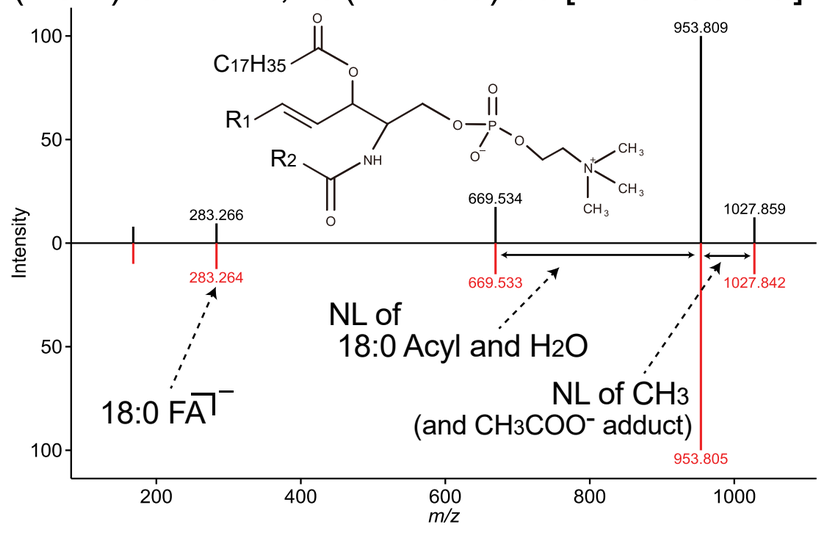

SHexCer 38:1;2O as $[M-H]^-$

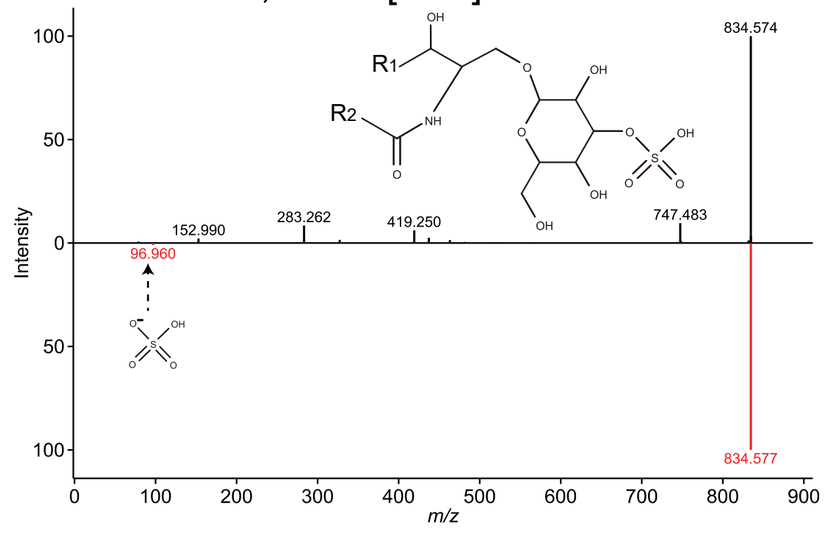

SHexCer 42:2;3O as $[M-H]^-$

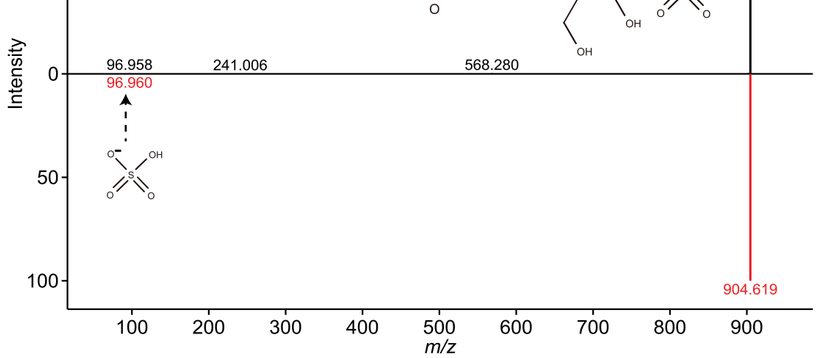

SL 18:0;O/16:0 as $[M-H]^-$

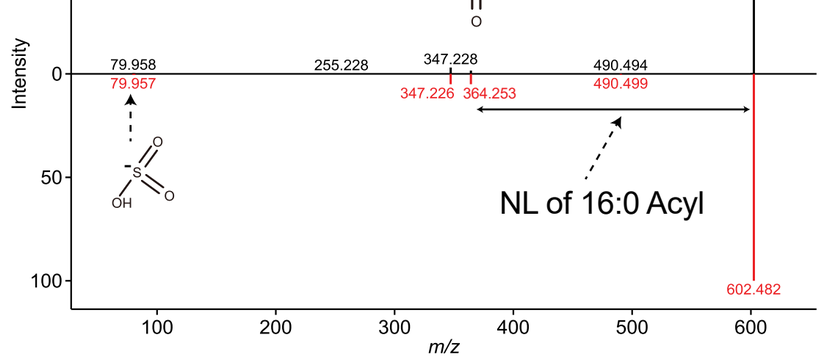

SL 18:0;O/16:1;O as $[M-H]^-$

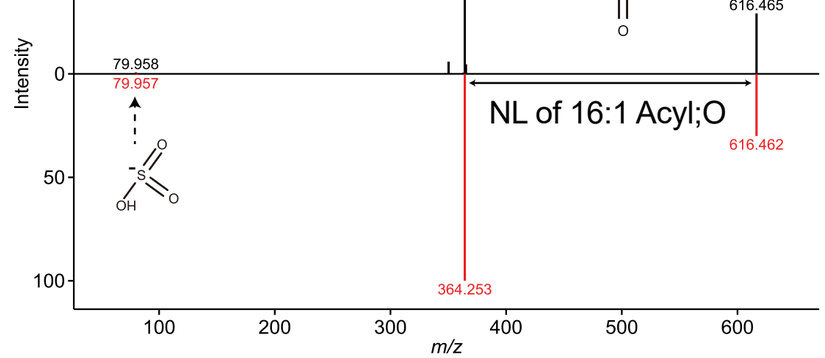

Sterol Lipids [SL]

ESI(+)-MS/MS for Sterol Lipids [SL]: Cholesterol, CE, SHex, BRSE, CASE, SISE, DCAE, STSE, AHexCS

Cholesterol as $[M-H_2O+H]^+$

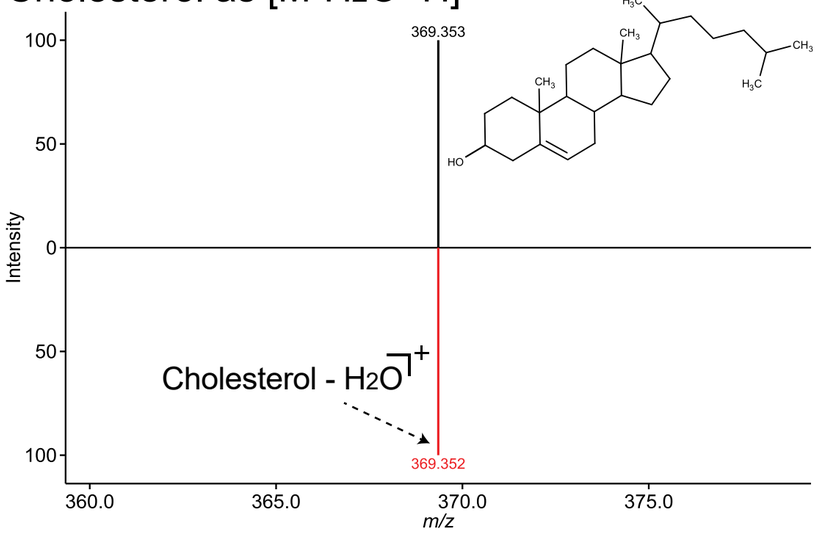

CE 18:1 as $[M+NH_4]^+$

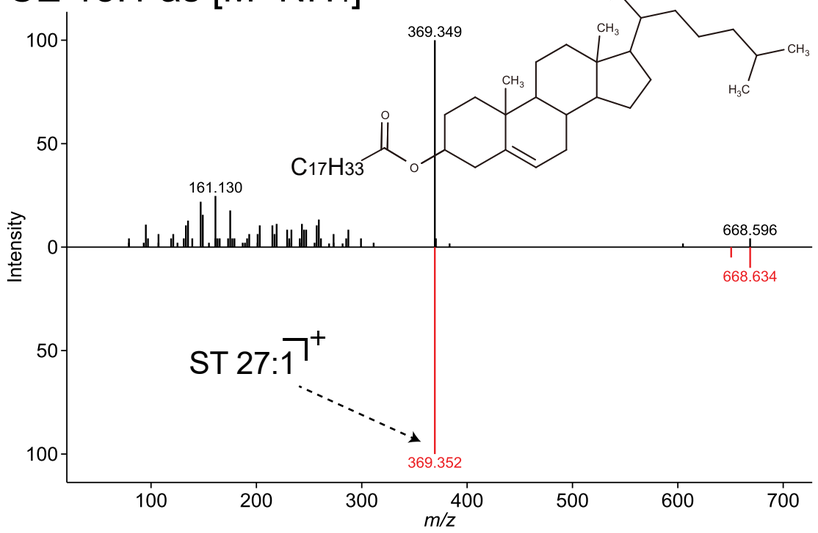

(SHex) ST 29:2;O;Hex as $[M+NH_4]^+$

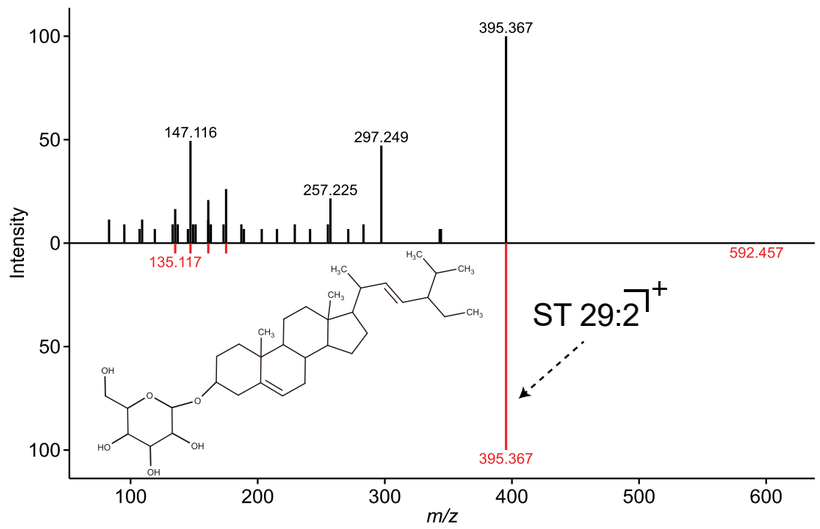

(BRSE) SE 28:2/22:6 as $[M+NH_4]^+$

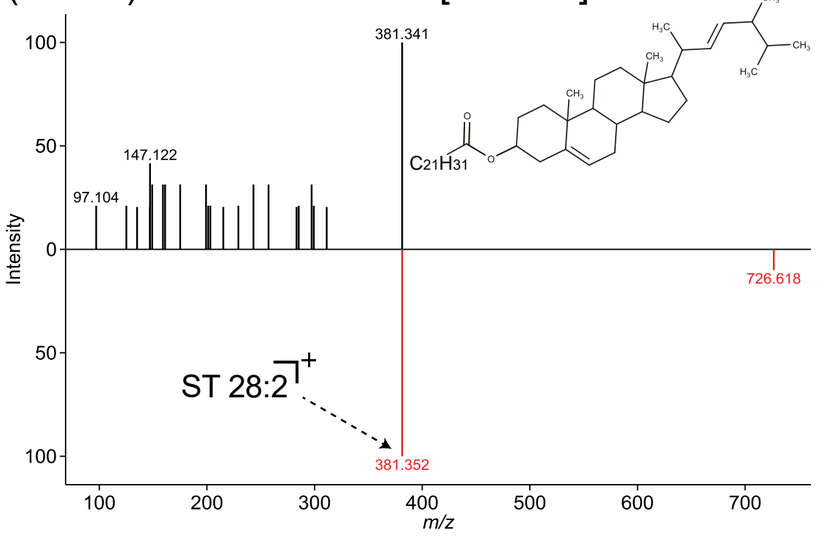

(CASE) SE 28:1/18:1 as $[M+NH_4]^+$

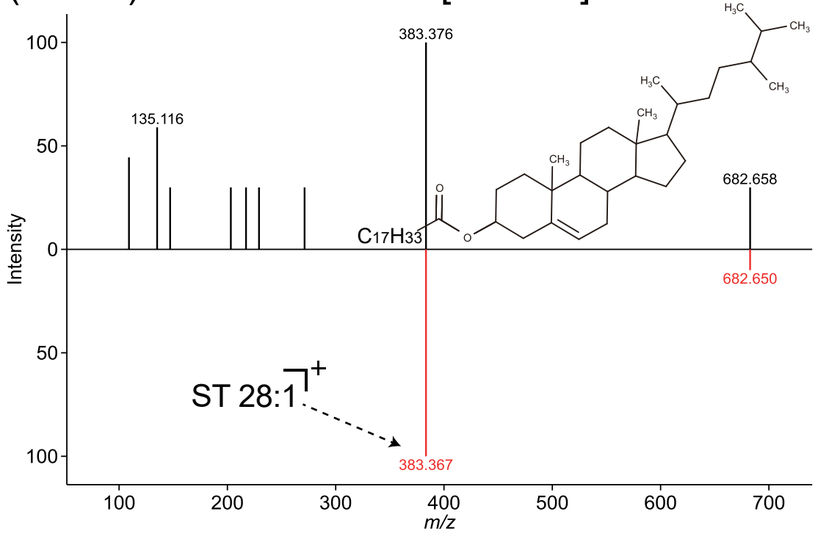

(SISE) SE 29:1/18:1 as $[M+NH_4]^+$

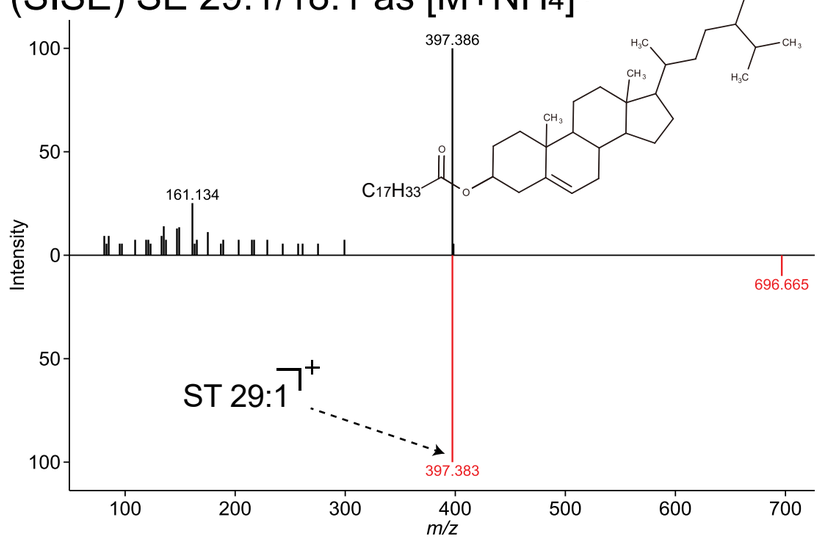

(DCAE) SE 24:1;O3/18:1 as $[M+NH_4]^+$

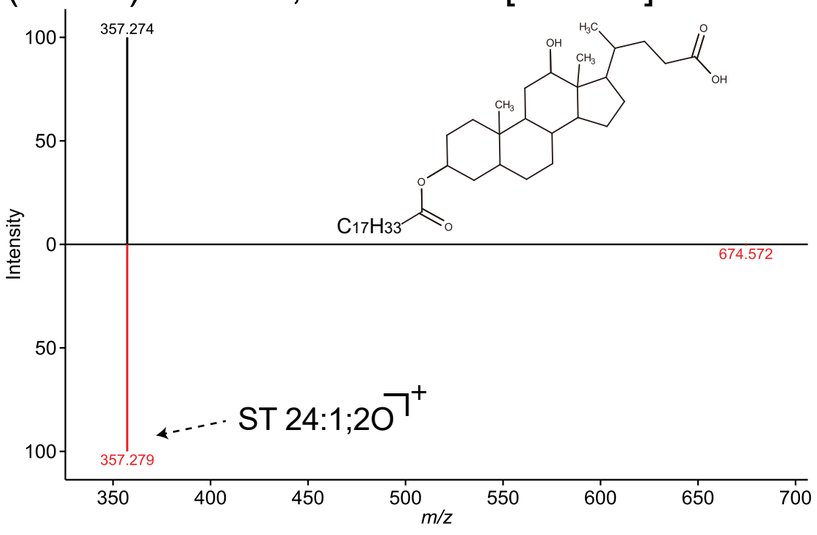

(STSE) SE 29:2/18:2 as $[M+NH_4]^+$

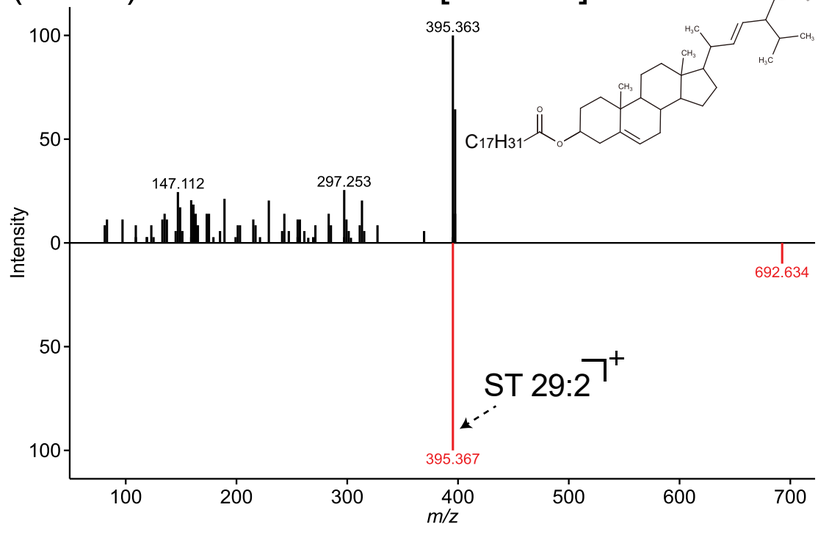

(AHexCS) ST 27:1;O;Hex;FA 16:0 as $[M+NH_4]^+$

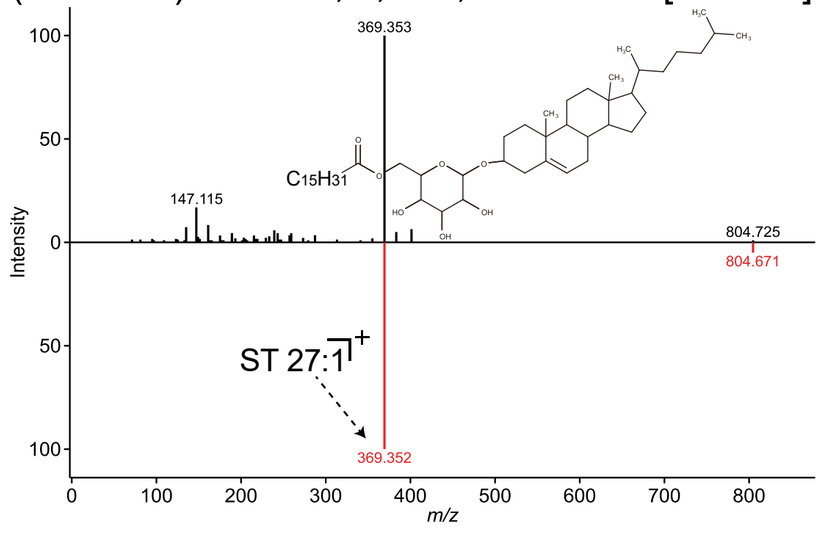

ESI(+)-MS/MS for Sterol Lipids [SL]: AHexCAS, AHexSIS, AHexSTS, Vitamin D

(AHexCAS) ST 28:1;O;Hex;FA 18:2 as $[M+NH_4]^+$

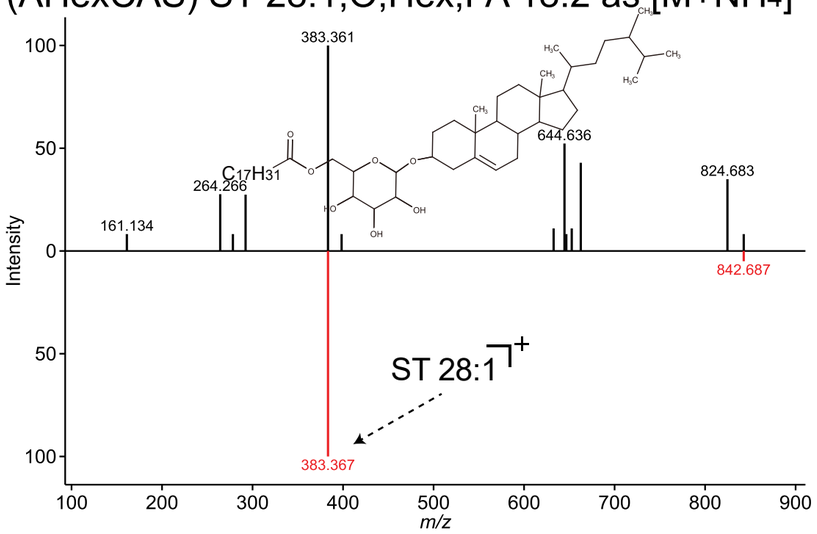

(AHexSIS) ST 29:1;O;Hex;FA 18:1 as $[M+NH_4]^+$

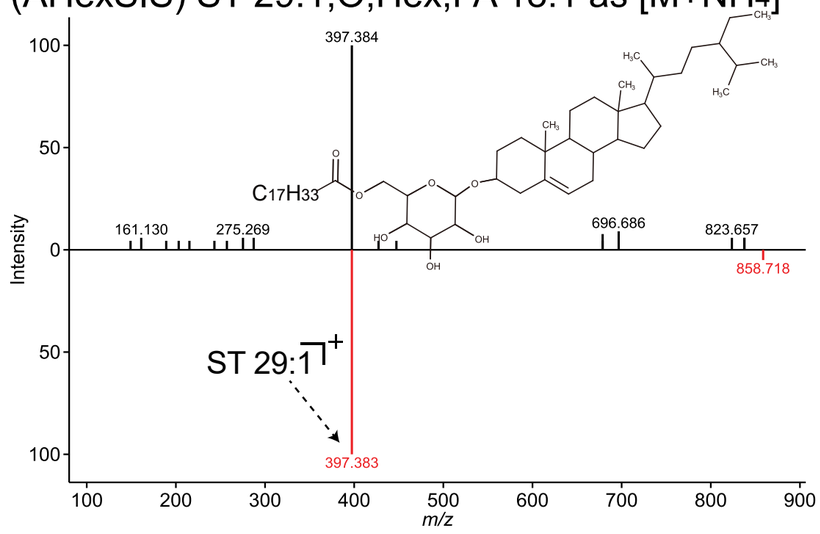

(AHexSTS) ST 29:2;O;Hex;FA 16:0 as $[M+NH_4]^+$

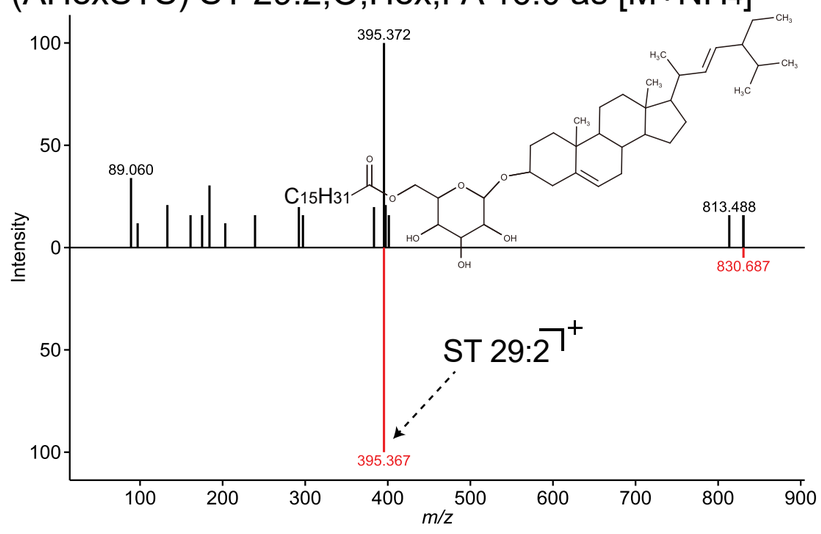

(Vitamin D) Calcidiol as $[M+H]^+$

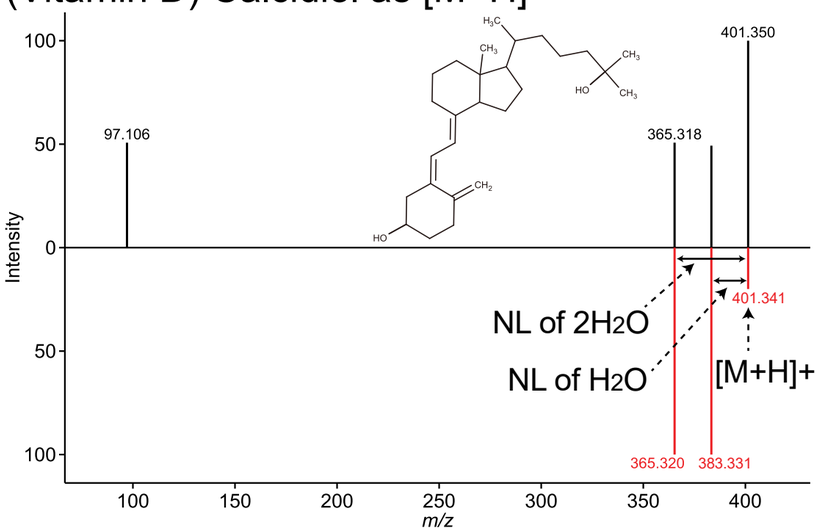

ESI(-)-MS/MS for Sterol Lipids [SL]: SSulfate, BASulfate, DCAE, SHex, AHexCS, AHexCAS, AHexSIS, AHexBRS, AHexSTS

(SSulfate) ST 27:1;O;S as [M-H]-

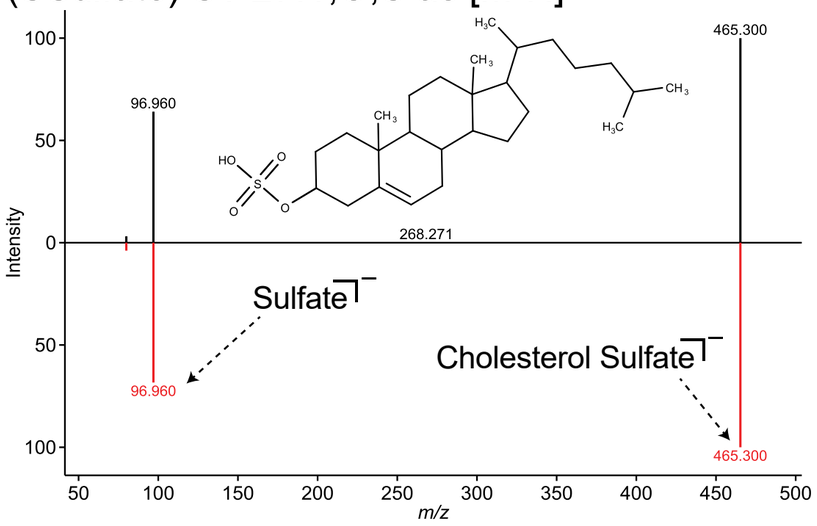

(BASulfate) ST 24:1;O5;S as [M-H]-

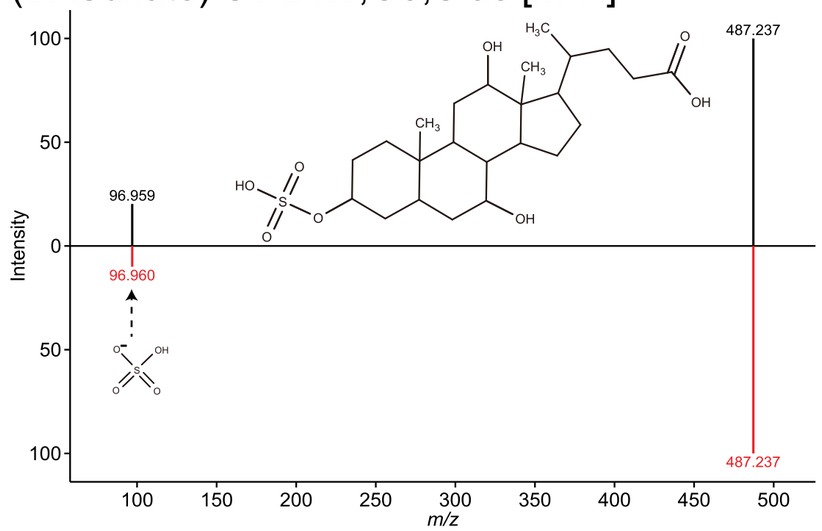

(SHex) ST 29:2;O;Hex as [M+CH3COO]-

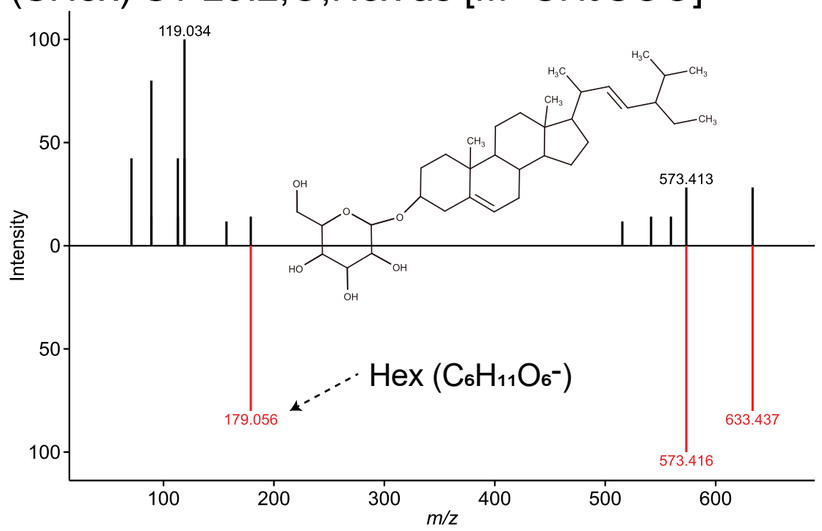

(AHexCS) ST 27:1;O;Hex;FA 18:1 as [M+CH3COO]-

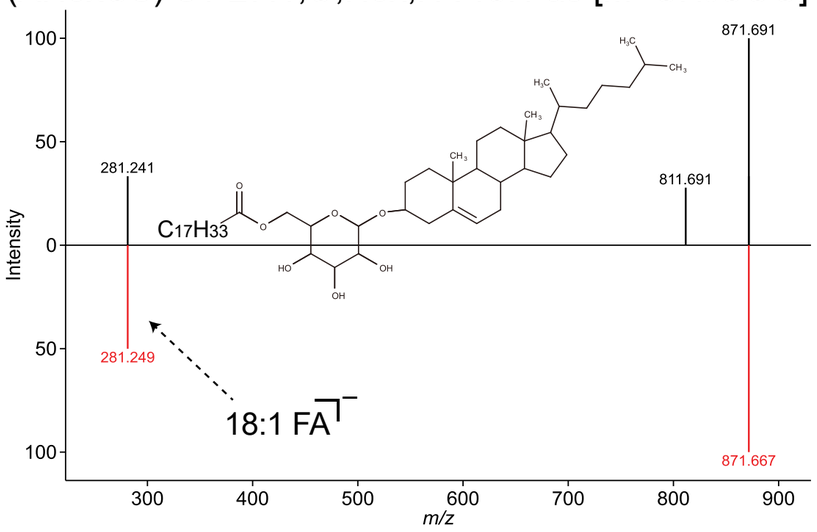

(AHexCAS) ST 28:1;O;Hex;FA 18:1 as [M+CH3COO]-

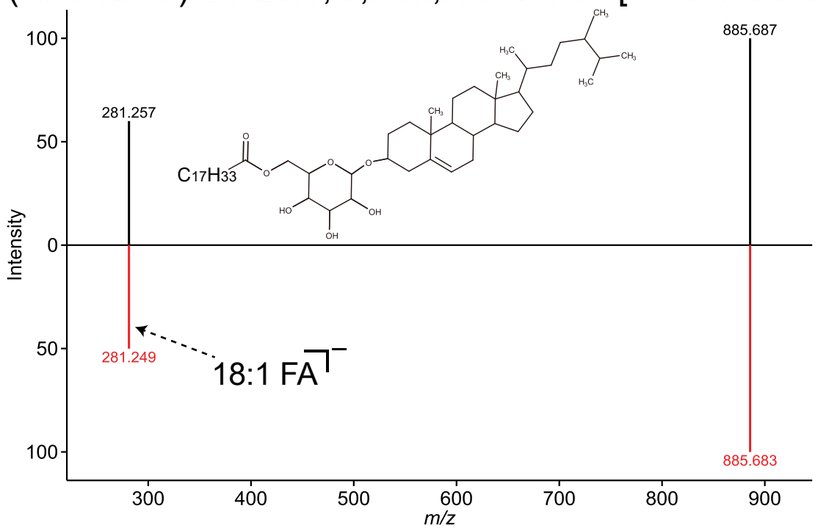

(AHexSIS) ST 29:1;O;Hex;FA 18:1 as [M+CH3COO]-

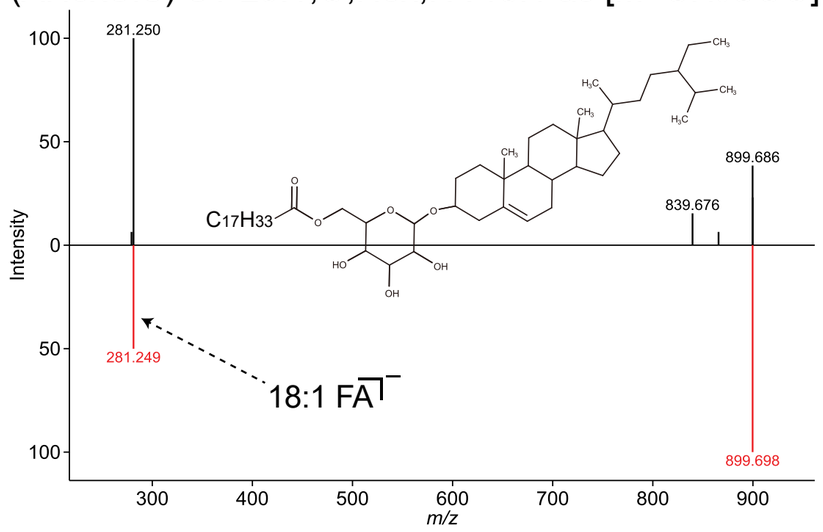

(AHexBRS) ST 28:2;O;Hex;FA 16:0 as [M+CH3COO]-

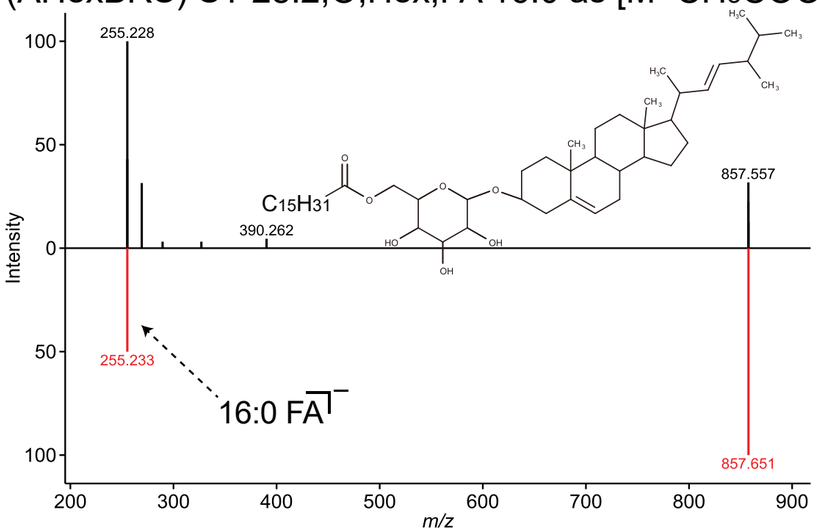

(AHexSTS) ST 29:2;O;Hex;FA 16:0 [M+CH3COO]-

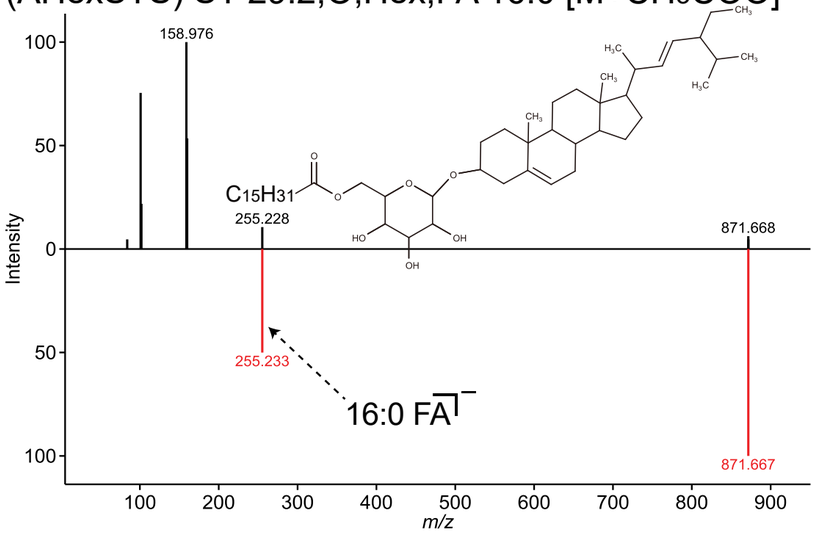

(DCAE) SE 24:1;O3/18:1 as [M-H]-

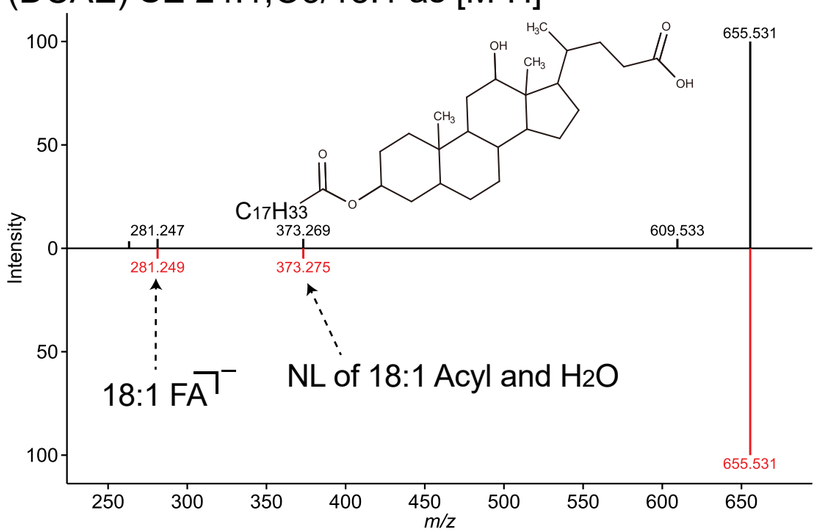

ESI(-)-MS/MS for Sterol Lipids [SL]: Bile acids (e.g. glycine or taurin conjugate)

(GDCA) ST 24:1;O3;G as [M-H]-

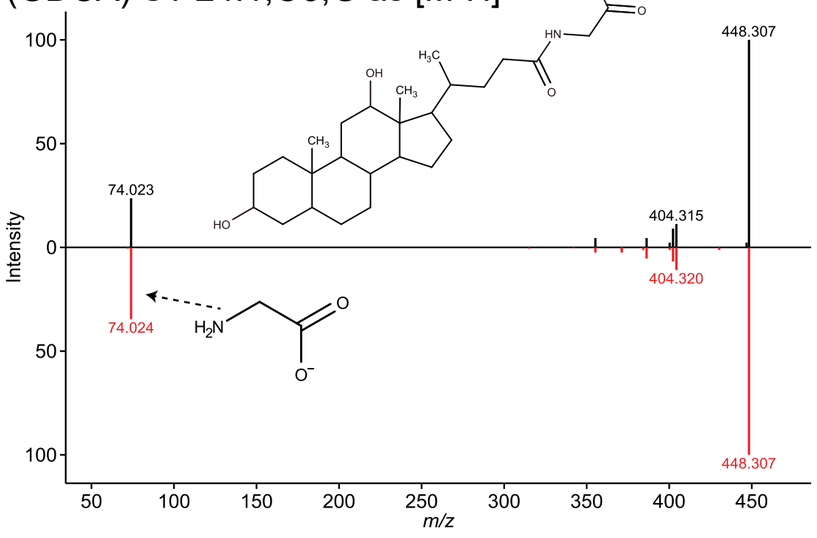

(TLCA) ST 24:1;O2;T as [M-H]-

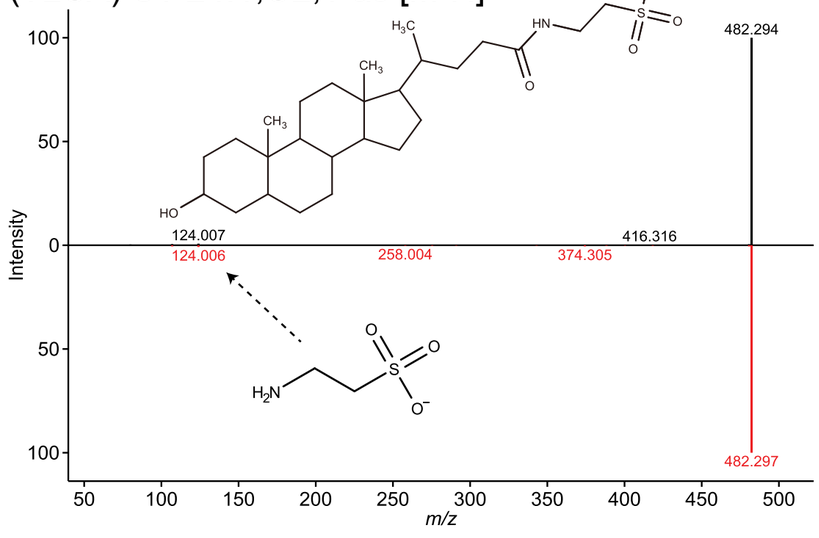

Prenol Lipids [PL]

ESI(+) and ESI(-)-MS/MS for Prenol Lipids [PL]: CoQ, VAE, Vitamin E

CoQ10 as $[M+H]^+$

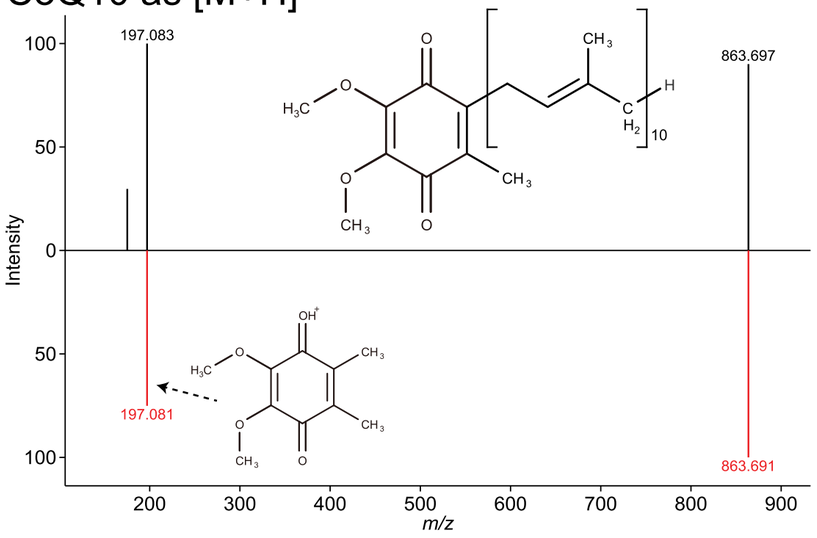

VAE 18:0 as $[M+Na]^+$

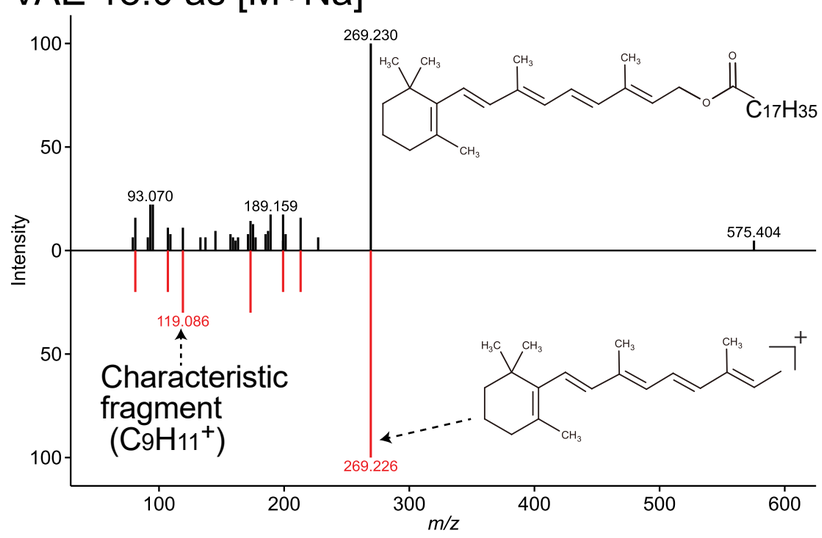

(Vitamin E) Tocopherol as $[M+CH_3COO]^-$